Controls on Erosion Patterns and Sediment Transport in a Monsoonal, Tectonically Quiescent Drainage, Song Gianh, Central Vietnam

Tara N. Jonell[1]*, Peter D. Clift[1], Long Van Hoang[2], Tina Hoang[3], Andrew Carter[4], Hella Wittmann[5], Philipp Böning[6], Katharina Pahnke[6] and Tammy Rittenour[7]

1 – Department of Geology and Geophysics, Louisiana State University, Baton Rouge, LA 70803, USA

2 - Hanoi University of Mining and Geology, Duc Thang, North Tu Liem, Ha Noi, Vietnam

3 - School of Geosciences, University of Louisiana at Lafayette, Lafayette LA 70504, USA

4 - Department of Earth and Planetary Sciences, Birkbeck College, London, WC1E 7HX, United Kingdom

5- Helmholtz Centre Potsdam, GFZ German Research Center for Geosciences, Telegrafenberg, 14473 Potsdam, Germany

6- Max Planck Research Group for Marine Isotope Geochemistry, Institute for Chemistry and Biology of the Marine Environment (ICBM), University of Oldenburg, 26129 Oldenburg, Germany

7 - Department of Geology, Utah State University, Logan UT 84322, USA

Abstract

Keywords: provenance, erosion, monsoon, Vietnam

The Song Gianh is a small, monsoon-dominated river in northern central Vietnam that can be used to understand how topography and climate control continental erosion. We present major element concentrations, together with Sr and Nd isotopic compositions, of siliciclastic bulk sediments to define sediment provenance and chemical weathering intensity. These data indicate preferential sediment generation in the steep, wetter upper reaches of the Song Gianh. In contrast, detrital zircon U-Pb ages argue for significant flux from the drier, northern Rao Tro tributary. We propose that this mismatch represents disequilibrium in basin erosion patterns driven by changing monsoon strength and the onset of agriculture across the region. Detrital apatite fission track and ^{10}Be data from modern sediment support slowing of regional bedrock exhumation rates through the

* Corresponding author – tjonell1@lsu.edu

Cenozoic. If the Song Gianh is representative of coastal Vietnam then the coastal mountains may have produced around 132,000–158,000 km^3 of the sediment now preserved in the Song Hong-Yinggehai Basin (17–21% of the total), the primary depocenter of the Red River. This flux does not negate the need for drainage capture in the Red River to explain the large Cenozoic sediment volumes in that basin but does partly account for the discrepancy between preserved and eroded sediment volumes. OSL ages from terraces cluster in the Early Holocene (7.4–8.5 ka), Pre-Industrial (550–320 yr BP) and in the recent past (~150 yr BP). The older terraces reflect high sediment production driven by a strong monsoon, while the younger are the product of anthropogenic impact on the landscape caused by farming. Modern river sediment is consistently more weathered than terrace sediment consistent with reworking of old weathered soils by agricultural disruption.

Introduction

Erosion of the continental crust is controlled by surface processes that in turn are partly influenced by climate, lithology, and tectonic deformation of the lithosphere. Debate continues about whether climatic or solid Earth forcing dominates the formation of sediment from bedrock (Burbank *et al.*, 2003; Bookhagen *et al.*, 2005a; Clift, 2006; Dortch *et al.*, 2011). Interpretation of the geologic record requires an understanding of modern sediment production and transport processes. Furthermore, long-term recycling of the continental crust is inherently tied to continental erosion, delivering material that can then be reincorporated via subduction back into the mantle (von Huene & Scholl, 1991; Clift *et al.*, 2009).

Previous studies investigating erosion have focused on active mountain belts where tectonic and climatic processes are often intimately linked (Pratt-Sitaula *et al.*, 2004; Kirby & Ouimet, 2011; Blöthe *et al.*, 2014). In many cases, it is hard to separate the relative influence of these primary drivers of erosion. In this study we address this issue by evaluating a fluvial system in a largely tectonically quiescent setting. By doing so we aim to isolate the effects of climate in controlling patterns and rates of erosion. We choose to do so in an Asian monsoonal system because this atmospheric phenomena is often cited as a type example for the influence of surface processes on solid Earth systems (Beaumont *et al.*, 2001; Hodges *et al.*, 2004). Furthermore, several Quaternary records of monsoonal strength exist across the region (Dykoski *et al.*, 2005; Yancheva *et al.*, 2007; Hu *et al.*, 2008) allowing us to directly correlate landscape evolution and climate variability.

We examine the development of the Song Gianh Basin (Gianh River Basin) since the start of the Holocene (~10 ka) to understand how changing monsoon strength has influenced sediment production and transport. The small size (~3500 km^2) and simplicity of its tectonic setting permits a comprehensive basin-wide analysis of sediment production in contrast to logistically more challenging, large fluvial systems (>1000 km) such as the Yangtze, Mekong, and Red Rivers, which also have more complex and long sediment transport systems. In addition, the Song Giang originates from the eastern Annamite Range and directly drains into the South China Sea across a relatively high topographic gradient from the mountainous terrain to the narrow coastal plain (Fig. 1). This means that sediment could potentially be transported rapidly through the Song Gianh with less possibility for storage and reworking in wide flood plains that can act as sediment buffers and result in signal shredding, as seen in larger rivers (Castelltort & Van Den Driessche, 2003; Wittmann *et al.*, 2011; Simpson & Castelltort, 2012; Bracken *et al.*, 2015).

Geological Setting

The Song Gianh drains the coastal Annamite Range of central Vietnam and flows to the Gulf of Tonkin. The Song Gianh does not have a well-developed delta but a simple river mouth. Longshore currents remove sediment delivered by the river and transport them southward. North of the river mouth is a large complex of dunes (~40 km^2) that might have acted as a source for sediment to the river but does not appear to influence the modern flux as this complex does not now drain into the Song Gianh (Fig. 1). The river has a relatively narrow coastal plain that rises to the SW where the backbone of the Annamite Range separates the Song Gianh from streams that flow to the west and into the Mekong River. The highest topography exceeds 2 km elevation, but much of the basin is more low lying with gorges in the upper reaches ~600–800 m deep. Aggradational river terraces are found in the upper reaches of the Song Gianh Basin, but are of very limited extent. However, in the middle reaches, more extensive aggradational terracing, involving at least three separate levels, is recognized. Terraces heights above the modern river level are ≤11 m. No terraces extend around or near the river mouth.

The continental margin formed during the opening of the South China Sea, starting in the Eocene (Ru & Pigott, 1986; Franke *et al.*, 2014). Located at the end of the Red River Fault, one of the largest strike-slip systems on Earth, the Song Hong-Yinggehai Basin is a major pull-apart structure linked to that fault (Rangin *et al.*, 1995; Zhong *et al.*, 2004). The Song Hong-Yinggehai Basin is the primary depocenter for the Red River and is also supplied by sediment by the Song Gianh, along with other small rivers draining the northern Ammanite Range. Although active opening of the Song Hong-Yinggehai Basin ceased at ~17 Ma, there was modest reactivation after ~5 Ma, at least in the northern part of the basin (Rangin *et al.*, 1995; Clift & Sun, 2006). The northern Vietnam margin faces the island of Hainan, which is known to have been affected by volcanism and surface uplift since the Pliocene (Tu *et al.*, 1991; Shi *et al.*, 2011). Further south the Central Highlands of Vietnam were affected by volcanism, uplift and erosion ~8 Ma (Carter *et al.*, 2000). Nonetheless, the expectation is that the Song Gianh has been largely unaffected by more recent phases of tectonic activity and is now in a state of slow subsidence linked to passive margin thermal processes. There are no seismic or GPS-related data to indicate active deformation of the bedrock (Michel *et al.*, 2001).

The bedrock of the Song Gianh is largely composed of a variety of Paleozoic to Triassic sedimentary and metasedimentary rocks, intruded by modest volumes of peraluminous granites and rhyolites (Fig. 2). The metamorphism and magmatism are linked to the Permo-Triassic Indosinian Orogeny (Carter *et al.*, 2001; Lepvrier *et al.*,

2004) that affected much of Indochina . It is unclear to what extent the basin was affected by Cenozoic extension, such as that documented further south in the Kontum Massif, but this is also now inactive (Nagy *et al.*, 2001). This means we can interpret erosion more simply, largely in terms of the climate and topography.

Here we address the Song Gianh's development since the start of the Holocene, which is a time over which detailed multiproxy records for monsoon intensity exist in SE Asia. In particular, speleothem records from Dongge Cave in SW China represent the closest high resolution reconstruction (Dykoski *et al.*, 2005; Duan *et al.*, 2014). Although some doubts have been cast concerning the interpretation of such cave records (Clemens *et al.*, 2010) they are broadly in accord with other paleoenvironmental records, such as loess or upwelling productivity proxies (Mohtadi *et al.*, 2011). These show an intensification of the East Asian summer monsoon after ~11 ka, reaching a maximum ~8 ka, followed by a long-term decrease until present, albeit sometimes in steps rather than a continual slow decline. Farther north in the Red River catchment, shifting erosion patterns are tied to Holocene changes in summer rainfall (Hoang *et al.*, 2010a). In general times of strong summer monsoon are associated with faster erosion and sediment supply to deltas across Asia (Goodbred & Kuehl, 2000).

Methods

We use several methods to constrain the source of sediment in the Song Gianh and to quantify how sediment is mixed downstream before reaching the ocean. Modern river sediments were collected across the basin to characterize the compositions of the major tributaries flowing into the Song Gianh mainstream and assess the relative impact of each tributary to the total budget. Samples were taken from active channel beds and point bars with care to avoid bank material and in facies that were recently reworked by the river (Table 1). The fine- to medium-grained sand fraction was preferentially sampled because this size fraction is targeted for single-grain mineral provenance techniques. Samples were also taken from selected aggradational terraces for optically stimulated luminescence (OSL) dating.

Major and Trace Element Geochemistry

Each bulk, unsieved sediment sample was analyzed for major and trace elements to provide a basic characterization of the material that was also assessed with other isotopic and thermochronologic methods and to constrain the degree of chemical weathering. Carbonate was not removed prior to digestion. During chemical weathering the ratios of water-mobile versus water-immobile elements change because of mineral breakdown. Alkali earth elements are commonly used in such proxies because they are relatively mobile, and when compared to immobile elements, track the degree of leaching (e.g., K/Al).

For elemental analysis all samples were freeze-dried and ground before mixing 600 mg of sample with 3600 mg of lithium tetraborate ($Li_2B_4O_7$, Spektromelt). The samples were pre-oxidized at 500°C with NH_4NO_3 and fused to glass-beads. Samples were then were analyzed for Si, Al, Ti, Fe, Na, Ca, K, P and Rb by X-Ray Fluorescence (XRF) using a Philips PW 2400 X-Ray spectrometer at the Institut für Chemie und Biologie des Meeres (ICBM) at the Carl von Ossietzky Universität, Oldenburg, Germany. XRF measurements were performed using the method of Böning *et al.* (2009). Overall analytical precision and accuracy were monitored by measurements of several in-house standards and the certified standard GSD-12, and were better than 3%. All data are presented in Table 2. Bulk sediment terrace OSL samples were analyzed separately by ICP-AES methods at the University of Utah, as described below, as part of the OSL methodology.

Isotope Geochemistry

Selected sediments were also analyzed for Sr and Nd isotopes because these systems have an established track record of being reliable provenance and chemical weathering proxies in sedimentary systems and have been applied successfully in the Mekong and Red Rivers (Liu *et al.*, 2007; Clift *et al.*, 2008b). Nd is a water-immobile element and is generally considered not to experience isotopic fractionation during weathering and erosion processes (Goldstein *et al.*, 1984). The Nd isotopic composition broadly reflects the average age and lithology of the crust being eroded so that sediments from ancient continental crust have different signatures compared to those derived from younger igneous bodies. Sr is water mobile and may be affected by weathering processes as well as the provenance (Derry & France-Lanord, 1996). Unweathered rocks show correlation between Nd and Sr isotopes, but $^{87}Sr/^{86}Sr$ values tend to increase with stronger alteration (Derry & France-Lanord, 1996; Hu *et al.*, 2013). Sr isotopes are strongly affected by the presence of carbonate and care was taken to decarbonate samples prior to analysis. This was especially important in the Song Gianh because of the presence of common limestone exposures, especially in the southern part of the basin (Fig. 2). This means that our analysis only constrains the provenance and alteration of the siliciclastic fraction. Much of the carbonate load is in any case dissolved and is not represented in the analyzed bedload (see the low CaO values, Table 2).

Prior to total digestion all samples were leached using buffered acetic acid to remove any carbonate-bound Sr. This was followed by a leach with 25% (v/v) acetic acid and 0.02 M hydroxylamine hydrochloride (HH) to remove Sr contained in authigenic Mn-Fe-oxides, which may also concentrate Nd. Hence, the Sr and Nd isotopic signatures is assumed to result solely from the silicate fraction (plus perhaps fractions of dolomite). The leached sediments were then digested in closed PTFE vessels (Böning *et al.*, 2004). The samples and the certified standard BCR-2 (50 mg), as well as a blank, were treated with HNO_3 overnight to oxidize any organic matter. After that HF and $HClO_4$ were added and the vessels were heated for 12 h at 180°C. All acids were of suprapure quality. After digestion, acids were evaporated on a heated metal block (180°C), residues were redissolved and fumed off three times with 6N HCl, and finally taken up in 1N HNO_3.

From the resulting solutions, rare earth elements (REEs) and Sr were isolated from major elements and separated from each other by two-step column chemistry using

Eichrom TRU-Spec resin. Nd was then isolated from interfering REEs using Eichrom LN-Spec resin with 0.23–0.25 N HCl as eluant. The TRU-Spec Sr-Rb cut was loaded on Eichrom Sr-Spec columns to isolate Sr using Milli-Q water.

The isotopic compositions of Nd and Sr were analyzed on a Thermo Neptune Plus Multicollector ICP-MS at the ICBM. For Nd isotope analyses, all samples were corrected for internal mass fractionation using $^{146}Nd/^{144}Nd = 0.7219$ and an exponential law. Each measurement session was accompanied by multiple analyses of the Nd standard JNdi-1 with sample-like concentrations, and $^{143}Nd/^{144}Nd$ ratios of all samples were normalized to the reported JNdi-1 value of $^{143}Nd/^{144}Nd = 0.512115$ (Tanaka *et al.*, 2000). The Nd isotopic composition is expressed in ε_{Nd} notation:

$$\varepsilon_{Nd} = [(^{143}Nd/^{144}Nd)_{sample} / (^{143}Nd/^{144}Nd)_{CHUR} - 1] * 10^4$$

$(^{143}Nd/^{144}Nd)_{CHUR}$ is the Chondritic Uniform Reservoir with a value of 0.512638 (Jacobsen & Wasserburg, 1980).The external reproducibility is calculated for each session separately using the analyses of JNdi-1 and was generally better than ±0.000015 or ± 0.3 ε_{Nd} units (2σ). The BCR-2 standard (n = 4) had an ε_{Nd} value of 0.1 (± 0.3, 2σ) and was well within the reported ε_{Nd} value of 0.0 ± 0.2 (Raczek *et al.*, 2003). The procedural blank was ≤ 30 pg Nd.

For Sr isotope analyses, all samples were corrected for mass fractionation using $^{86}Sr/^{88}Sr = 0.1194$ and the exponential law. Measurements were accompanied by multiple analyses of NBS987 with sample-like concentrations, and $^{87}Sr/^{86}Sr$ ratios of all samples were normalized to the reported value of 0.710248 (Thirlwall, 1991). Furthermore, Kr, Rb and Ba contents were monitored and found to be negligible. The external reproducibility is calculated using the analyses of NBS987 and was generally better than 50 ppm (2σ). The BCR-2 standard (n = 4) had a $^{87}Sr/^{86}Sr$ ratio of 0.70502 ± 0.00004 (2σ) and was within the reported $^{87}Sr/^{86}Sr$ ratio of 0.70496 ± 0.00002 (Raczek *et al.*, 2003). The procedural blanks were negligible throughout. Results are reported in Table 3.

Detrital zircon U-Pb geochronology

Detrital zircon U-Pb dating has become a popular and effective technique for evaluating sediment provenance in clastic systems because zircon is a common mineral in continental rocks of many compositions, and is chemically and mechanically durable enough to survive multiple cycles of erosion, transport and sedimentation. Grains >50 µm across were analyzed, reflecting the spot size of the laser employed. Yang *et al.* (2012) revealed that younger zircons were larger or more variable in size than the older grains in the Yangtze River, indicating the potential influence of hydrodynamic fractionation on zircon size and age. Yang *et al.* (2012) concluded that the 63–125 µm size fraction yielded almost the same age distribution as the total zircon population, and can effectively demonstrate all significant age populations. Our analysis may thus be expected to be representative of the bulk composition. Given that the Song Gianh is so much shorter than the Yangtze any grain size effect would be even less significant, because there must be less abrasion of zircons during transport.

Detrital zircons were dated using the U-Pb method at the London Geochronology Centre facilities at University College London, using a New Wave Nd:YAG 193 nm laser ablation system, coupled to an Agilent 7700 quadrupole ICP-MS. Around 100–120 grains are considered generally sufficient for characterizing sand eroded from a geologically complicated drainage basin (Vermeesch, 2004). Real time U-Pb data were processed using GLITTER 4.4 data reduction software. Repeated measurements of external zircon standard Plesovice (TIMS reference age 337.13±0.37 Ma)(Sláma *et al.*, 2008) and NIST 612 silicate glass (Pearce *et al.*, 1997) were used to correct for instrumental mass bias and depth-dependent inter-element fractionation of Pb, Th and U. For this study $^{206}Pb/^{238}U$ ages are used for grains younger than 1000 Ma, and for zircon grains older than 1000 Ma we used the $^{207}Pb/^{206}Pb$ ages to calculate the crystallization age. Because some grains are discordant we chose to only plot those grains when the discordance was less than 15%. Table 4.

Detrital Apatite Fission Track Geochronology

Two samples were analyzed for apatite fission track dating. The low-temperature apatite fission-track method, which records cooling through ~60–125°C over timescales of 1–10 m.y. (Green *et al.*, 1989) is particularly sensitive to exhumation driven by erosion and has been widely used in exhumation studies worldwide. Fission track analyses were performed at University College, London, UK. Polished grain mounts of apatite were etched with 5N HNO_3 at 20˚C for 20 s to reveal the spontaneous fission-tracks. Etched grain mounts were packed with mica external detectors and corning glass (CN5) dosimeters and irradiated in the FRM 11 thermal neutron facility at the University of Munich in Germany. Following irradiation the external detectors were etched using 48% HF at 20°C for 25 minutes. Sample ages were determined using the zeta calibration method and IUGS recommended age standards (Hurford, 1990). The results of the fission track analyses are presented in Table 5.

In situ ^{10}Be cosmogenic nuclide data

In situ-produced cosmogenic isotopes (e.g.,^{10}Be) are routinely measured in quartz from river sediment for estimating denudation rates in steady-state hill-slope settings over time scales relevant to soil formation processes, i.e., millennial (Bierman & Steig, 1996; von Blanckenburg, 2005; Granger & Riebe, 2007). These estimates can be compared with other methods, such as fission track to determine the temporal stability of erosion rates. In this study we only analyzed the river mouth sample using this method in order to determine the basin-wide integrated denudation rate in the recent past. Sample processing was done at the Deutsches GeoForschungszentrum (GFZ), in Potsdam, Germany. The sample was dried, sieved into a grain size range of 90 to 300 μm, and pure quartz was separated using magnetic separation followed by etching with weak HF, flotation, and ortho-phosphoric acid treatments until Al concentrations (being indicative of feldspar contents) were below 300 ppm (as subsequently evaluated using optical emission spectroscopy, OES). We used the simplified method of von Blanckenburg *et al.* (2004) to separate in situ-produced ^{10}Be from the sample matrix. Prior to final decomposition using concentrated HF and Fe and Be column chemistry, a final leach in aqua regia was done to remove remaining atmospherically-produced ^{10}Be. About 0.42 g of a ^{9}Be carrier with a concentration of 372 ppm was added to the sample, determined to contain a ^{10}Be/^{9}Be ratio of $3.4 \pm 0.5\times10^{-15}$, whose amount was subtracted from the measured ^{10}Be concentration. After column chemistry and alkaline precipitation, the sample was oxidized and pressed into accelerator mass spectrometer (AMS) cathodes and was measured at the Cologne University AMS facility (Dewald *et al.*, 2013) relative to standards KN1-6-2 and KN1-5-3 (having nominal ^{10}Be/^{9}Be ratios of 5.35×10^{-13} and 6.32×10^{-12}, respectively) normalized to a ^{10}Be half life of 1.39 m.y. (Chmeleff *et al.*, 2010; Korschinek *et al.*, 2010).

Conversion of a blank-corrected ^{10}Be concentration (Table 6) to a denudation rate was done using the atmospheric time-independent scaling scheme of Dunai (2000), calculated for pixel-based altitudes derived from 90 m resolution DEM, relative to a total sea level high latitude (SLHL) ^{10}Be nuclide production rate of 4.682 at/g×yr (Roller *et al.*, 2012). These calculations resulted in a total mean basin-wide ^{10}Be production rate of 3.37 at/g×yr (Table 6) for the Song Gianh catchment. This basin-wide production rate is lowered to a rate of 2.90 at/g×yr (Table 6) when a lithology correction is employed for areas of karstic limestone (not producing any ^{10}Be). These areas, identified mainly as Devonian limestones (Fig. 2), were excluded from production rate calculations. An uncertainty of 5% incorporating production rate and scaling errors was propagated into the calculated denudation rate error (yielding an external error for inter-method comparison). Note that a correction for geomagnetic variation in the intensity of Earth's magnetic dipole field was not carried out for the derived production rate. Topographic shielding on production rates was deemed negligible for the studied catchment.

Optically Stimulated Luminescence Dating

Depositional ages of sediment in the terraces were determined by optically stimulated luminescence (OSL) dating of quartz sand. While OSL dating can be challenging in fluvial environments, deposits from these settings can be accurately dated by selecting depositional facies most likely to have been reset by sunlight exposure (Fuchs & Owen, 2008; Rittenour, 2008; Wyshnytzky *et al.*, 2015). We preferentially targeted well-sorted, horizontally bedded sand lenses from fluvial deposits to reduce the influence of incomplete resetting (partial bleaching) of the luminescence signal.

Samples for OSL dating were collected by pounding opaque metal pipes into target horizons within the sediment exposures and sealing the ends of the tightly packed tubes to prevent light exposure and sediment mixing. Samples were sent to the Utah State University Luminescence Laboratory for processing to purified quartz separates for analysis. Samples were treated with dilute HCl and chlorine bleach to remove carbonates and organics followed by heavy mineral separation (sodium polytungstate, 2.7 g/cm^3) and treatment in concentrated HF to remove feldspars and etch the quartz grains. The purity of the quartz separates was checked by monitoring response to infra-red stimulation; contaminated aliquots were not used for age calculation.

Samples for environmental dose rate determination were collected from a 30 cm diameter area surrounding the OSL sample tube. Sediments were homogenized and representative samples were analyzed for radioisotope concentration using ICP-MS and ICP-AES techniques (Table 7). These concentration values were converted to dose rate following the conversion factors of Guérin *et al.* (2011) and beta attenuation values of Brennan (2003). Contribution of cosmic radiation to the dose rate was calculated using sample depth, elevation and latitude/longitude following Prescott and Hutton (1994). Total dose rates were calculated based on water content, radioisotope concentration, and cosmic contribution (Adamiec & Aitken, 1998; Aitken, 1998).

Small aliquots (50–200 grains) of quartz sand were analysed using the single-aliquot regenerative-dose (SAR) technique (Murray & Wintle, 2000) on Risø OSL/TL DA-20 luminescence readers with blue-green (470 nm, 36 W/m^2) stimulation and detection through 7.5-mm UV filters (U-340). Stimulation was conducted at 125°C following 240°C preheats (10 s) for regenerative and natural doses. OSL ages were calculated from 28–41 aliquots that passed rejection criteria related to feldspar contamination (IRSL signal to background ratio >2) and performance related to repeat-point (>15% difference) and zero-dose tests (>5% signal recuperated). Equivalent dose (D_E) values were calculated using either the central age model (CAM) or minimum age model (MAM) of Galbraith and Roberts (2012).

Results

Major Elements

The major element compositions of the samples show a typical range for quartz-rich sands. Rarely is the major element geochemistry diagnostic for provenance but it can be effective in determining the intensity of chemical weathering. This can be assessed using the "Chemical Index of Alteration" (CIA) proxy developed by Nesbitt *et al.* (1980) and expressed as:

$$\mathrm{CIA} = \left(\frac{\mathrm{Al_2O_3}}{\mathrm{Al_2O_3+Na_2O+K_2O+CaO^*}}\right) * 100$$

CIA compares the relative leaching of mobile elements K, Na, and silicate-only Ca against immobile Al as minerals, such as feldspar, weather to clay. CIA values close to 100 indicate intense weathering, where values around 50 indicate negligible weathering. Where excess CaO is present in carbonates and phosphates, a correction is made by assuming reasonable Ca/Na ratios from the silicate material and correcting for CaO in phosphate (Singh *et al.*, 2005).

Figure 3 indicates that CIA values range from 57 to 73 and vary in relation to the SiO_2 content, which can serve as a proxy for the quartz content of the sediment. Our samples show negative correlation to CIA with increasing silica content, which is typical of grain size variation in fluvial sediments.

There is a general decrease in CIA variation downstream towards the river mouth as shown in Figure 4. The highest values are seen in the upper reaches of the mainstream but decrease rapidly towards the river mouth. The Song Trac is noteworthy in that it has relatively high CIA values that contrast with the lower values seen in all other tributaries. Sediments in the terraces within the upper reaches and within the Song Trac have lower CIA values than the modern adjacent rivers.

Sr and Nd Isotopes

Figure 5 shows the variation in Sr and Nd isotopes for the Song Gianh and other SE Asian rivers, as well as potential source terranes in the Kontum Massif and Central Highlands (Fig. 1). The isotope compositions of Song Gianh indicate more negative ε_{Nd} values than other major SE Asian rivers and generally high $^{87}Sr/^{86}Sr$ values. We note that when considering only the Song Gianh samples there is no coherent correlation between the isotopic systems.

Along the mainstream, much variation is recognized in $^{87}Sr/^{86}Sr$ values of decarbonated sediment (Fig. 6A) with most variation occurring in the upper reaches of the mainstream. It is noteworthy that the Rao Tro and Mai Hoa tributaries have relatively high $^{87}Sr/^{86}Sr$ values compared to the mainstream. The $^{87}Sr/^{86}Sr$ values of the mainstream fall from upstream to downstream of the Mai Hoa. After this confluence, there is little compositional variability downstream. The Song Trac and Song Nan tributary $^{87}Sr/^{86}Sr$ values lie close to the values of the mainstream.

Similar to the Sr isotopes, the ε_{Nd} values of the mainstream are stable downstream of the Mai Hoa confluence (Fig. 6B). The northern tributaries, the Rao Tro and Mai Hoa, show distinctive, more positive ε_{Nd} values than the mainstream river. The mainstream ε_{Nd} values do not vary significantly downstream after the confluences of these tributaries. In contrast, the Song Nan and Song Trac have ε_{Nd} values that are slightly more negative than the mainstream.

Detrital Zircon

The distribution of ages for detrital zircons can be best compared graphically with kernel density estimation (KDE) diagrams. Figure 7 shows the range of measured zircon ages younger than 3.5 Ga for all the samples in our study, together with basement analyses from the Kontum Massif, Khorat Plateau, and Central Highlands. Although these do not directly source the Song Gianh they represent basement data from the Indochina Block that might have equivalents within our drainage. Each sample has a unique age spectrum but there are resolvable age peaks that can be identified in many samples. One prominent peak spans 100–380 Ma, with a maximum age ~250 Ma; this peak characterizes many rocks in SE Asia and is typically indicative of the Indosinian Orogeny (Carter *et al.*, 2001; Lepvrier *et al.*, 2004). Another common population at ~450 Ma is sometimes referred to as “the Caledonian event” (Chen & Jahn, 1998) or the Wuyi-Yunkai (or occasionally Kwangsian) Orogeny (Li *et al.*, 2010). A broad population of ages spanning 700–1100 Ma are correlative with rocks of that age from the Yangtze Craton, commonly referred to as the Jinningian (Li, 1999). An older group of zircons ages from 1750–2200 Ma match similar aged rock are referred to as the Luliangian from eastern Asia (Chen & Jahn, 1998). The number of older grains are somewhat fewer, although peaks are identified at ~2500 Ma and rarely ~2800 Ma.

It is noteworthy that the river mouth is characterized by a particularly large peak at ~250 Ma, a characteristic that is shared by the Rao Tro tributary. This peak is common in many of the Song Gianh zircon spectra, but other tributaries' spectra include other prominent, older populations as well. These older peaks are not dominant at the river mouth or Rao Tro spectra.

Apatite Fission Track

A single sample (14052705) yielded sufficient apatite to generate a statistically meaningful result that allows us to examine the average cooling history of bedrock in the Song Trac (Fig. 8). A single age population exists in the Song Trac with a central age of 54.5 ± 3.5 Ma as shown by a radial plot (Fig. 8A) and a KDE diagram (Fig. 8B) that also highlights the tail of older ages back to 120 Ma.

Denudation rates from detrital ^{10}Be concentrations

The measured *in situ* cosmogenic denudation rate at the river mouth is 29.5 ± 2.4 mm/k.y. (calculated using the limestone-corrected production rate). The integration time scale of this denudation rate is 33 k.y., corresponding to the time necessary to erode one attenuation depth scale (60 cm in rock or 100 cm in soil).

OSL dates

Results of OSL dating indicate four possible times of terrace construction within the basin (Table 7). In the upper reaches two samples within a single prominent, 11 m high terrace, show that it was constructed ~7.4–8.5 ka, during the Early Holocene. This terrace or an equivalent aged surface were not found in the lower reaches. A younger terrace, around 8 m above the modern stream, was identified nearby within the Mai Hoa confluence area and was dated at 550 ± 190 years ago. A slightly younger terrace was dated at ~320 ± 90 years ago within the Song Trac, standing 3–4 m above the modern river level. The youngest terrace, also found in the Song Trac, is elevated only ~1.5 m above the modern river and constructed against the 320 ± 90 years terrace. This was dated at 150 ± 140 years ago.

Discussion

Chemical Weathering

The degree of chemical weathering in the Song Gianh is not especially high but is largely a function of the quartz-rich, coarse-grained character of the sediments. Figure 3 compares our samples with bulk sediments from the Mekong, Pearl and Red Rivers (Liu *et al.*, 2007). Analyses from the Pearl and Mekong Rivers are limited to fine-grained sediments and are not surprisingly more altered than Song Gianh sediment. Red River sediments, however, also span sandier compositions and are generally lower in CIA (Clift *et al.*, 2008b) than the Song Gianh at any given silica composition. This implies that the Song Gianh sediments are more altered than those found in the Red River. Sediments from the Song Gianh reach extremely high silica contents by the river mouth. Because the Red River and the Song Gianh have very similar climates, we argue this stronger degree of chemical weathering is a reflection of the long-term tectonic stability of the Song Gianh Basin compared with the still tectonically active drainage basin of the Red River (Michel *et al.*, 2001; Zuchiewicz *et al.*, 2013). This is despite the fact that the Song Gianh is a smaller basin than the Red River, and would be expected to have much shorter sediment transport time. If relief and tectonic activity are lower in the Song Gianh than the Red River then this would favor longer residence of sediment on hillslopes that would allow more alteration to occur.

The downstream variation in CIA might suggest reduced chemical weathering with longer sediment transport (Fig. 4), but we believe that this trend is largely a grain-size and quartz content effect. Longer transport typically produces increased chemical weathering in contrast to what we observe here.

It is noteworthy that the terrace sediments, regardless of age, have lower CIA values than the adjacent modern river (Fig. 4), although the youngest terraces are the least weathered. This may imply that the modern river is in a state of disequilibrium and presently carries more weathered material than what has been carried in the geologic past. This observation is surprising because sediment stored in terraces has more time to become weathered than sediment recently derived from bedrock. Evidence from the Amazon Basin suggests that the amount of weathering in flood plains may be rather low (Bouchez *et al.*, 2012), but even if that were true we would not expect terraces to be less weathered than sediment in the adjacent river. We suggest the current highly weathered character of the modern river sediments reflects reworking of old weathered soils as a result of agriculture and/or deforestation, as noted in the Red River and Pearl River systems (Hu *et al.*, 2013; Wan *et al.*, 2015). Although settlement in northern Vietnam is known from ~11 ka population densities remained low and early communities were reliant on hunter-gatherer methods that did not greatly impact erosion (Rabett, 2012). However, rice cultivation spread to the Red River delta after ~3300 yr BP (Li *et al.*, 2006; Sweeney & McCouch, 2007; Fuller, 2011) and would have spread further south after that time. Plowing related to the spread in agriculture into the Song Gianh Basin may have disturbed old, strongly weathered soils that have been reworked into the modern river. This process should continue as the region becomes more densely settled today.

Sediment Provenance

Provenance of the bulk sediment can in part be constrained by the Sr and Nd isotopic values. Figure 5 shows that one Song Trac sample overlaps, with sediments from the Red Rivers (Liu *et al.*, 2007), suggesting erosion from similar bedrock types. It is clear that there is no sediment derivation from bedrock in the Central Highlands or other equivalent sources because the Song Gianh does not drain these areas. The high $^{87}Sr/^{86}Sr$ values may reflect higher chemical weathering and are not simply provenance driven, as shown by the lack of close correlation between the Sr and Nd isotopes (Fig. 5). Sr isotopes do not correlate closely with CIA or other weathering proxies either because there is also a provenance influence on these values. Nonetheless, Song Gianh samples largely have more negative ε_{Nd} values compared to the Red River or the basement rocks of the Kontum Massif, which is the closest characterized bedrock exposure known in the literature (Lan *et al.*, 2003). The data from the Red River and Kontum Massif may be interpreted as possibly representative of the average bedrock sources of Indochina. These data suggest that the Song Gianh is preferentially eroding more ancient crustal material (negative ε_{Nd}) than is typical of Indochina and may likely represent local compositional heterogeneity within the Indochina Block.

Variability in Sr isotopes in the upper reaches of the Song Gianh is followed by little variation downstream of the Mai Hoa confluence (Fig. 6). This pattern suggests that there is significant sediment addition upstream of that point and that there is little addition downstream. In particular, we note that the mainstream does not change substantially downstream of the Mai Hoa and Rao Tro confluences in terms of the Sr isotope compositions. This argues that these tributaries are not significant sources of sediment, although it is possible that influx from the Rao Tro is balanced by the more negative ε_{Nd} contributions from the southern tributaries. The $^{87}Sr/^{86}Sr$ values for the southern tributaries, however, argue against this possibility because their values lie quite close to the mainstream $^{87}Sr/^{86}Sr$ values. If there had been significant sediment input from the Rao Tro, in order to produce the $^{87}Sr/^{86}Sr$ values seen at the river mouth, very large quantities of sediment would have to be supplied from the southern tributaries to balance that addition. We consider this to be unlikely.

To help understand the different influences from individual tributaries Kolmogorov-Smirnov distances between samples were fed into a multidimensional scaling (MDS) algorithm to convert the data into a 'map' (Fig. 9) to display the relative distances (similarities) between the data (Vermeesch, 2013). The map shows most samples cluster on the right hand side of the plot reflecting a mixing of sources and similarity in the spectrum of U-Pb ages. A notable exception is the sample from Rao Tro (12061712), which has a narrow range of ages, mostly confined to the early Mesozoic. The upper reaches of the Rao Tro include granites of this age. The drainage of a nearby sample (12061711) from the middle reaches of the mainstream contains a much wider range of older zircon ages reflecting erosion of Triassic clastic sedimentary rocks. Granites also dominate in the southwest of the catchment, however samples from the Song Trac, which drains this area, show a mix with older zircons ages indicating that the Triassic sedimentary rocks from the upper reaches are mixing with eroded granite. Interestingly, the sample from the river mouth only contains a moderate component of the older ages diagnostic of Triassic clastic rocks and shows similarities to the sample from the Rao Tro in containing a larger proportion of granitic ages. This suggests that the granite-rich northeastern part of the catchment is producing a significant amount of the zircons.

This provenance model for at least the 63–250 μm fraction can be further tested by examination of the KDE plots. A wide variety of different spectra are found across the basin (Fig. 7) but the Rao Tro and mainstream river show distinctive similarity in having a prominent Indosinian ~250 Ma peak. The source of sediment to the river mouth is clearly more complicated because of the appearance of older zircon populations that are uncommon in the Rao Tro sample. Note that the river mouth does not plot directly with the Rao Tro sample in Figure 9. The ~1800 Ma peak observed in the upper reaches of the mainstream has disappeared in the river mouth sample, suggesting that substantial volumes of zircon-bearing sediment has been added to the mainstream, downstream of sample 12961711. Significant Rao Tro sediment flux to the mainstream is required to dilute the sediment from the upper reaches and generate the spectrum from the river mouth. Modest flux from the Song Nan may account for the smaller age peak at ~450 Ma seen at the river mouth. Likewise, major input from the Song Trac can be ruled out based on the lack of prominent peaks older than ~700 Ma in the river mouth sample but which are typical of the Song Trac.

We can further evaluate the input of sediment if we track the relative abundance of diagnostic zircon age populations downstream (Figs. 10A-E). Using the KDE diagrams we define the following as diagnostic populations, whose abundance can be used to understand sediment mixing: 100–380 Ma, 380–500 Ma, 700–1100 Ma, 1750–2200 Ma, and 2200–2800 Ma. Zircon populations not included in these groups are ubiquitous across samples or very rarely occur. We normalized to 100% the budgets of each sample, excluding zircon outside these five groups. Figure 10 demonstrates the evolution of the Song Gianh downstream, as well as the character of each of the major contributing tributaries. We note that there is an increase in the 100–380 Ma (Fig. 10A) zircon group from the upper reaches of the mainstream (20%) to the river mouth (50%). Low proportions of these 100–380 Ma grains in the southern tributaries preclude them from driving this trend. The Rao Tro could in part control this evolution because 100–380 Ma grains are prevalent in this tributary. This interpretation is consistent with the trends observed in the 1750–2200 Ma (Fig. 10D) and 2200–2800 Ma (Fig. 10E) plots, although contribution from the southern tributaries could explain the changes in these two groups downstream.

In contrast, the downstream increase in 380–500 Ma (Fig. 10B) and 700–1100 Ma (Fig. 10C) zircons would seem to argue for influx from the southern tributaries that are relatively rich in those zircon groups compared to the northern Rao Tro. This inconsistency suggests that our samples are not perfect representatives of the long-term flux of the river. Furthermore, we have not fully characterized all the smaller tributaries contributing to the mainstream, such as along the middle reaches. Nonetheless, based on the data that we do have and statistically supported by MDS, the Rao Tro or other rivers rich in 100–380 Ma zircon must be important contributors to the total zircon budget of the 63–250 μm fraction. In particular, the fact that the 100–380 Ma zircon group accounts for almost half of the total zircon at the river mouth is striking. We note that more analyzed grains (Pullen *et al.*, 2014) would provide a more accurate estimate of the frequency of each age population, but we are confident in that no analytical bias can account for the 20% to 50% change in 100–380 Ma zircons.

Fluvial Disequilibrium

If we accept the conclusions of the detrital zircon budget there is clearly a discrepancy between the results of our bulk sediment isotope and zircon data. The former suggests large-scale sediment generation in the upper reaches of the mainstream, while the latter argues for significant input from the Rao Tro (Figs. 6 and 10). One possible solution to this mismatch is that the bulk sediment is dominated by material finer than the analyzed zircon fraction (63–250 µm). Although possible, our bulk samples tended to be sandy and not contain large amounts of fine material. Alternatively it is conceivable that phases rich in Nd are travelling through the river at a different speed than the zircons, so that if erosion patterns changed in the past the two systems might not be in agreement in a river that is in disequilibrium. Garçon *et al.* (2014) showed that monazite strongly controls the Nd content of bulk sediments. Monazite however, has a high density similar to that of zircon, so it is questionable whether these two phases would be separated by hydrodynamic sorting, despite moderate differences in crystal morphology. Garçon *et al.* (2014) recognized the possible role of biotite, clay, and titanite as other Nd controlling phases. Consequently preferential sorting of biotite and clay compared to zircon may explain this discrepancy provided erosion patterns have changed in the past. Effectively, the lag time in zircon transport relative to micaceous Nd-rich phases is significant because of their morphology and density. Changing monsoon strength and settlement/farming patterns might be expected to change erosion patterns so that the river sediment compositions change on millennial timescales. Because these erosional signals travel at variable rates through the river depending on the mineral phase, different proxies yield contrasting results from the same sample. Although we have no independent control on how quickly the river composition has changed we anticipate that this would be on millennial and centennial time scales if climatic and anthropogenic processes are the primary controls on erosion.

Lithological variability between tributaries might be an additional reason why different provenance proxies tell different stories about the source of the sediment. It is possible that the upper reaches might contain many source rocks rich in Nd while the Rao Tro contains rocks rich in zircon, but we consider this less likely. Using Zr contents as a proxy for zircon abundance (Amidon *et al.*, 2005) would suggest that the Song Nan and parts of the Song Trac might be rich in zircon, not the Rao Tro (Fig. 2). It is possible that rocks rich in 100–380 Ma zircons but with mainstream type ε_{Nd} values are exposed in the slopes that provide sediment directly into the mainstream along its upper reaches and that these might dominate the sediment budget and explain the apparent mismatch. A combination of these factors may explain the contrasting provenance proxies of the Song Gianh.

The central and southern parts of the Song Gianh Basin expose large areas of karstic limestone (Fig. 2), which clearly do not contribute to the Sr and Nd isotopes or the zircon data presented here. The abundance of limestone in the southern parts of the Song

Trac could explain why little sediment is apparently produced from this tributary, despite locally heavy rainfall, high relief and steep slopes (Fig. 11). It is likely that much of the eroded carbonate is carried in solution, and so consequently cannot be resolved with the methods we employ here.

Exhumation History

With a central age of ~54.5 Ma, the Song Gianh Basin yields apatite ages that are broadly consistent with others in SE Asia (Fig. 8). Bedrock ages from the Kontum Massif and Khorat Plateau indicate average central ages at ~43 Ma suggesting that the Song Gianh has a typical Cenozoic exhumation history for the region. If we assume an average geothermal gradient of 25–30°C/km, then cooling from the base of the partial annealing zone (~110°C)(Green *et al.*, 1989) would be equivalent to 3.7–4.4 km of exhumation during the Cenozoic. Although central ages can be misleading if exhumation is slow, we lack sufficient number of grains to complete detailed modelling of the process and we assume a relatively simple exhumation history. If we calculate long-term exhumation rates, fission track data suggest rates of 67–81 mm/ky, equivalent to 610–737 t/yr of sediment flux.

Cosmogenic nuclide analysis indicates a denudation rate of ~30 mm/ky (Table 6), equivalent to only 273 t/yr discharge. This is somewhat lower than rates derived by fission track analysis. At the first-order level we can say that recent rates of exhumation of the siliciclastic bedrock are slower than the long-term average, so must therefore have decreased over the Cenozoic. This is consistent with thermal models for passive margin evolution with rapid erosion and cooling during the early stages of rifting and break-up followed by a slowing of rates during passive margin thermal subsidence (Gallagher *et al.*, 1995; Brown *et al.*, 2002; Persano *et al.*, 2002).

Constraints on the erosion history for the Song Gianh have implications for our understanding for how the adjacent Song Hong-Yinggehai Basin has been filled since its opening in the Eocene. This basin is typically considered to have been filled by flux from the Red River, and it has been noted that the volume of sediment in the basin far exceeds the amount of erosion within the modern Red River catchment (Clift *et al.*, 2006). This observation was used to argue for a paleo-Red River that far exceeds the modern catchment, in agreement with models that proposed the Red River as a former dominant drainage of East Asia prior to large-scale Tibetan Plateau uplift (Brookfield, 1998; Clark *et al.*, 2004). However, this approach ignored possible flux into the basin from Hainan Island and coastal Vietnam. While fission track studies confirm that erosion from Hainan has been modest (Shi *et al.*, 2011) and largely directed to the south (Clift & Sun, 2006), the same is not true of the coastal ranges of northern Vietnam. Hoang *et al.* (2010b) noted that clinoforms prograde from the Vietnamese coast into the basin indicating significant flux from Vietnam.

If 3.7–4.4 km of rock has been eroded over the 3500 km^2 of the Song Gianh then we can estimate the possible flux from the whole Annamite Range adjacent to the Song Hong-Yinggehai Basin, assuming that the Song Gianh is representative of the coastal area.

Our fission track data would estimate that 110,000–132,000 km^3 of rock have been eroded during the Cenozoic from the Song Gianh and equivalent rivers draining the Annamite Range. This would be equivalent to 132,000–158,000 km^3 of sediment produced, assuming an average porosity of ~20%, as previously applied to the Song Hong-Yinggehai Basin by Clift *et al.* (2006). Using an estimate of 750,000 km^3 for the total volume of the Song Hong-Yinggehai Basin, this implies that 17–21% of the total volume could be accounted for by erosion of coastal Vietnam. While significant, this is insufficient to completely account for the ~455,000 km^3 deficit between eroded and deposited volumes estimated by Clift *et al.* (2006). Our study suggests that drainage capture for the paleo-Red River must have been important but was perhaps less than previously envisaged (Brookfield, 1998; Clark *et al.*, 2004).

Controls on Erosion Patterns

Our study identifies the upper reaches of the Song Gianh mainstream as the primary source of sediment in the basin. The zircon U-Pb data suggest a potential important contribution from the Rao Tro in the recent geologic past, reflecting the slower transport of zircon downstream relative to other mineral phases. Because the basin is tectonically inactive we can exclude tectonism as a primary driver of erosion in this particular case. Previous studies have proposed that precipitation distribution can control the efficiency of erosion in fluvial systems (Hodges *et al.*, 2004; Bookhagen *et al.*, 2005b). Figure 11A shows that there is a two-fold increase of rainfall annually in the western side of the Song Gianh Basin than in the eastern floodplains. We note that the western part of the basin experiencing the greatest annual rainfall currently produces the bulk of the sediment delivered to the river mouth. This is despite the fact that unconsolidated sediment in the floodplains would be physically easier to remobilize. We also note that the southern Song Trac experiences heavy precipitation, but contains predominantly carbonate lithologies so does not produce siliciclastic sediment as quantified in this study. Hillslopes in the Song Gianh are also steepest in areas producing the most sediment (Fig. 11B) and contain the greatest local relief (Fig. 11C). Henck *et al.* (2011) suggest that erosion patterns in rivers experiencing low rock uplift rates (i.e., Yangtze River) are most strongly influenced by rainfall distribution in contrast to quickly uplifting regions (i.e., Salween and Mekong River basins) where patterns are controlled by local relief. While it is beyond the scope of this study to separate the relative influence of precipitation versus internal basin parameters, the coincidence of rainfall in areas of steeper slope and higher relief suggests correlation between these factors.

Terracing

Sedimentation in terraces reflects times when deposition was occurring as a result of the sediment load exceeding the carrying capacity of the river. This requires that the supply of sediment from the sources upstream was particularly high at times of valley filling. The subsequent incision of these sedimented valleys is not well dated but must come after the ages derived from the OSL dating. These ages represent the time of deposition, not terrace abandonment and incision. The highest and oldest terrace was constructed during the early Holocene (7.4–8.5 ka), which was a time of strong monsoon precipitation (Dykoski *et al.*, 2005; Hu *et al.*, 2008). Terracing of this age is also known in other monsoonal regions, such as the Western Himalaya (Bookhagen *et al.*, 2005b; Srivastava *et al.*, 2008). Stronger erosion often correlates with times of heavy rainfall, which massively increases the sediment supply to the river. Our observation of an Early Holocene terrace is consistent with earlier work suggesting rapid erosion and sediment delivery occurs during times of strong summer monsoon (Goodbred & Kuehl, 2000; Clift *et al.*, 2008a). Early Holocene strong rainfall is reconstructed both in South and East Asia (Enzel *et al.*, 1999; Dykoski *et al.*, 2005; Hu *et al.*, 2008) and we suggest that the landscape response to this climate change was the same in Southeast Asia, as previously demonstrated in the monsoonal Himalayas (Bookhagen *et al.*, 2005b). Because topographic relief is more subdued in northern Vietnam the importance of landsliding may be less in our study area compared to the South Asian examples (Dortch *et al.*, 2009), but the correlation between terracing and monsoon strength is nonetheless clear.

The younger, lower terraces observed in the Song Gianh do not clearly correlate with any known monsoon intensification, although there is some indication of a possible modest strengthening in recent times (Dykoski *et al.*, 2005). We suggest that it is much more likely that the increased sediment flux in the river was instead driven by the establishment of widespread agriculture. The impact of deforestation and farming, especially ploughing, is known to have generated large-scale soil erosion and sediment delivery to rivers both in Asia and worldwide (Syvitski *et al.*, 2005; Montgomery, 2007). The extremely young age of the terracing here suggests that these younger, lower terraces are a direct result of intensified soil erosion driven by human settlement of the basin, possibly in two phases, one medieval and one 18–19th century. We note that this disruption is too young and volumetrically too small to have greatly impacted the cosmogenic denudation rates reported here.

Conclusions

Our study highlights the utility of tectonically quiescent, monsoonally-controlled river basins for evaluating connections between the production, weathering, storage and flux of sediment. Study of a small basin moreover allows us to better characterize the erosion patterns throughout the catchment in a way that is impractical in larger river systems, where more complete sampling of all major source terranes is often impossible.

Multiple geochemical datasets from the Song Gianh indicate greatest production of siliciclastic sediment from the steep, wettest upper reaches of the basin and modest input from the tributaries downstream. However, detrital U-Pb zircon dating pinpoints large volumes of sediment flux from the northern Rao Tro tributary in a drier, lower relief part of the catchment. This apparent contrast between U-Pb zircon and bulk sediment Sr and Nd isotopic data requires that the Song Gianh River be in disequilibrium. Bulk sediment composition and flux are largely controlled by topographic and climatic processes. These are modified through the Holocene as a result of a weakening monsoon and are also influenced by sediment reworking triggered by human settlement/farming.

Together these result in large scale millennial to centennial scale changes in sediment provenance.

The modern river is marked by more chemically weathered sediment than found in the river terraces. Terrace construction occurred in three pulses, the Early Holocene, 550–320 yrs ago and since ~150 yr ago. We infer that the river was oversupplied by sediment at those times. The strong monsoon of the Early Holocene correlates with greater sediment supply and terrace construction here, as elsewhere in South Asia. Younger terraces are most likely a result of anthropogenic erosion related to agriculture because there is no evidence for a strengthening of the monsoon at that time.

Song Gianh exhumation rates derived from detrital apatite fission track and concurrent ^{10}Be-derived denudation rates ^{10}Be are largely consistent with accepted models for a tectonically quiescent passive margin, undergoing thermal subsidence. Exhumation is seen to slow through time since the start of the opening of the Song Hong-Yinggehai Basin in the Eocene. Our study highlights that although rivers along the margins of central Vietnam are small, the total sediment volumes fluxed from these catchments to the Song Hong-Yinggehai Basin are significant (132,000–158,000 km^3; 17–21% of the total). If one-fifth of the total sediment budget for the Song Hong-Yinggehai Basin is sourced from central Vietnam and not from the Red River, less significant drainage capture in the paleo-Red River is required compared to earlier models.

Acknowledgements

This work was supported by the Charles T. McCord Jr. chair in petroleum geology at LSU.

Conflict of Interest

No conflict of interest declared.

References

Adamiec, G. & Aitken, M.J. (1998) Dose Rate Conversion Factors: Update. *Ancient TL*, **16,** 37-50.

Aitken, M.J. (1998) *An Introduction to Optical Dating*. Oxford University Press, Oxford.

Amidon, W.H., Burbank, D.W. & Gehrels, G.E. (2005) U-Pb Zircon Ages as a Sediment Mixing Tracer in the Nepal Himalaya. *Earth and Planetary Science Letters*, **235,** 244-260.

Beaumont, C., Jamieson, R.A., Nguyen, M.H. & Lee, B. (2001) Himalayan Tectonics Explained by Extrusion of a Low-Viscosity Crustal Channel Coupled to Focused Surface Denudation. *Nature*, **414,** 738-742.

Bierman, P.R. & Steig, E. (1996) Estimating Rates of Denudation and Sediment Transport Using Cosmogenic Isotope Abundances in Sediment. *Earth Surface Processes and Landforms*, **21,** 125-139.

Blöthe, J.H., Munack, H., Korup, O., Fülling, A., Garzanti, E., Resentini, A. & Kubik, P.W. (2014) Late Quaternary Valley Infill and Dissection in the Indus River, Westerntibetan Plateau Margin. *Quaternary Science Reviews*, **94,** 102-119.

Böning, P., Brumsack, H.J., Böttcher, M.E., Schnetger, B., Kriete, C., Kallmeyer, J. & Borchers, S.L. (2004) Geochemistry of Peruvian near-Surface Sediments. *Geochimica et Cosmochimica Acta*, **68,** 4429-4451.

Böning, P., Brumsack, H.-J., Schnetger, B. & Grunwald, M. (2009) Trace Metal Signatures of Chilean Upwelling Sediments at ~36°S. *Marine Geology*, **259,** 112-121.

Bookhagen, B., Thiede, R.C. & Strecker, M.R. (2005a) Abnormal Monsoon Years and Their Control on Erosion and Sediment Flux in the High, Arid Northwest Himalaya. *Earth and Planetary Science Letters*, **231,** 131-146.

Bookhagen, B., Thiede, R.C. & Strecker, M.R. (2005b) Late Quaternary Intensified Monsoon Phases Control Landscape Evolution in the Northwest Himalaya. *Geology*, **33,** 149-152.

Bouchez, J., Gaillardet, J., Lupker, M., Louvat, P., France-Lanord, C., Maurice, L., Armijos, E. & Moquet, J.-S. (2012) Floodplains of Large Rivers: Weathering Reactors or Simple Silos? *Chemical Geology*, **332-333,** 166-184.

Bracken, L.J., Turnbull, L., Wainwright, J. & Bogaart, P. (2015) Sediment Connectivity: A Framework for Understanding Sediment Transfer at Multiple Scales. *Earth Surface Processes and Landforms*, **40,** 177–188.

Brennan, B.J. (2003) Beta Doses to Spherical Grains. *Radiation Measurements*, **37,** 299–303.

Brookfield, M.E. (1998) The Evolution of the Great River Systems of Southern Asia During the Cenozoic India-Asia Collision; Rivers Draining Southwards. *Geomorphology*, **22,** 285-312.

Brown, R.L., Summerfield, M. & Gleadow, A.J.W. (2002) Denudational History Along a Transect across the Drakensberg Escarpment of Southern Africa Derived from Apatite Fission Track Thermochronology. *Journal of Geophysical Research*, **107, 2350**.

Burbank, D.W., Blythe, A.E., Putkonen, J., Pratt-Sitaula, B., Gabet, E., Oskins, M., Barros, A. & Ojha, T.P. (2003) Decoupling of Erosion and Precipitation in the Himalayas. *Nature*, **426,** 652–655.

Carter, A. & Moss, S.J. (1999) Combined Detrital-Zircon Fission-Track and U-Pb Dating: A New Approach to Understanding Hinterland Evolution. *Geology*, **27,** 235–238.

Carter, A., Roques, D. & Bristow, C.S. (2000) Denudation History of Onshore Central Vietnam: Constraints on the Cenozoic Evolution of the Western Margin of the South China Sea. *Tectonophysics*, **322,** 265–277.

Carter, A., Roques, D., Bristow, C. & Kinny, P.D. (2001) Understanding Mesozoic Accretion in Southeast Asia: Significance of Triassic Thermotectonism (Indosinian Orogeny) in Vietnam. *Geology*, **29,** 211–214.

Carter, A. & Bristow, C.S. (2003) Linking Hinterland Evolution and Continental Basin Sedimentation by Using Detrital Zircon Thermochronology; a Study of the Khorat Plateau Basin, Eastern Thailand. *Basin Research*, **15,** 271–285.

Castelltort, S. & Van Den Driessche, J. (2003) How Plausible Are High-Frequency Sediment Supply-Driven Cycles in the Stratigraphic Record? *Sedimentary Geology*, **157,** 3–13.

Chen, J. & Jahn, B.-M. (1998) Crustal Evolution of Southeastern China: Nd and Sr Isotopic Evidence. *Tectonophysics*, **284,** 101–133.

Chmeleff, J., von Blanckenburg, F., Kossert, K. & Jakob, D. (2010) Determination of the 10be Half-Life by Multicollector Icp-Ms and Liquid Scintillation Counting. *Nuclear Instruments & Methods in Physics Research Section B- Beam Interactions with Materials and Atoms*, **268,** 192-199.

Clark, M.K., Schoenbohm, L.M., Royden, L.H., Whipple, K.X., Burchfiel, B.C., Zhang, X., Tang, W., Wang, E. & Chen, L. (2004) Surface Uplift, Tectonics, and Erosion of Eastern Tibet from Large-Scale Drainage Patterns. *Tectonics*, **23, TC1006**.

Clemens, S.C., Prell, W.L. & Sun, Y. (2010) Orbital-Scale Timing and Mechanisms Driving Late Pleistocene Indo-Asian Summer Monsoons: Reinterpreting Cave Speleothem ∂^{18}o. *Paleoceanography*, **25**.

Clift, P.D. (2006) Controls on the Erosion of Cenozoic Asia and the Flux of Clastic Sediment to the Ocean. *Earth and Planetary Science Letters*, **241,** 571-580.

Clift, P.D., Blusztajn, J. & Nguyen, D.A. (2006) Large-Scale Drainage Capture and Surface Uplift in Eastern Tibet-Sw China before 24 Ma Inferred from Sediments of the Hanoi Basin, Vietnam. *Geophysical Research Letters*, **33**.

Clift, P.D. & Sun, Z. (2006) The Sedimentary and Tectonic Evolution of the Yinggehai-Song Hong Basin and the Southern Hainan Margin, South China Sea; Implications for Tibetan Uplift and Monsoon Intensification. *Journal of Geophysical Research*, **111**.

Clift, P.D., Giosan, L., Blusztajn, J., Campbell, I.H., Allen, C.M., Pringle, M., Tabrez, A., Danish, M., Rabbani, M.M., Carter, A. & Lückge, A. (2008a) Holocene Erosion of the Lesser Himalaya Triggered by Intensified Summer Monsoon. *Geology*, **36,** 79–82.

Clift, P.D., Hoang, V.L., Hinton, R., Ellam, R., Hannigan, R., Tan, M.T. & Nguyen, D.A. (2008b) Evolving East Asian River Systems Reconstructed by Trace Element and Pb and Nd Isotope Variations in Modern and Ancient Red River-Song Hong Sediments. *Geochemistry Geophysics Geosystems*, **9**.

Clift, P.D., Vannucchi, P. & Phipps Morgan, J. (2009) Crustal Redistribution, Crust-Mantle Recycling and Phanerozoic Evolution of the Continental Crust. *Earth Science Reviews*, **97,** 80-104.

Derry, L.A. & France-Lanord, C. (1996) Neogene Himalayan Weathering History and River ^{87}sr/^{86}sr; Impact on the Marine Sr Record. *Earth and Planetary Science Letters*, **142,** 59-74.

Dewald, A., Heinze, S., Jolie, J., Zilges, A., Dunai, T., Rethemeyer, J., Melles, M., Staubwasser, M., Kuczewski, B., Richter, J., Radtke, U., von Blanckenburg, F. & Klein, M. (2013) Cologneams, a Dedicated Center for Accelerator Mass Spectrometry in Germany. *Nuclear Instruments and Methods in Physics Research Section B: Beam Interactions with Materials and Atoms*, **294,** 18-23.

Dortch, J., Owen, L.A., Haneberg, W.C., Caffee, M.W., Dietsch, C. & Kamp, D.U. (2009) Nature and Timing of Large-Landslides in the Himalaya and Transhimalaya of Northern India. *Quaternary Science Reviews*, **28,** 1037–1054.

Dortch, J.M., Dietsch, C., Owen, L.A., Caffee, M.W. & Ruppert, K. (2011) Episodic Fluvial Incision of Rivers and Rock Uplift in the Himalaya and Transhimalaya. *Journal of the Geological Society*, **168,** 783-804.

Duan, F., Wang, Y., Shen, C.-C., Wang, Y., Cheng, H., Wu, C.-C., Hu, H.-M., Kong, X., Liu, D. & Zhao, K. (2014) Evidence for Solar Cycles in a Late Holocene Speleothem Record from Dongge Cave, China. *Nature Scientific Reports*, **4**.

Dunai, T.J. (2000) Scaling Factors for Production Rates of in Situ Produced Cosmogenic Nuclides: A Critical Reevaluation. *Earth and Planetary Science Letters*, **176,** 157-169.

Dykoski, C.A., Edwards, R.L., Cheng, H., Yuan, D., Cai, Y., Zhang, M., Lin, Y., Qing, J., An, Z. & Revenaugh, J. (2005) A High-Resolution, Absolute-Dated Holocene and Deglacial Asian Monsoon Record from Dongge Cave, China. *Earth and Planetary Science Letters*, **233,** 71-86.

Enzel, Y., Ely, L.L., Mishra, S., Ramesh, R., Amit, R., Lazar, B., Rajaguru, S.N., Baker, V.R. & Sandle, A. (1999) High-Resolution Holocene Environmental Changes in the Thar Desert, Northwestern India. *Science*, **284,** 125–128.

Franke, D., Savva, D., Pubellier, M., Steuer, S., Mouly, B., Auxietre, J.-L., Meresse, F. & Chamot-Rooke, N. (2014) The Final Rifting Evolution in the South China Sea. *Marine and Petroleum Geology*, **58B,** 704–720.

Fromaget, J., Saurin, E. & Fontaine, H. (1971) Geological Map of Vietnam, Cambodia and Laos, National Geographic Directorate of Vietnam. Dalat.

Fuchs, M. & Owen, L.A. (2008) Luminescence Dating of Glacial and Associated Sediments: Review, Recommendations and Future Directions. *Boreas*, **37,** 636-659.

Fuller, D. (2011) Pathways to Asian Civilizations: Tracing the Origins and Spread of Rice and Rice Cultures. *Rice*, **4,** 78-92.

Galbraith, R.F. & Roberts, R.G. (2012) Statistical Aspects of Equivalent Dose and Error Calculation and Display in Osl Dating: An Overview and Some Recommendations. *Quaternary Geochronology*, **11,** 1-27.

Gallagher, K., Hawkesworth, C.J. & Mantovani, M.S.M. (1995) Denudation, Fission Track Analysis and the Long-Term Evolution of Passive Margin Topography: Application to the S.E. Brazilian Margin. *Journal of South American Earth Sciences*, **8,** 65-77.

Garçon, M., Chauvel, C., France-Lanord, C., Limonta, M. & Garzanti, E. (2014) Which Minerals Control the Nd–Hf–Sr–Pb Isotopic Compositions of River Sediments? *Chemical Geology*, **364,** 42–55.

Goldstein, S.L., O'Nions, R.K. & Hamilton, P.J. (1984) A Sm-Nd Isotopic Study of Atmospheric Dusts and Particulates from Major River Systems. *Earth and Planetary Science Letters*, **70,** 221-236.

Goodbred, S.L. & Kuehl, S.A. (2000) Enormous Ganges-Brahmaputra Sediment Discharge During Strengthened Early Holocene Monsoon. *Geology (Boulder)*, **28,** 1083-1086.

Granger, D.E. & Riebe, C.S. (2007) Cosmogenic Nuclides in Weathering and Erosion. In: *Surface and Ground Water, Weathering, and Soils* (Ed. by J. I. Drever), *Treatise on Geochemistry*, **5**. Elsevier, London.

Green, P.F., Duddy, I.R., Laslett, G.M., Hegarty, K.A., Gleadow, A.J.W. & Lovering, J.F. (1989) Thermal Annealing of Fission Tracks in Apatite; 4, Quantitative Modelling Techniques and Extension to Geological Timescales. *Chemical Geology; Isotope Geoscience Section*, **79,** 155-182.

Guerin, G., Mercier, N. & Adamiec, G. (2011) Dose Rate Conversion Factors: Update. *Ancient Thermo Luminesence*, **29,** 5-8.

Henck, A.C., Huntington, K.W., Stone, J.O., Montgomery, D.R. & Hallet, B. (2011) Spatial Controls on Erosion in the Three Rivers Region, Southeastern Tibet and Southwestern China. *Earth and Planetary Science Letters*, **303,** 71-83.

Hoa, T.T., Anh, T.T., Phuong, N.T., Dung, P.T., Anh, T.V., Izokh, A.E., Borisenko, A.S., Lan, C.Y., Chung, S.L. & Lo, C.H. (2008) Permo-Triassic Intermediate–Felsic Magmatism of the Truong Son Belt, Eastern Margin of Indochina. *Comptes Rendus Geoscience*, **340,** 112–126.

Hoang, L.V., Clift, P.D., Mark, D., Zheng, H. & Tan, M.T. (2010a) Ar-Ar Muscovite Dating as a Constraint on Sediment Provenance and Erosion Processes in the Red and Yangtze River Systems, Se Asia. *Earth and Planetary Science Letters*, **295,** 379–389.

Hoang, L.V., Clift, P.D., Schwab, A.M., Huuse, M., Nguyen, D.A. & Zhen, S. (2010b) Large-Scale Erosional Response of Se Asia to Monsoon Evolution Reconstructed from Sedimentary Records of the Song Hong-Yinggehai and Qiongdongnan Basins, South China Sea. In: *Monsoon Evolution and Tectonic-Climate Linkage in Asia* (Ed. by P. D. Clift, R. Tada & H. Zheng), *Special Publication*, **342**, 219–244. Geological Society, London.

Hoang, N., Flower, M.F.J. & Carlson, R.W. (1996) Major, Trace Element, and Isotopic Compositions of Vietnamese Basalts: Interaction of Hydrous Em1-Rich Asthenopshere with Thinned Eurasian Lithosphere. *Geochimica et Cosmochimica Acta*, **60,** 4329–4351.

Hodges, K.V., Wobus, C., Ruhl, K., Schildgen, T. & Whipple, K. (2004) Quaternary Deformation, River Steepening, and Heavy Precipitation at the Front of the Higher Himalayan Ranges. *Earth and Planetary Science Letters*, **220,** 379-389.

Hu, C., Henderson, G.M., Huang, J., Xie, S., Sun, Y. & Johnson, K.R. (2008) Quantification of Holocene Asian Monsoon Rainfall from Spatially Separated Cave Records. *Earth and Planetary Science Letters*, **266,** 221–232.

Hu, D., Clift, P.D., Böning, P., Hannigan, R., Hillier, S., Blusztajn, J., Wang, S. & Fuller, D.Q. (2013) Holocene Evolution in Weathering and Erosion Patterns in the Pearl River Delta. *Geochemistry Geophysics Geosystems*, **14**.

Hurford, A. (1990) Standardization of Fission Track Dating Calibration: Recommendation by the Fission Track Working Group of the Iugs Subcommission on Geochronology. *Chemical Geology*, **80,** 177–178.

Jacobsen, S.B. & Wasserburg, G.J. (1980) Sm-Nd Isotopic Evolution of Chondrites. *Earth and Planetary Science Letters* **50,** 139-155.

Kirby, E. & Ouimet, W. (2011) Tectonic Geomorphology Along the Eastern Margin of Tibet: Insights into the Pattern and Processes of Active Deformation Adjacent to the Sichuan Basin. In: *Growth and Collapse of the Tibetan Plateau* (Ed. by R. Gloaguen & L. Ratschbacher), *Special Publications*, **353**, 165-188. Geological Society, London.

Korschinek, G., Bergmaier, A., Faestermann, T., Gerstmann, U.C., Knie, K., Rugel, G., Wallner, A., Dillmann, I., Dollinger, G., von Gostomski, C.L., Kossert, K., Maiti, M., Poutivtsev, M. & Remmert, A. (2010) A New Value for the Half-Life of 10be by Heavy-Ion Elastic Recoil Detection and Liquid Scintillation Counting., . *Nuclear Instruments & Methods in Physics Research Section B - Beam Interactions with Materials and Atoms* **268,** 187-191.

Lan, C.-Y., Chung, S.-L., Trinh, V.L., Lo, C.-H., Lee, T.-Y., Mertzman, S.A. & Shen, J.J.-S. (2003) Geochemical and Sr–Nd Isotopic Constraints from the Kontum Massif, Central Vietnam on the Crustal Evolution of the Indochina Block. *Precambrian Research*, **122,** 7-27.

Lepvrier, C., Maluski, H., Vu, V.T., Leyreloup, A., Phan, T.T. & Vuong, N.V. (2004) The Early Triassic Indosinian Orogeny in Vietnam (Truong Son Belt and Kontum Massif); Implications for the Geodynamic Evolution of Indochina. *Tectonophysics*, **393,** 87-118.

Li, X.H. (1999) U-Pb Zircon Ages of Granites from the Southern Margin of the Yangtze Block; Timing of Neoproterozoic Jinning; Orogeny in Se China and Implications for Rodinia Assembly. *Precambrian Research*, **97,** 43–57.

Li, Z., Saito, Y., Matsumoto, E., Wang, Y., Tanabe, S. & Vu, Q.L. (2006) Climate Change and Human Impact on the Song Hong (Red River) Delta, Vietnam, During the Holocene. *Quaternary International*, **144,** 4–28.

Li, Z.X., Li, X.H., Wartho, J.A., Clark, C., Li, W.X., Zhang, C.L. & Bao, C. (2010) Magmatic and Metamorphic Events During the Early Paleozoic Wuyi-Yunkai Orogeny, Southeastern South China: New Age Constraints and Pressure-Temperature Conditions. *Geological Society of America Bulletin*, **122,** 772–793.

Liu, Z., Colin, C., Huang, W., Le, K.P., Tong, S., Chen, Z. & Trentesaux, A. (2007) Climatic and Tectonic Controls on Weathering in South China and Indochina Peninsula: Clay Mineralogical and Geochemical Investigations from the Pearl, Red, and Mekong Drainage Basins. *Geochemistry Geophysics Geosystems*, **8, Q05005**.

Michel, G.W., Yu, Y.Q., Zhu, S.Y., Christoph, R., Becker, M., Reinhart, E., Simons, W., Ambrosius, B., Vigny, C., Chamot-Rooke, N., Le-Pichon, X., Morgan, P. & Matheussen, S. (2001) Crustal Motion and Block Behaviour in Se-Asia from Gps Measurements. *Earth and Planetary Science Letters*, **187**.

Mohtadi, M., Oppo, D.W., Steinke, S., Stuut, J.-B.W., Pol-Holz, R.D., Hebbeln, D. & Lückge, A. (2011) Glacial to Holocene Swings of the Australian-Indonesian Monsoon. *Nature Geoscience*, **4,** 540-544.

Montgomery, D.R. (2007) *Dirt: The Erosion of Civilizations*. University of California Press, Berkeley.

Murray, A.S. & Wintle, A.G. (2000) Luminescence Dating of Quartz Using an Improved Single-Aliquot Regenerative-Dose Protocol. *Radiation Measurements*, **32,** 57-72.

Nagy, E.A., Schärer, U. & Nguyen, T.M. (2000) Oligo-Miocene Granitic Magmatism in Central Vietnam and Implications for Continental Deformation in Indochina. *Terra Nova*, **12,** 67–76.

Nagy, E.A., Maluski, H., Lepvrier, C., Schärer, U., Phan, T.T., Leyreloup, A. & Vu, V.T. (2001) Geodynamic Significance of the Kontum Massif in Central Vietnam; Composite 40ar/39ar and U-Pb Ages from Paleozoic to Triassic. *Journal of Geology*, **109,** 755–770.

Nesbitt, H.W., Markovics, G. & Price, R.C. (1980) Chemical Processes Affecting Alkalis and Alkaline Earths During Continental Weathering. *Geochimica et Cosmochimica Acta*, **44,** 1659–1666.

Pearce, N.J.G., Perkins, W.T., Westgate, J.A., Gorton, M.P., Jackson, S.E., Neal, C.R. & Chenery, S.P. (1997) A Compilation of New and Published Major and Trace Element Data for Nist Srm 610 and Nist Srm 612 Glass Reference Materials. *Geostandards Newsletter-the Journal of Geostandards and Geoanalysis*, **21,** 115-144.

Persano, C., Stuart, F.M., Bishop, P. & Barfod, D.N. (2002) Apatite (U–Th)/He Age Constraints on the Development of the Great Escarpment on the Southeastern Australian Passive Margin. *Earth and Planetary Science Letters*, **200,** 79–90.

Pratt-Sitaula, B., Burbank, D.W., Heimsath, A. & Ojha, T. (2004) Landscape Disequilibrium on 1000-10,000 Year Scales Marsyandi River, Nepal, Central Himalaya. *Geomorphology*, **58,** 223-241.

Prescott, J.R. & Hutton, J.T. (1994) Cosmic Ray Contributions to Dose Rates for Luminescence and Esr Dating: Large Depths and Long-Term Time Variations. *Radiation Measurements*, **23,** 497-500.

Pullen, A., Ibanez-Mejia, M., Gehrels, G.E., Ibanez-Mejia, J.C. & Pecha, M. (2014) What Happens When N¼ 1000? Creating Large-N Geochronological Datasets with La-Icp-Ms for Geologic Investigations. *Journal of Analytical Atomic Spectrometry*, **29,** 971-980.

Rabett, R.J. (2012) *Human Adaptation in the Asian Palaeolithic*. Cambridge University Press.

Raczek, I., Jochum, K.P. & Hofmann, A.W. (2003) Neodymium and Strontium Isotope Data for Usgs Reference Materials Bcr-1, Bcr-2, Bhvo-1, Bhvo-2, Agv-1, Agv-2, Gsp-1, Gsp-2 and Eight Mpi-Ding Reference Glasses. *Geostandards Newsletter*, **27,** 173–179.

Rangin, C., Klein, M., Roques, D., Le Pichon, X. & Trong, L.V. (1995) The Red River Fault System in the Tonkin Gulf, Vietnam. *Tectonophysics*, **243,** 209–222.

Rittenour, T.M. (2008) Luminescence Dating of Fluvial Deposits: Applications to Geomorphic, Palaeoseismic and Archaeological Research. *Boreas* **37,** 613-635.

Roller, S., Wittmann, H., Kastowski, M. & Hinderer, M. (2012) Erosion of the Rwenzori Mountains, East African Rift, from in Situ-Produced Cosmogenic 10be. *Journal of Geophysical Research*, **117**.

Ru, K. & Pigott, J.D. (1986) Episodic Rifting and Subsidence in the South China Sea. *AAPG Bulletin*, **70,** 1136–1155.

Shi, X., Kohn, B., Spencer, S., Guo, X., Li, Y., Yang, X., Shi, H. & Gleadow, A. (2011) Cenozoic Denudation History of Southern Hainan Island, South China Sea: Constraints from Low Temperature Thermochronology. *Tectonophysics*, **504,** 100–115.

Simpson, G. & Castelltort, S. (2012) Model Shows That Rivers Transmit High-Frequency Climate Cycles to the Sedimentary Record. *Geology*, **40,** 1131–1134.

Singh, M., Sharma, M. & Tobschall, H.J. (2005) Weathering of the Ganga Alluvial Plain, Northern India: Implications from Fluvial Geochemistry of the Gomati River. *Applied Geochemistry*, **20,** 1–21.

Sláma, J., Košler, J., Condon, D.J., Crowley, J.L., Gerdes, A., Hanchar, J.M., Horstwood, M.S.A., Morris, G.A., Nasdala, L., Norberg, N., Schaltegger, U., Schoene, B., Tubrett, M.N. & Whitehouse, M.J. (2008) Plezovice Zircon a New Natural Reference Material for U–Pb and Hf Isotopic Microanalysis. *Chemical Geology*, **249,** 1-35.

Srivastava, P., Tripathi, J.K., Islam, R. & Jaiswal, M.K. (2008) Fashion and Phases of Late Pleistocene Aggradation and Incision in Alaknanda River, Western Himalaya India. *Quaternary Research*, **70,** 68–80.

Sweeney, M. & McCouch, S. (2007) The Complex History of the Domestication of Rice. *Annals of Botany*, **100,** 951-957.

Syvitski, J.P.M., C., V., Kettner, A.J. & Green, P. (2005) Impact of Humans on the Flux of Terrestrial Sediment to the Global Coastal Ocean. *Science*, **308,** 376-380.

Tanaka, T., Togashi, S., Kamioka, H., Amakawa, H., Kagami, H., Hamamoto, T., Yuhara, M., Orihashi, Y., Yoneda, S., Shimizu, H., Kunimaru, T., Takahashi, K., Yanagi, T., Nakano, T., Fujimaki, H., Shinjo, R., Asahara, Y., Tanimizu,

M. & Dragusanu, C. (2000) Jndi-1: A Neodymium Isotopic Reference in Consistency with Lajolla Neodymium. *Chemical Geology*, **168,** 279–281.

Thirlwall, M.F. (1991) Long-Term Reproducibility of Multicollector Sr and Nd Isotope Ratio Analysis. *Chemical Geology: Isotope Geoscience section*, **94,** 85-104.

Tu, K., Flower, M.F.J., Carlson, R.W., Zhang, M. & Xie, G. (1991) Sr, Nd, and Pb Isotopic Compositions of Hainan Basalts (South China): Implications for a Subcontinental Lithosphere Dupal Source. *Geology*, **19,** 567–569.

Vermeesch, P. (2004) How Many Grains Are Needed for a Provenance Study? *Earth and Planetary Science Letters*, **224,** 351–441.

Vermeesch, P. (2013) Multi-Sample Comparison of Detrital Age Distributions. *Chemical Geology*, **341,** 140–146.

von Blanckenburg, F., Hewawasam, T. & Kubik, P. (2004) Cosmogenic Nuclide Evidence for Low Weathering and Denudation in the Wet Tropical Highlands of Sri Lanka. *Journal of Geophysical Research*, **109**.

von Blanckenburg, F. (2005) The Control Mechanisms of Erosion and Weathering at Basin Scale from Cosmogenic Nuclides in River Sediment. *Earth and Planetary Science Letters*, **237,** 462-479.

von Huene, R. & Scholl, D.W. (1991) Observations at Convergent Margins Concerning Sediment Subduction, Subduction Erosion, and the Growth of Continental Crust. *Reviews of Geophysics*, **29,** 279-316.

Wan, S., Toucanne, S., Clift, P.D., Zhao, D., Bayon, G., Yu, Z., Cai, G., Yin, X., Révillon, S., Wang, D., Li, A. & Li, T. (2015) Human Impact Overwhelms Long-Term Climate Control of Weathering and Erosion in Southwest China. *Geology*.

Wittmann, H., von Blanckenburg, F., Maurice, L., Guyot, J.L., Filizola, N. & Kubik, P.W. (2011) Sediment Production and Delivery in the Amazon River Basin Quantified by in Situ—Produced Cosmogenic Nuclides and Recent River Loads. *Geological Society of America Bulletin*, **123,** 934–950.

Wyshnytzky, C.E., Rittenour, T.M., Nelson, M.S. & Thackray, G. (2015) Luminescence Dating of Late Pleistocene Proximal Glacial Sediments in the Olympic Mountains, Washington. *Quaternary International*, **362,** 116–123.

Yancheva, G., Nowaczyk, N.R., Mingram, J., Dulski, P., Schettler, G., Negendank, J.F.W., Liu, J., Sigman, D.M., Peterson, L.C. & Haug, G.H. (2007) Influence of the Intertropical Convergence Zone on the East Asian Monsoon. *Nature*, **445,** 74-77.

Yang, S., Zhang, F. & Wang, Z. (2012) Grain Size Distribution and Age Population of Detrital Zircons from the Changjiang (Yangtze) River System, China. *Chemical Geology*, **296-297,** 26-38.

Zhong, Z., Wang, L., Xia, B., Dong, W., Sun, Z. & Shi, Y. (2004) The Dynamics of Yinggehai Basin Formation and Its Tectonic Significance. *Acta Geologica Sinica*, **78,** 302-309.

Zuchiewicz, W., Nguyen, Q.C., Zasadni, J. & Nguyen, T.Y. (2013) Late Cenozoic Tectonics of the Red River Fault Zone, Vietnam, in the Light of Geomorphic Studies. *Journal of Geodynamics*, **69,** 11– 30.

Tables

Table 1. Location of river sediment and terrace samples analyzed during this study.

Table 2. Major and trace element compositions of river and terrace samples from the Song Gianh. Major element concentrations are in weight %, whereas trace elements are in ppm.

Table 3. Sr and Nd isotope compositions of samples taken from the modern Song Gianh basin.

Table 4. Analytical data for U-Pb dating of detrital zircon grains from the river sediment samples.

Table 5. Results of apatite fission track analysis.

Table 6. *In situ* ^{10}Be cosmogenic nuclide data. Second line of table shows rates corrected for carbonate exposure.

Table 7. Data and depositional ages from the OSL analysis of terrace sediments.

Figure Captions

Figure 1. Study location in reference to southeast Asia. (A) Regional geographic map of southeast Asia outlining Song Gianh basin (black polygon) and political border of Vietnam (gray line), AR = Annamite Range, CH = Central Highlands, H = Hainan, KM = Kontum Massif, KP = Khorat Plateau, RR = Red River, and SH-Y = Song Hong-Yinggehai Basin; (B) Shaded topographic map derived from void-filled SRTM90 v.4.1 digital elevation model (DEM) grid data (http://www.cgiar-csi.org/data) with delineated stream network (black line). Sample locations denoted by open circles.

Figure 2. Geological map of the Song Gianh basin showing the simplified geology overlain with the modern drainage network. Map is redrawn from Fromaget (1971).

Figure 3. Plot of Chemical Index of Alteration (CIA) versus silica content of the samples considered in this study. SiO_2 is used as a proxy for the quartz sand content. Fields showing fine grained material from the Pearl and Mekong Rivers are from Liu *et al.* (2007). Red River field includes fine grained sediments from this source and sandy sediment analyzed by Clift *et al.* (2008b). Lack of SiO_2 data precludes plotting terraces here.

Figure 4. Downstream evolution in CIA within the Song Gianh basin. Note the general decrease in CIA downstream and that the terrace sediments are generally lower in CIA compared to the modern river at that location. Terrace samples are from the mainstream, except for those labeled ST that are from the Song Trac. Ages in parentheses are OSL ages.

Figure 5. Cross plot of Sr versus Nd isotope compositions for the Song Gianh compared with river sediments measured from the Red, Mekong and Pearl Rivers by Liu *et al.* (2007) and Clift *et al.* (2008b). Basement samples from central and northern Vietnam are from Hoa *et al.* (2008), Lan *et al.* (2003) and Nagy *et al.* (2000). Central Highland volcanic rocks are compiled from various sources from Hoang *et al.* (1996).

Figure 6. Plots showing the downstream evolution in (A) Sr and (B) ε_{Nd} isotope compositions within the Song Gianh. Note that the mainstream stabilizes in composition in its middle reaches and does not seem much affected by flow from either of the northern tributaries. Error bars smaller than symbol size for Sr in Fig. 6A and propagated error for ε_{Nd} in Fig. 6B are gray brackets.

Figure 7. KDE plots of U-Pb zircon dates from Song Gianh sediments, compared with bed rock data from the Kontum Massif from Nagy *et al.* (2001), and the Khorat Plateau from Carter & Moss (1999) and Carter & Bristow (2003), and the Vietnamese Central Highlands from Carter *et al.* (2001).

Figure 8. (A) Radial plot of apatite fission track data from the Song Trac tributary showing an approximately single population clustered around a central age of 54 Ma. (B) A KDE plot of the apatite fission track data.

Figure 9. Multidimensional scaling (MDS) plot showing the Kolmogorov-Smirnov distances between sample zircon age spectra, following the method of Vermeesch (2013).

Figure 10. Plots showing downstream variation in specific age populations (A-E) within the mainstream (black dots linked by a solid line) and major tributaries showing how addition of sediment from the tributaries acts (or not) to influencing the bulk composition downstream of the confluence.

Figure 11. Annual rainfall, local mean slope, and local relief maps for the Song Gianh basin. (A) Annual rainfall values derived from TRMM 3B42 data from 1998–2009 at 0.25° × 0.25° resolution (http://www.geog.ucsb.edu/wbodo/TRMM/); (B) Average mean local slope calculated from void-filled SRTM90 DEM for Song Gianh basin. Black lines and open circles denote stream network and sample locations, respectively; (C) Mean local relief map, expressed as maximum elevation difference, using a moving ~1 km radius window on SRTM90 data.

Supporting Figure Captions:

Supplementary Figure 1. OSL dose rate diagrams for the five terrace samples analyzed with this study.

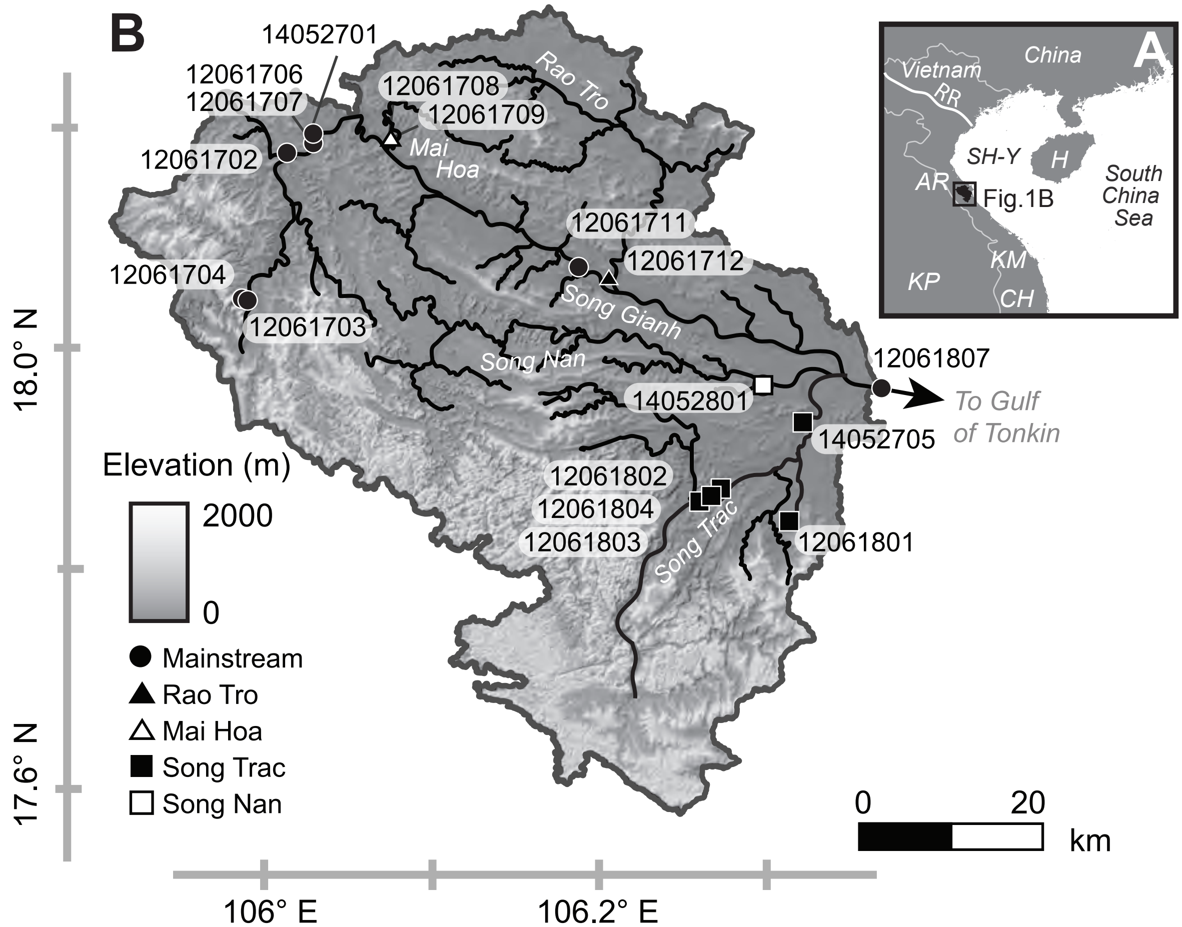
B
14052701
12061706
12061707
12061708
12061709
Rao Tro
Mai
Hoa
12061702
12061711
12061712
12061704
12061703
Song Gianh
Song Nan
12061807
14052801
To Gulf
of Tonkin
14052705
Elevation (m)
2000
0
12061802
12061804
12061803
Song Trac
12061801
Mainstream
Rao Tro
Mai Hoa
Song Trac
Song Nan
0
20
km
18.0° N
17.6° N
106° E
106.2° E
A
China
Vietnam
RR
SH-Y
H
AR
Fig.1B
South
China
Sea
KM
KP
CH

Figure 1

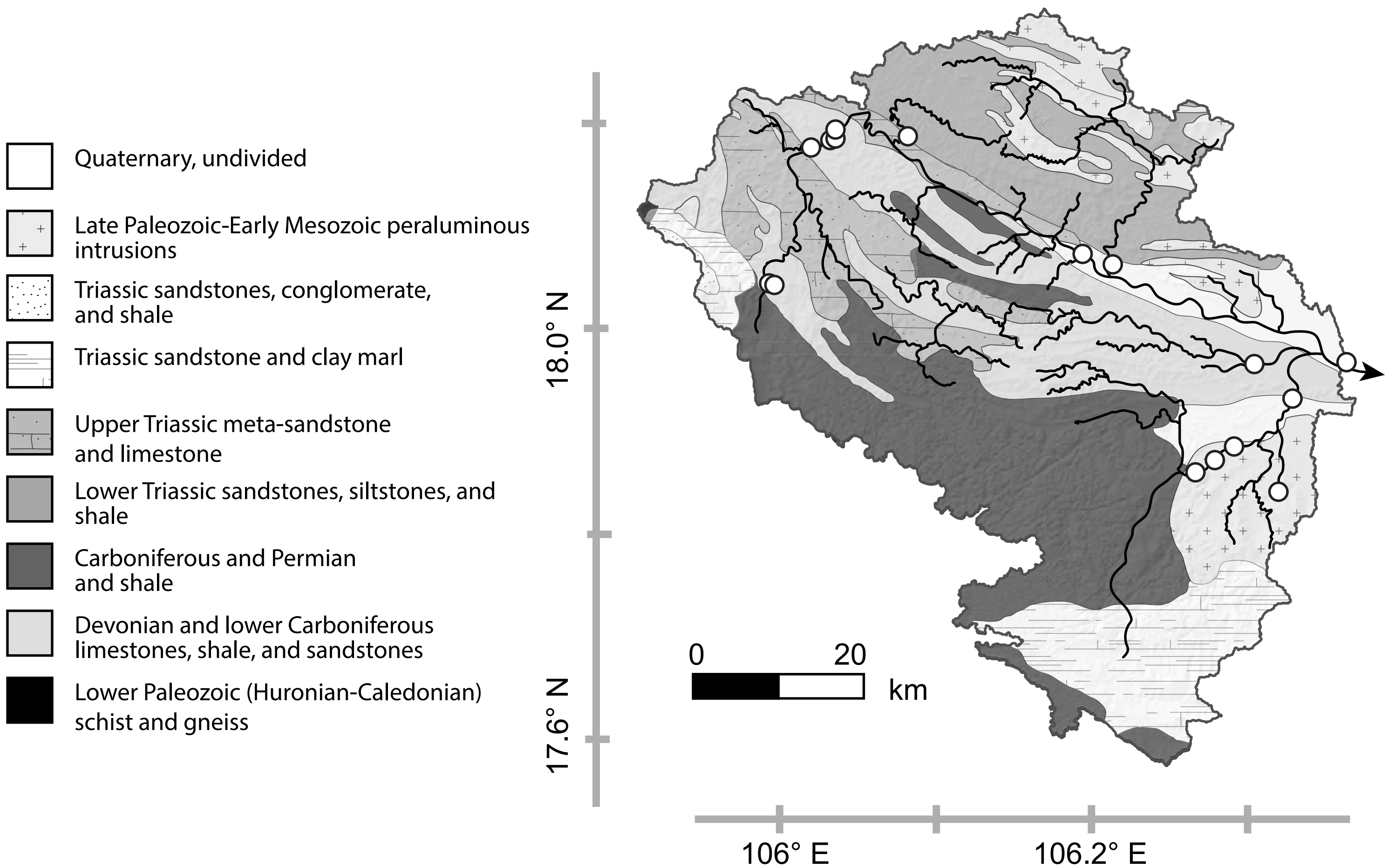

Quaternary, undivided
Late Paleozoic-Early Mesozoic peraluminous intrusions
Triassic sandstones, conglomerate, and shale
Triassic sandstone and clay marl
Upper Triassic meta-sandstone and limestone
Lower Triassic sandstones, siltstones, and shale
Carboniferous and Permian and shale
Devonian and lower Carboniferous limestones, shale, and sandstones
Lower Paleozoic (Huronian-Caledonian) schist and gneiss
18.0° N
17.6° N
0
20
km
106° E
106.2° E

Figure 2

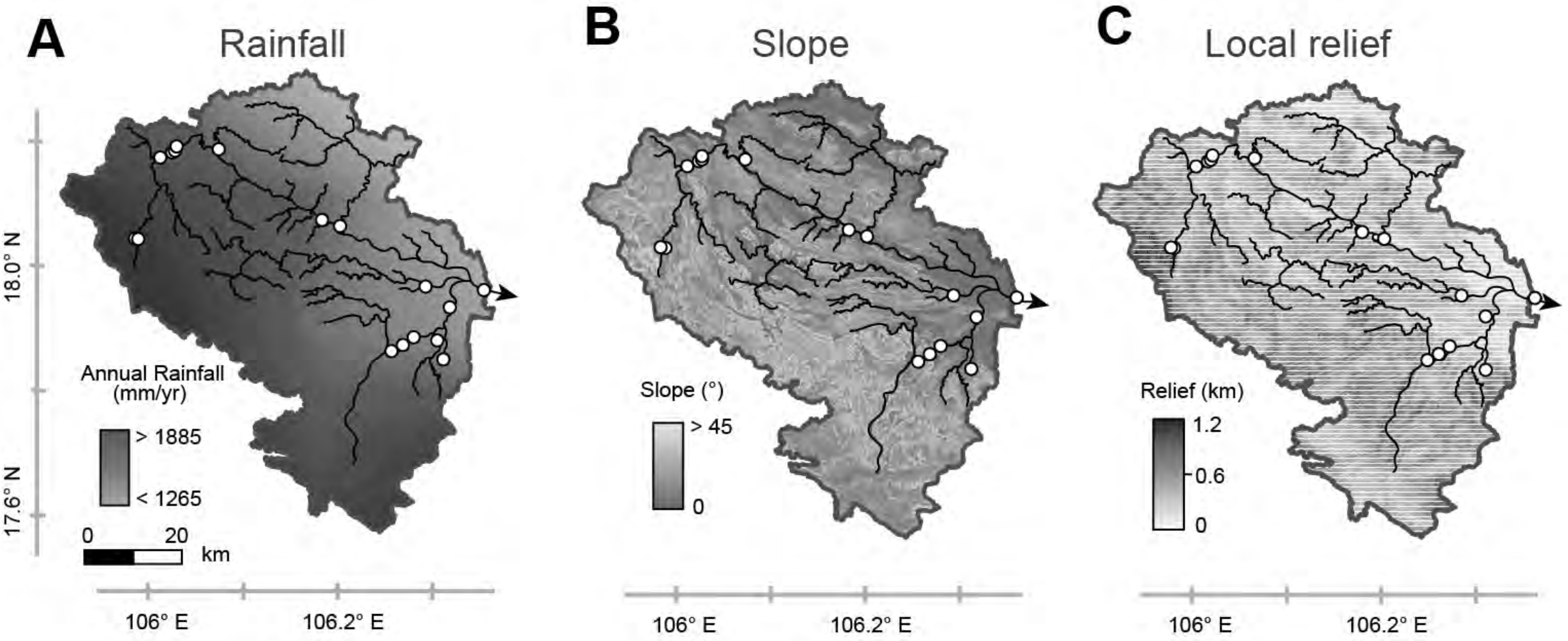
A
Rainfall
B
Slope
C
Local relief
18.0° N
17.6° N
Annual Rainfall
(mm/yr)
> 1885
< 1265
0
20
km
Slope (°)
> 45
0
Relief (km)
1.2
0.6
0
106° E
106.2° E
106° E
106.2° E
106° E
106.2° E

Figure 3

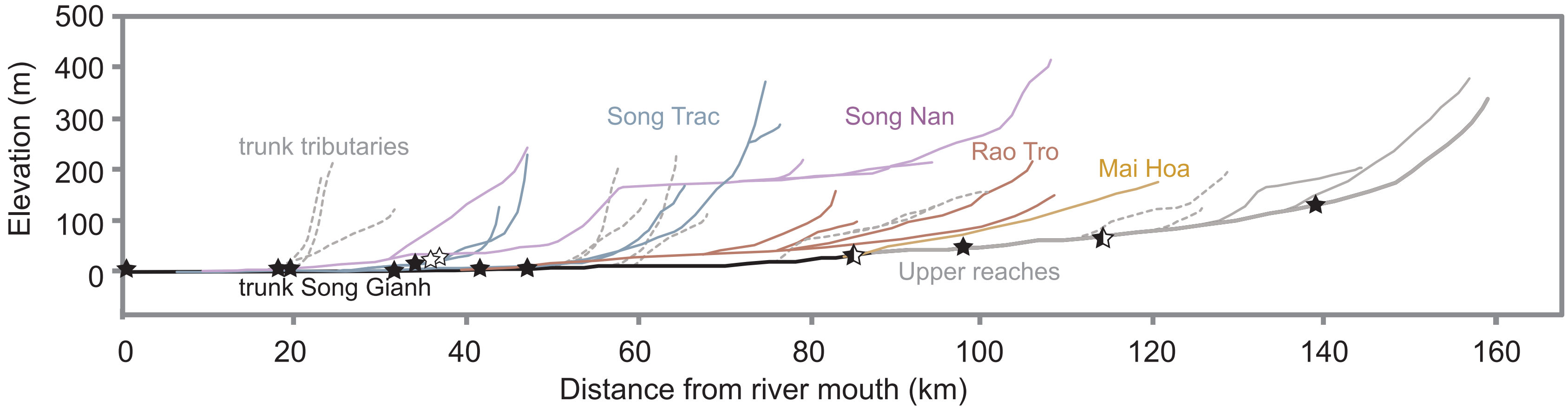

500
400
300
200
100
0
Elevation (m)
0
20
40
60
80
100
120
140
160
Distance from river mouth (km)
trunk tributaries
Song Trac
Song Nan
Rao Tro
Mai Hoa
Upper reaches
trunk Song Gianh

Figure 4

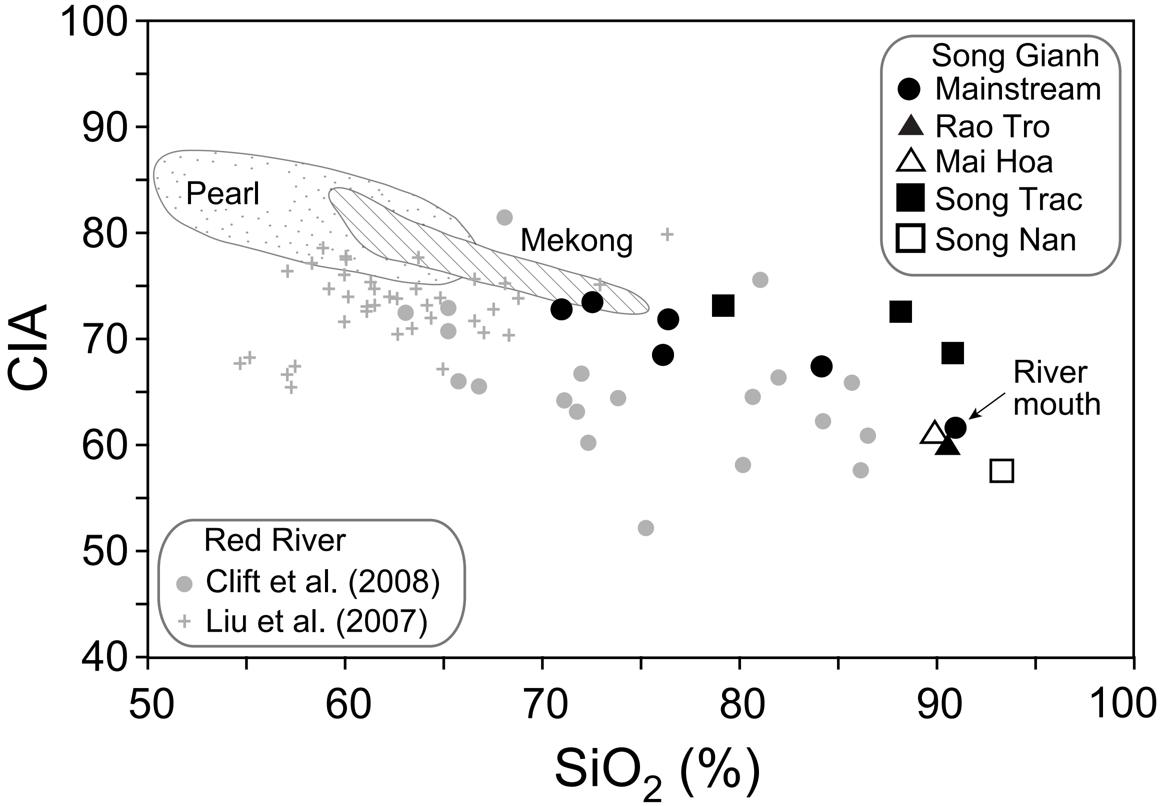

100
90
80
70
60
50
40
CIA
50
60
70
80
90
100
SiO2 (%)
Pearl
Mekong
Song Gianh
Mainstream
Rao Tro
Mai Hoa
Song Trac
Song Nan
River mouth
Red River
Clift et al. (2008)
Liu et al. (2007)

Figure 5

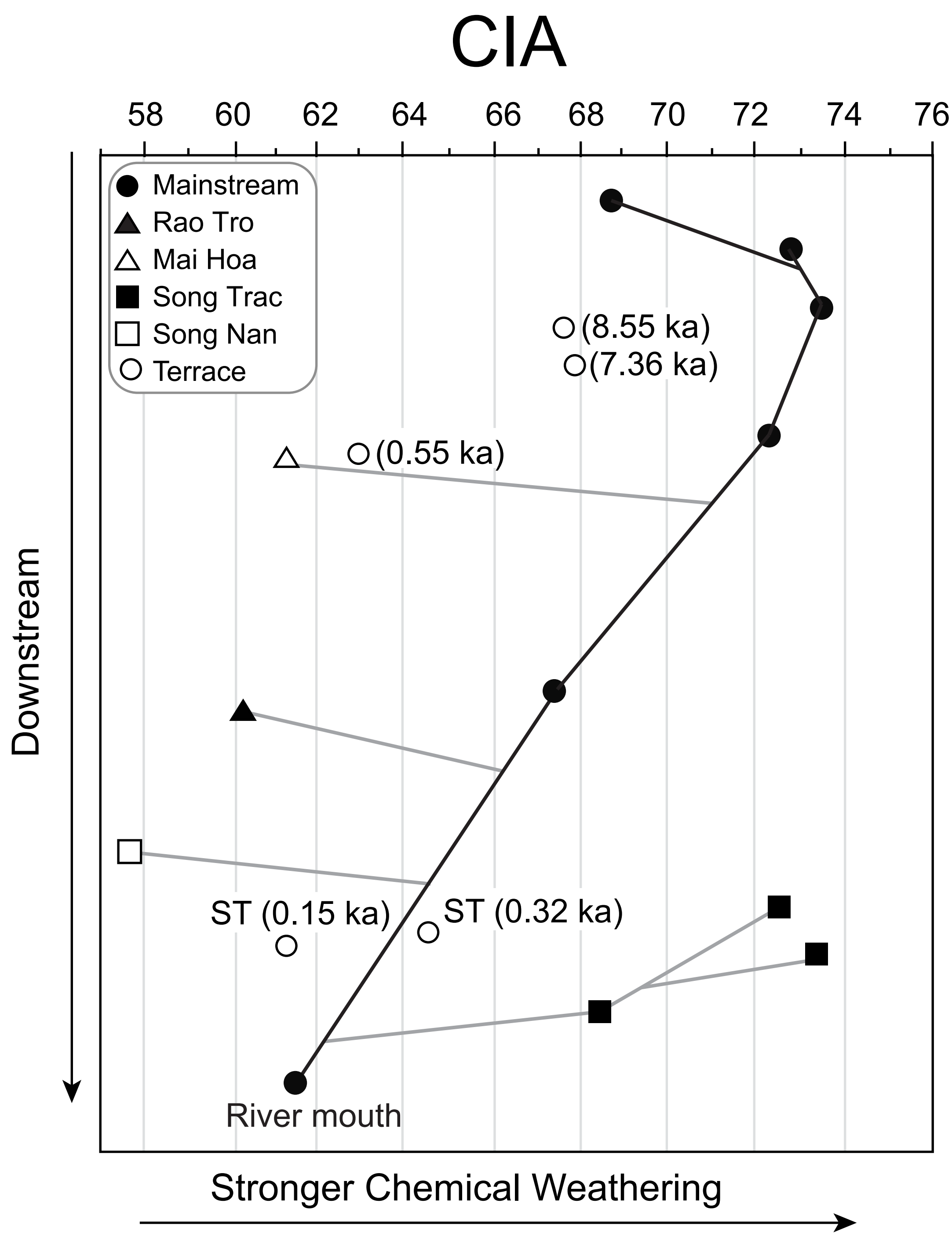
CIA
58
60
62
64
66
68
70
72
74
76
Mainstream
Rao Tro
Mai Hoa
Song Trac
Song Nan
Terrace
(8.55 ka)
(7.36 ka)
(0.55 ka)
ST (0.15 ka)
ST (0.32 ka)
River mouth
Downstream
Stronger Chemical Weathering

Figure 6

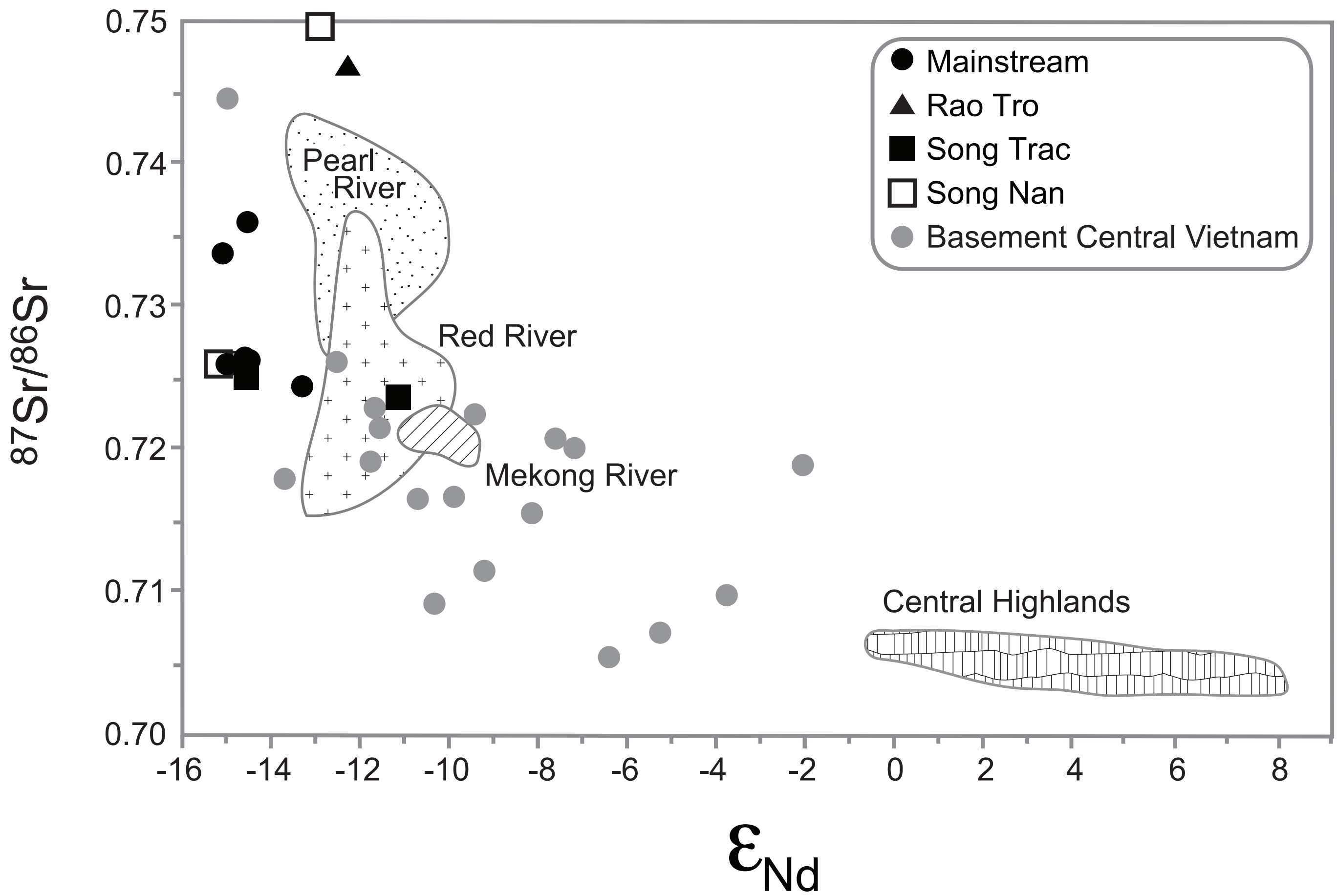
0.75
0.74
0.73
0.72
0.71
0.70
-16
-14
-12
-10
-8
-6
-4
-2
0
2
4
6
8
$^{87}Sr/^{86}Sr$
ε_{Nd}
Mainstream
Rao Tro
Song Trac
Song Nan
Basement Central Vietnam
Pearl River
Red River
Mekong River
Central Highlands

Figure 7

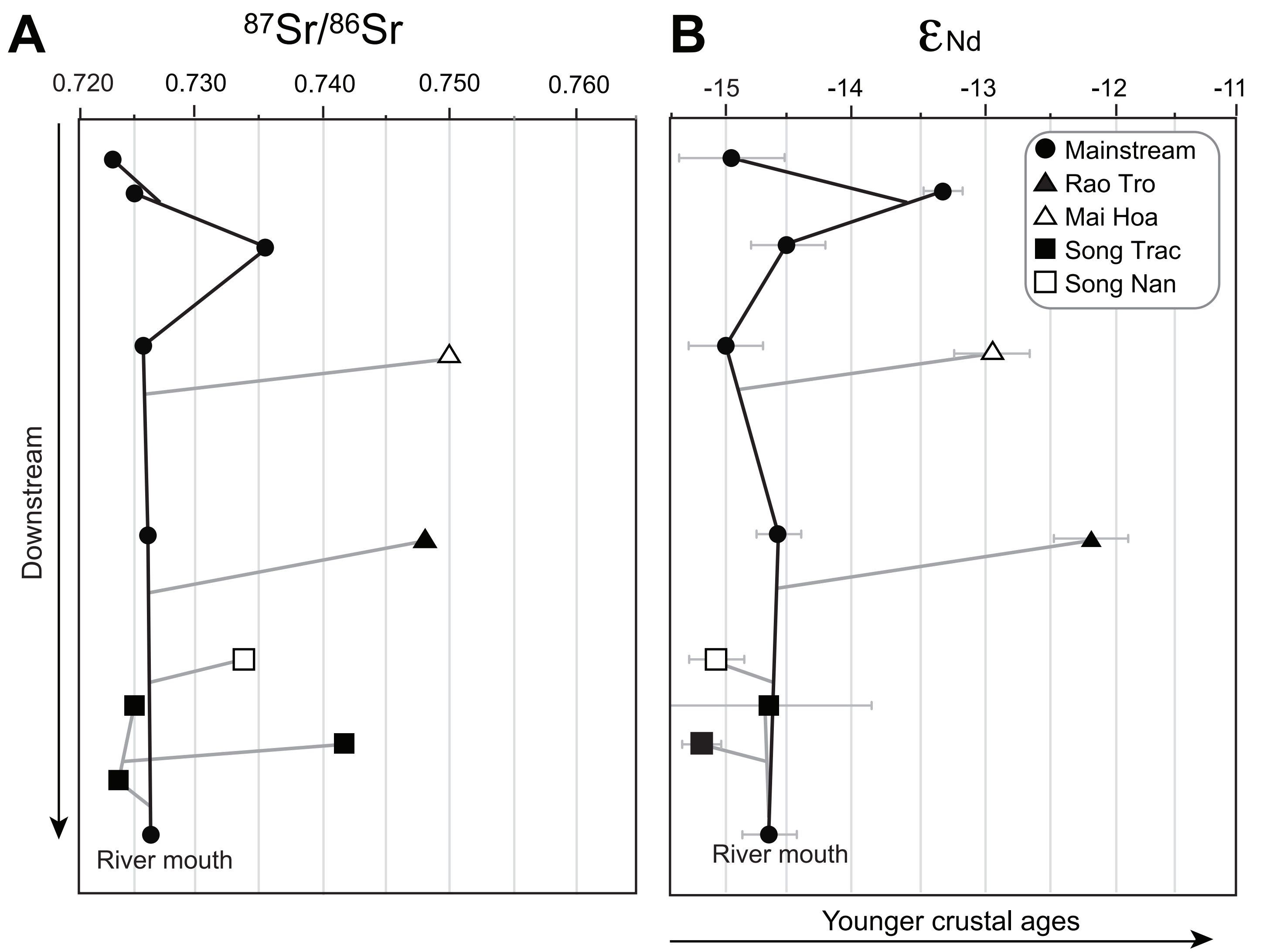
A
$^{87}Sr/^{86}Sr$
0.720
0.730
0.740
0.750
0.760
Downstream
River mouth
B
ε_{Nd}
-15
-14
-13
-12
-11
Mainstream
Rao Tro
Mai Hoa
Song Trac
Song Nan
River mouth
Younger crustal ages

Figure 8

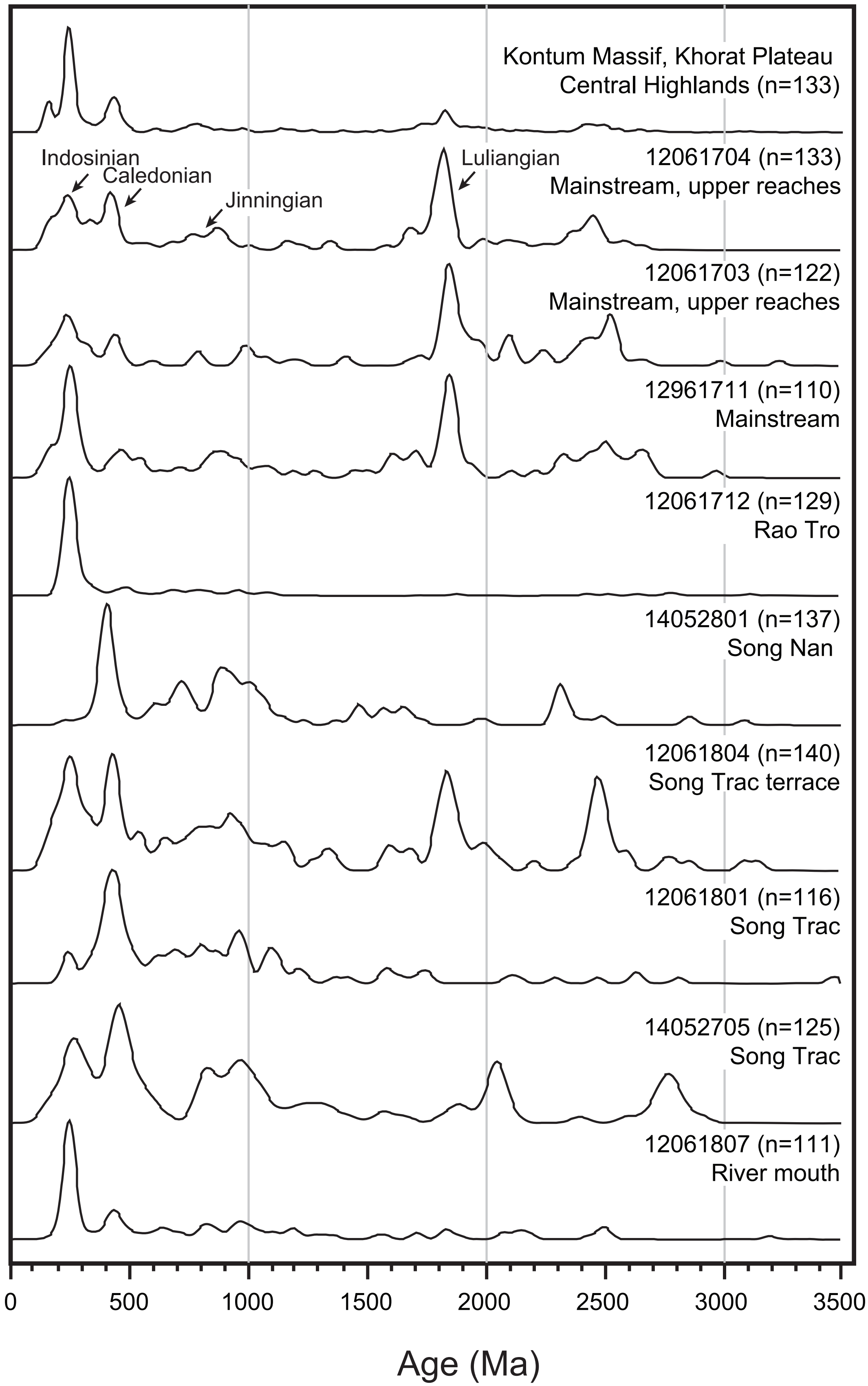

Kontum Massif, Khorat Plateau
Central Highlands (n=133)
Indosinian
Caledonian
Jinningian
Luliangian
12061704 (n=133)
Mainstream, upper reaches
12061703 (n=122)
Mainstream, upper reaches
12961711 (n=110)
Mainstream
12061712 (n=129)
Rao Tro
14052801 (n=137)
Song Nan
12061804 (n=140)
Song Trac terrace
12061801 (n=116)
Song Trac
14052705 (n=125)
Song Trac
12061807 (n=111)
River mouth
0
500
1000
1500
2000
2500
3000
3500
Age (Ma)

Figure 9

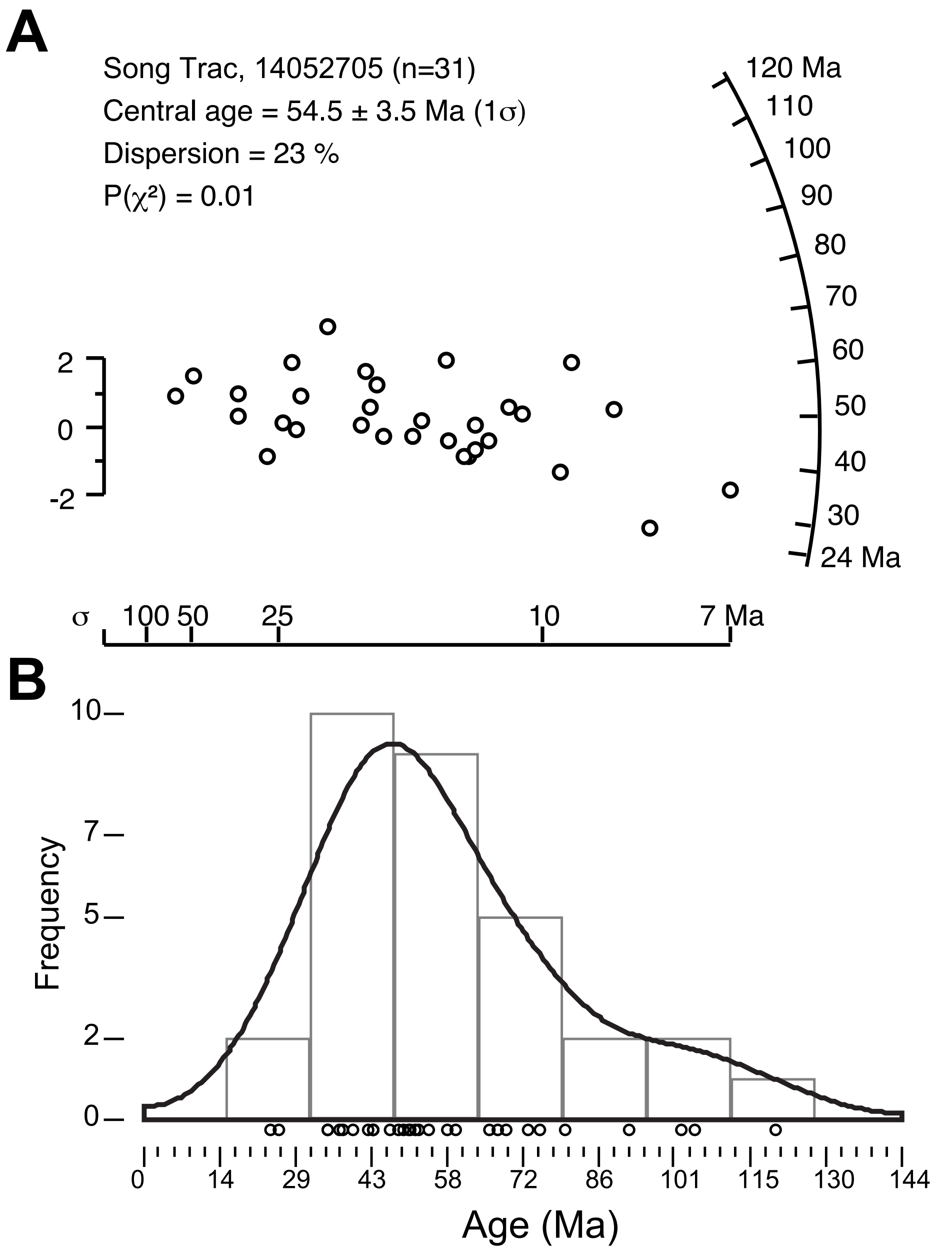
A
Song Trac, 14052705 (n=31)
Central age = 54.5 ± 3.5 Ma (1σ)
Dispersion = 23 %
P(χ²) = 0.01
120 Ma
110
100
90
80
70
60
50
40
30
24 Ma
2
0
-2
σ
100 50
25
10
7 Ma
B
10
7
5
2
0
Frequency
0
14
29
43
58
72
86
101
115
130
144
Age (Ma)

Figure 10

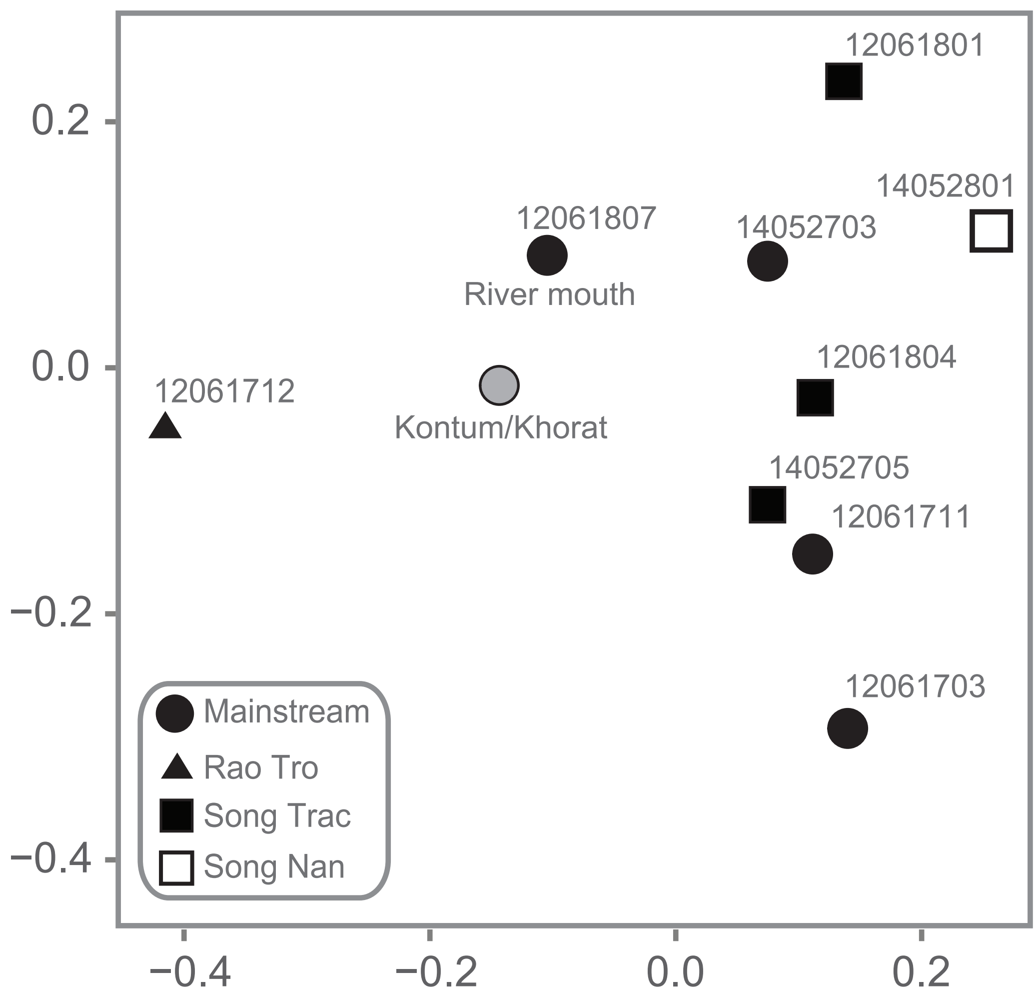
12061801
14052801
12061807
14052703
River mouth
12061804
12061712
Kontum/Khorat
14052705
12061711
12061703
Mainstream
Rao Tro
Song Trac
Song Nan
0.2
0.0
−0.2
−0.4
−0.4
−0.2
0.0
0.2

Figure 11

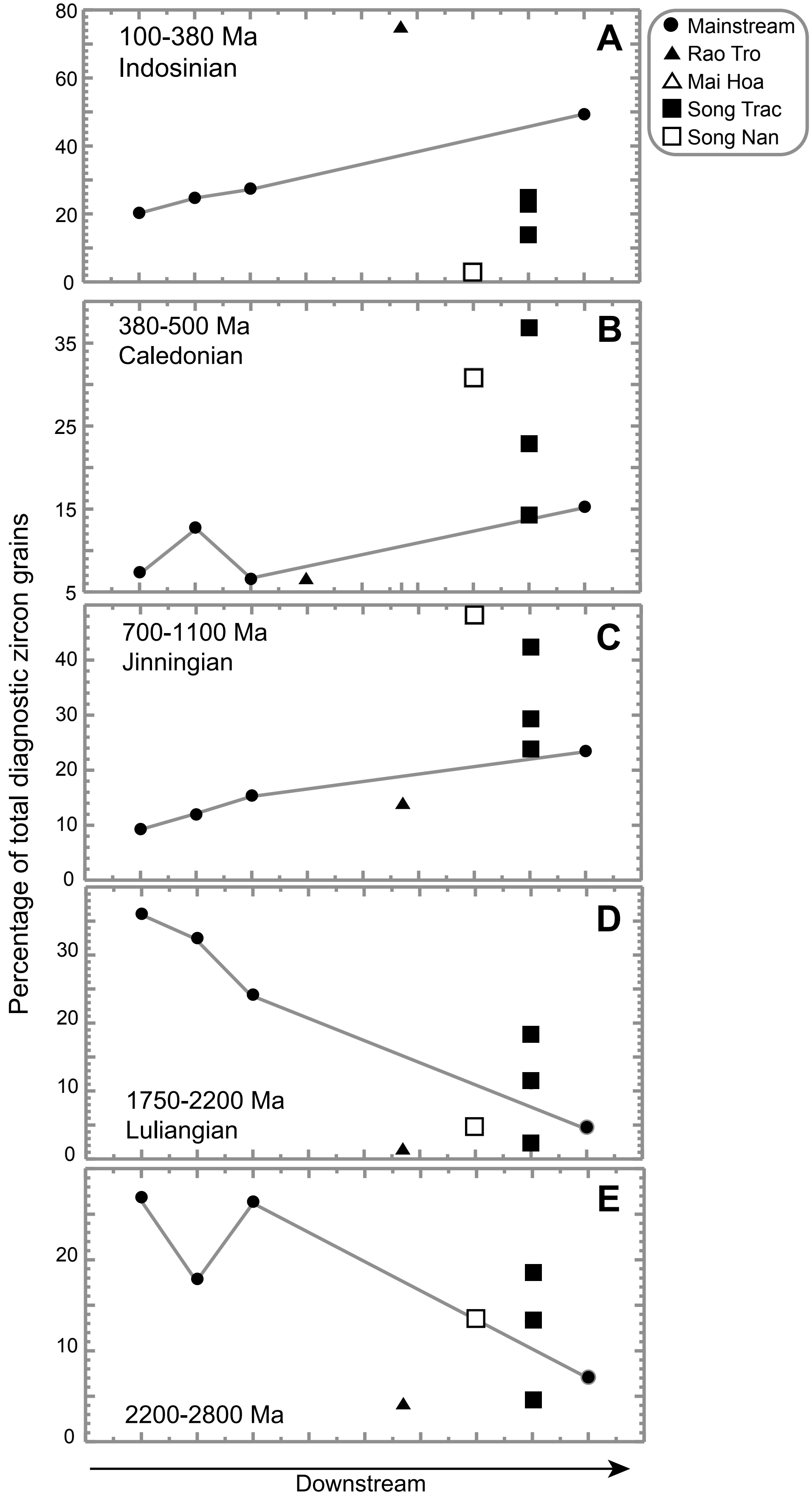

100-380 Ma
Indosinian
A
380-500 Ma
Caledonian
B
700-1100 Ma
Jinningian
C
1750-2200 Ma
Luliangian
D
2200-2800 Ma
E
Mainstream
Rao Tro
Mai Hoa
Song Trac
Song Nan
Percentage of total diagnostic zircon grains
Downstream

Figure 12

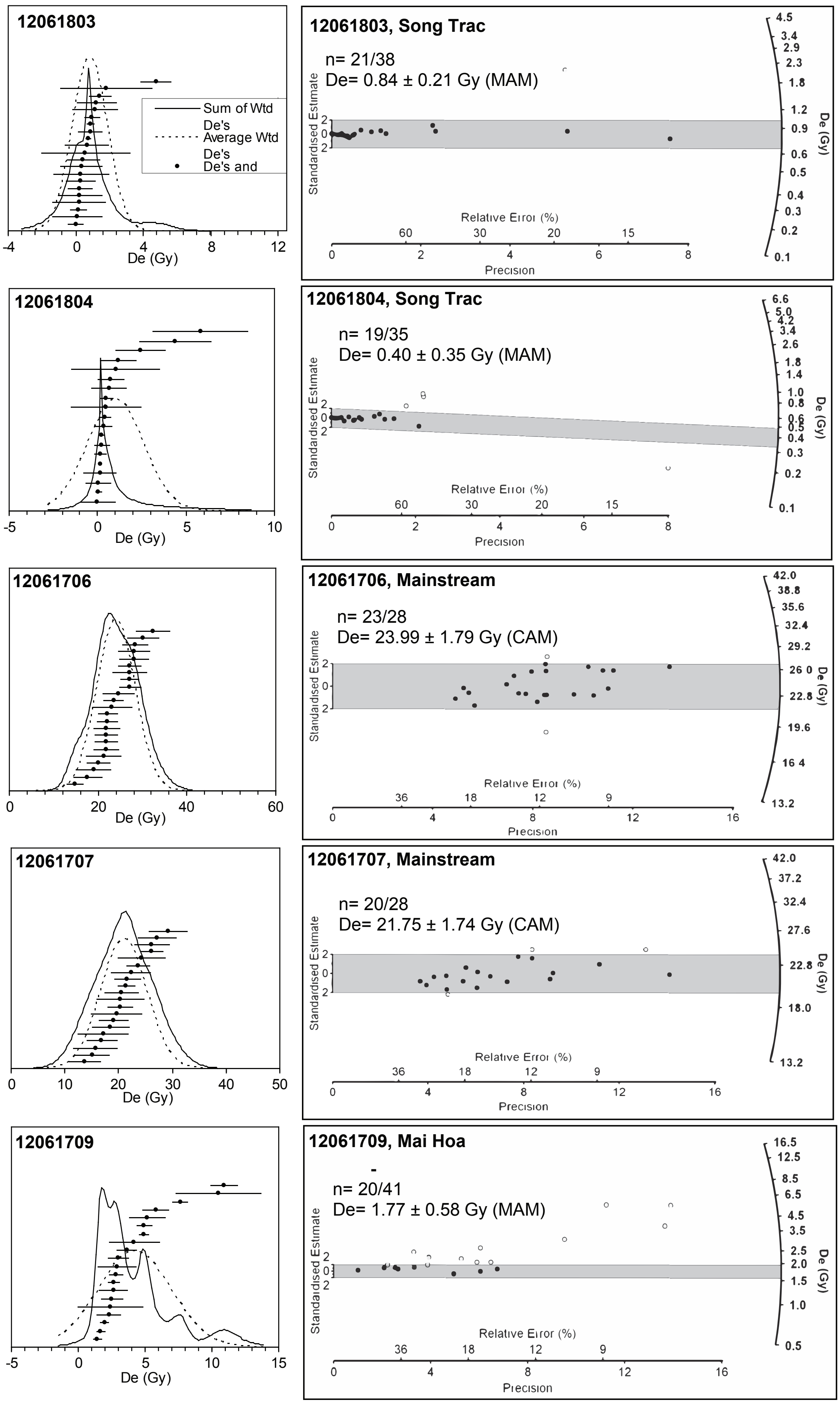
12061803
Sum of Wtd De's
Average Wtd De's
De's and
De (Gy)
12061803, Song Trac
n= 21/38
De= 0.84 ± 0.21 Gy (MAM)
Standardised Estimate
Relative Error (%)
Precision
De (Gy)
12061804
De (Gy)
12061804, Song Trac
n= 19/35
De= 0.40 ± 0.35 Gy (MAM)
Standardised Estimate
Relative Error (%)
Precision
De (Gy)
12061706
De (Gy)
12061706, Mainstream
n= 23/28
De= 23.99 ± 1.79 Gy (CAM)
Standardised Estimate
Relative Error (%)
Precision
De (Gy)
12061707
De (Gy)
12061707, Mainstream
n= 20/28
De= 21.75 ± 1.74 Gy (CAM)
Standardised Estimate
Relative Error (%)
Precision
De (Gy)
12061709
De (Gy)
12061709, Mai Hoa
n= 20/41
De= 1.77 ± 0.58 Gy (MAM)
Standardised Estimate
Relative Error (%)
Precision
De (Gy)

Figure SI-1

Table 1

Sample	Location	Latitude	Longitude	Elevation (m)
Modern river samples				
12061704	Upper reaches mainstream	17.82820	105.76820	160
12061703	Upper reaches mainstream	17.81815	105.77533	130
12061702	Upper reaches mainstream	17.96003	105.81230	48
14052701	Upper reaches mainstream	17.99917	105.86592	42
12061708	Mai Hoa	17.97928	105.92873	19
12061711	Middle reaches mainstream	17.84280	106.14482	1
12061712	Rao Tro	17.82463	106.17650	0
14052801	Song Nan	17.71797	106.35292	3
12061802	Song Trac	17.61637	106.31567	3
12061801	Song Trac	17.59690	106.42347	10
14052705	Song Trac	17.67200	106.39223	4
12061807	River Mouth	17.71438	106.44660	0
Terraces				
12061707	Mainstream terrace	17.99923	105.86595	51
12061706	Mainstream terrace	17.99923	105.86595	51
12061709	Mainstream terrace	17.97928	105.92873	19
12061803	Terrace Southern Song Trac	17.59463	106.28560	8
12061804	Terrace Southern Song Trac	17.61260	106.30465	3

Table 2

Sample	Location	SiO_2	TiO_2	Al_2O_3	Fe_2O_3	MnO	MgO	CaO	Na_2O	K_2O	P_2O_5
Modern river samples											
12061711	Middle reaches mainstream	84.17	0.36	5.21	2.68	0.020	0.35	0.16	0.38	1.17	0.05
12061712	Rao Tro	90.57	0.34	4.57	1.16	0.015	0.16	0.10	0.23	2.10	0.03
12061708	Mai Hoa	90.00	0.24	5.08	1.46	0.013	0.13	0.07	0.18	2.42	0.04
12061807	River Mouth	90.97	0.49	3.68	1.47	0.027	0.23	0.15	0.36	1.02	0.03
12061801	Song Trac	79.22	0.42	9.70	3.45	0.034	1.04	0.16	0.26	2.48	0.05
12061802	Song Trac	88.20	0.36	5.05	1.93	0.023	0.45	0.49	0.29	0.88	0.05
14052705	Song Trac	90.84	0.17	3.83	1.06	0.009	0.33	0.33	0.26	0.82	0.03
14052801	Song Nan	93.28	0.25	1.56	0.86	0.008	0.20	0.53	0.26	0.27	0.05
14052701	Upper reaches mainstream	76.48	0.46	10.60	4.94	0.041	0.72	0.20	0.47	2.26	0.09
12061703	Upper reaches mainstream	70.98	0.54	12.66	6.54	0.069	1.37	0.56	0.64	2.42	0.1
12061702	Upper reaches mainstream	72.57	0.43	9.70	4.89	0.050	2.06	2.34	0.38	2.07	0.09
12061704	Upper reaches mainstream	76.16	0.43	9.72	3.82	0.046	1.08	0.35	0.72	1.94	0.06
Terraces											
12061706	Mainstream terrace		0.26	5.58	3.30		0.35	0.07	0.28	1.60	
12061707	Mainstream terrace		0.30	5.77	2.94		0.34	0.08	0.32	1.54	
12061709	Mainstream terrace		0.27	4.60	2.11		0.16	0.03	0.15	2.03	
12061803	Terrace Southern tributary		0.23	3.93	1.92		0.34	0.33	0.27	1.17	
12061804	Terrace Southern tributary		0.15	2.73	1.47		0.20	0.17	0.23	0.86	

Table 2

Sample	As	Ba	Ce	Co	Cr	Cu	Ga	Mo	Ni	Nb	Pb	Rb	Sr	Th	Y	V	U	Zn	Zr
Modern river samples																			
12061711	3	184	40	8	27	5	6	0	14	10	12	51	42	7	6	33	9	34	104
12061712	7	317	12	7	13	1	5	0	5	10	8	80	30	6	3	20	7	18	83
12061708	6	321	15	8	15	4	5	0	7	8	13	105	37	7	6	18	7	17	84
12061807	2	170	38	6	22	2	5	0	13	10	10	36	34	7	11	24	10	25	418
12061801	0	452	30	10	48	10	12	0	21	11	22	115	45	7	13	61	6	54	95
12061802	5	158	10	9	33	7	7	-1	13	9	9	43	39	8	14	34	7	30	271
14052705	0	181	-7	7	20	1	5	-1	6	7	6	36	37	6	5	17	6	14	90
14052801	0	40	-30	6	24	0	3	0	7	7	5	16	24	5	11	15	6	16	465
14052701	8	337	57	17	55	13	13	0	24	12	21	112	61	11	15	64	4	65	145
12061703	11	336	59	15	67	16	17	0	33	13	23	103	83	9	16	86	6	79	132
12061702	9	301	50	15	63	13	12	-2	25	12	19	102	58	11	13	60	8	60	142
12061704	5	347	53	12	43	20	12	-5	21	11	17	77	73	9	3	62	13	47	121
Terraces																			
12061706	7.9	340	61.9	13	131	23.5	14.1	0.55	27.6	9.3	19.6	102	53.5	12.5	13.2	67	2.3	71	50.8
12061707	6.6	330	67.3	12.7	113	20.5	14.2	0.51	26.5	11.9	20.2	97.8	55.5	13.1	15.6	67	3.1	66	59.6
12061709	8.2	370	63.7	8.2	129	16.1	11.4	0.57	12.6	8.7	19.9	124	36.1	12.8	13.2	48	2.6	33	42.1
12061803	3.9	270	66.7	8.5	178	15.7	9.77	0.48	19.2	8.1	16.9	69.5	50	13.8	13.9	49	2.5	50	47.4
12061804	2.8	230	69.2	5.3	171	10	6.72	0.42	13.2	11.3	12.2	47.1	43.9	14.1	14.8	32	4	32	35.9

Table 3

Sample	Normalized $^{143}Nd/^{144}Nd$	2 sigma	ε_{Nd}	2 sigma	Normalized $^{87}Sr/^{86}Sr$	2 sigma
14052701	0.511871	0.000007	-15.0	0.14	0.73414	0.000018
14052801	0.511862	0.000003	-15.1	0.06	0.72566	0.000020
14052705	0.512068	0.000008	_	_	0.72358	0.000002
12061704	0.511874	0.000016	-14.9	0.31	0.72621	0.000019
12061802	0.511889	0.000042	-14.6	0.82	0.72518	0.000030
12061708	0.511978	0.000007	-12.9	0.15	0.75034	0.000018
12061702	0.511895	0.000013	-14.5	0.26	0.73591	0.000007
12061712	0.512014	0.000014	-12.2	0.28	0.74707	0.000022
12061703	0.511957	0.000003	-13.3	0.06	0.72469	0.000020
12061711	0.511890	0.000009	-14.6	0.18	0.72648	0.000007
12061807	0.511889	0.000008	-14.6	0.16	0.72679	0.000010
12061801	0.511857	0.000005	-15.2	0.16	0.74290	0.000026

Table 4

				Ratios						Ages (Ma)									
Gr. No.	Pb (ppm)	U (ppm)	Atomic Th/U	206/238	± s.e.	207/235	± s.e.	207/206	± s.e.	206/238	± 2s	207/235	± 2s	207/206	± 2s	% concord. (206/238 207/235)	% concord. (206/238 207/206)	Best Age (Ma)	±2s
12061711 Middle reaches																			
G1	19	48	0.85	0.3369	0.0033	5.2922	3.6232	0.1149	0.0087	1871.8	31.4	1867.6	130.7	1878.5	131.5	-0.2	0.4	1878.5	131.5
G2	116	441	1.40	0.1905	0.0032	2.0712	4.1212	0.0767	0.0088	1123.9	34.5	1139.3	158.0	1113.9	157.6	1.4	-0.9	1113.9	157.6
G3	10	204	0.27	0.0470	0.0044	0.3462	0.1557	0.0525	0.0016	295.8	54.7	301.9	51.3	308.5	18.2	2.0	4.1	295.8	54.7
G4	114	420	1.29	0.2028	0.0022	2.3616	0.0298	0.0841	0.0006	1190.6	24.0	1231.1	18.8	1293.9	12.3	3.3	8.0	1293.9	12.3
G5	17	418	0.19	0.0425	0.0006	0.3111	0.0097	0.0519	0.0013	268.0	7.9	275.0	13.5	279.7	13.6	2.6	4.2	268.0	7.9
G6	70	119	1.15	0.4388	0.0024	9.1038	0.0381	0.1502	0.0008	2345.4	21.7	2348.5	13.7	2348.2	11.0	0.1	0.1	2348.2	11.0
G7	145	411	0.16	0.3473	0.0005	5.6465	0.0062	0.1151	0.0008	1921.5	5.1	1923.2	12.5	1881.1	13.9	0.1	-2.1	1881.1	13.9
G8	217	677	0.20	0.3147	0.0041	4.9501	0.0792	0.1133	0.0008	1764.0	39.9	1810.8	25.0	1853.5	14.1	2.6	4.8	1853.5	14.1
G9	104	625	0.57	0.1519	0.0024	1.4922	0.0488	0.0697	0.0010	911.3	27.0	927.2	25.2	918.1	18.2	1.7	0.7	911.3	27.0
G10	257	465	0.39	0.4932	0.0037	12.0799	0.0710	0.1746	0.0008	2584.6	31.9	2610.6	16.7	2602.5	10.7	1.0	0.7	2602.5	10.7
G11	92	584	0.59	0.1415	0.0058	1.3669	0.1760	0.0675	0.0012	853.1	65.4	874.8	51.8	852.9	22.9	2.5	0.0	853.1	65.4
G12	9	154	1.54	0.0414	0.0012	0.3263	0.0210	0.0573	0.0012	261.6	14.2	286.8	17.6	502.7	18.9	8.8	48.0	261.6	14.2
G13	121	359	0.59	0.2969	0.0017	4.2707	0.0210	0.1027	0.0006	1676.1	16.7	1687.7	13.6	1673.1	11.6	0.7	-0.2	1673.1	11.6
G14	40	1016	0.24	0.0403	0.0006	0.2907	0.0096	0.0517	0.0015	254.9	7.2	259.1	14.4	272.2	15.2	1.6	6.4	254.9	7.2
G15	38	920	0.25	0.0417	0.0035	0.2985	0.0627	0.0519	0.0008	263.6	43.2	265.2	39.7	282.8	9.2	0.6	6.8	263.6	43.2
G16	131	349	0.59	0.3309	0.0005	5.4303	0.0046	0.1151	0.0006	1842.5	4.7	1889.7	8.9	1881.9	10.4	2.5	2.1	1881.9	10.4
G17	157	437	0.15	0.3539	0.0005	5.7042	0.0045	0.1149	0.0005	1953.1	4.7	1932.0	8.2	1878.2	9.5	-1.1	-4.0	1878.2	9.5
G18	94	211	1.42	0.3218	0.0039	5.0152	0.0823	0.1127	0.0009	1798.4	38.0	1821.9	24.5	1843.1	15.2	1.3	2.4	1843.1	15.2
G19	22	135	0.44	0.1513	0.0042	1.5206	0.0813	0.0709	0.0008	908.5	46.5	938.7	36.2	955.4	16.4	3.2	4.9	908.5	46.5
G20	23	130	1.65	0.1325	0.0038	1.4056	0.0824	0.0758	0.0010	802.2	43.5	891.3	37.1	1089.0	18.5	10.0	26.3	802.2	43.5
G21	10	71	1.97	0.0894	0.0018	0.7724	0.0269	0.0617	0.0008	552.0	21.7	581.2	21.1	663.0	14.0	5.0	16.7	552.0	21.7
G22	16	30	0.79	0.4337	0.0012	9.1829	0.0183	0.1563	0.0011	2322.5	10.4	2356.4	13.8	2415.9	14.7	1.4	3.9	2415.9	14.7
G23	56	225	0.54	0.2252	0.0021	2.8645	0.0495	0.0916	0.0011	1309.3	22.0	1372.6	22.4	1458.1	19.8	4.6	10.2	1458.1	19.8
G24	30	984	0.59	0.0275	0.0054	0.1881	0.2188	0.0502	0.0016	174.7	67.6	175.0	64.5	205.2	13.6	0.2	14.9	174.7	67.6
G25	103	236	0.56	0.3873	0.0027	8.2190	0.0434	0.1508	0.0008	2110.2	24.7	2255.4	15.5	2354.5	11.1	6.4	10.4	2354.5	11.1
G26	21	616	0.94	0.0275	0.0003	0.1963	0.0029	0.0517	0.0006	174.9	4.1	182.0	5.3	270.8	6.8	3.9	35.4	174.9	4.1
G27	32	398	0.67	0.0703	0.0045	0.5370	0.1199	0.0545	0.0011	437.8	54.7	436.4	47.6	389.7	15.0	-0.3	-12.3	437.8	54.7
G28	14	344	0.43	0.0393	0.0003	0.2832	0.0033	0.0516	0.0007	248.5	4.1	253.2	6.7	267.7	7.7	1.9	7.2	248.5	4.1
G29	67	755	0.14	0.0929	0.0008	0.8364	0.0085	0.0659	0.0006	572.8	9.9	617.2	11.7	802.6	11.5	7.2	28.6	572.8	9.9
G30	80	119	1.14	0.4987	0.0005	11.3395	0.0051	0.1673	0.0007	2608.1	4.1	2551.5	8.2	2530.5	9.8	-2.2	-3.1	2530.5	9.8
G31	108	307	0.33	0.3338	0.0011	5.4111	0.0117	0.1151	0.0006	1856.5	10.5	1886.6	9.9	1881.3	9.9	1.6	1.3	1881.3	9.9
G32	67	393	0.95	0.1401	0.0039	1.2923	0.0782	0.0664	0.0009	845.1	44.2	842.3	35.3	818.7	16.6	-0.3	-3.2	845.1	44.2
G33	97	227	1.08	0.3345	0.0022	5.2215	0.0340	0.1120	0.0007	1860.3	21.3	1856.1	15.9	1831.6	12.9	-0.2	-1.6	1831.6	12.9
G34	6	120	0.69	0.0423	0.0017	0.3016	0.0192	0.0510	0.0006	267.2	20.4	267.7	18.9	241.7	6.7	0.2	-10.5	267.2	20.4
G35	166	335	1.60	0.3455	0.0007	5.5649	0.0111	0.1145	0.0017	1912.9	6.2	1910.7	25.4	1872.3	26.8	-0.1	-2.2	1872.3	26.8
G36	13	29	1.57	0.3304	0.0005	5.1016	0.0089	0.1123	0.0021	1840.5	4.4	1836.4	32.4	1837.3	34.1	-0.2	-0.2	1837.3	34.1
G37	397	913	0.08	0.4313	0.0040	9.2576	0.0810	0.1541	0.0009	2311.4	36.4	2363.8	20.2	2391.5	12.4	2.2	3.3	2391.5	12.4

Table 4

Gr. No.	Pb (ppm)	U (ppm)	Atomic Th/U	Ratios 206/238	± s.e.	207/235	± s.e.	207/206	± s.e.	Ages (Ma) 206/238	± 2s	207/235	± 2s	207/206	± 2s	% concord. (206/238 207/235)	% concord. (206/238 207/206)	Best Age (Ma)	±2s
G38	9	24	0.89	0.3055	0.0043	4.4554	0.1390	0.1054	0.0015	1718.6	42.0	1722.7	33.1	1721.1	25.5	0.2	0.1	1721.1	25.5
G39	110	183	0.85	0.4795	0.0050	11.1188	0.1257	0.1656	0.0011	2525.1	43.7	2533.1	23.3	2513.9	14.5	0.3	-0.4	2513.9	14.5
G40	52	77	0.94	0.5429	0.0040	16.2770	0.1313	0.2199	0.0016	2795.6	33.6	2893.2	19.8	2979.8	15.6	3.4	6.2	2979.8	15.6
G41	48	283	0.86	0.1434	0.0056	1.3803	0.1717	0.0681	0.0013	864.1	63.5	880.6	50.9	871.9	24.1	1.9	0.9	864.1	63.5
G42	118	497	0.70	0.2066	0.0067	2.3049	0.3779	0.0802	0.0021	1210.7	71.2	1213.8	58.3	1202.2	38.1	0.3	-0.7	1202.2	38.1
G43	105	528	0.69	0.1743	0.0017	1.7752	0.0212	0.0726	0.0006	1035.5	18.6	1036.4	16.9	1001.7	13.0	0.1	-3.4	1035.5	18.6
G44	385	957	0.93	0.3252	0.0024	5.9702	0.0339	0.1315	0.0007	1815.3	23.5	1971.5	15.7	2117.4	10.9	7.9	14.3	2117.4	10.9
G45	43	127	0.85	0.2827	0.0020	3.9583	0.0257	0.0991	0.0006	1604.8	20.5	1625.7	15.4	1607.8	11.8	1.3	0.2	1607.8	11.8
G46	142	333	0.32	0.3977	0.0038	8.2402	0.0812	0.1463	0.0010	2158.5	34.9	2257.8	21.1	2303.0	14.2	4.4	6.3	2303.0	14.2
G47	15	343	0.51	0.0395	0.0047	0.2796	0.1270	0.0513	0.0012	249.5	57.9	250.4	53.4	252.5	12.2	0.4	1.2	249.5	57.9
G48	115	308	0.50	0.3364	0.0005	5.4176	0.0080	0.1138	0.0011	1869.3	4.9	1887.6	16.8	1861.4	18.4	1.0	-0.4	1861.4	18.4
G49	40	797	1.08	0.0405	0.0005	0.2885	0.0051	0.0517	0.0007	256.1	5.9	257.4	8.4	270.4	8.4	0.5	5.3	256.1	5.9
G50	36	68	0.58	0.4605	0.0040	10.0902	0.0844	0.1608	0.0010	2441.8	34.9	2443.1	19.4	2463.6	12.9	0.1	0.9	2463.6	12.9
G51	51	83	1.35	0.4455	0.0005	9.2787	0.0044	0.1487	0.0006	2375.2	4.3	2365.9	7.1	2331.3	8.5	-0.4	-1.9	2331.3	8.5
G52	18	128	0.68	0.1227	0.0057	1.0923	0.2318	0.0641	0.0017	745.9	65.0	749.6	55.9	745.6	29.1	0.5	0.0	745.9	65.0
G53	123	492	0.23	0.2477	0.0054	3.4873	0.1855	0.1001	0.0014	1426.6	55.4	1524.3	40.7	1626.5	24.7	6.4	12.3	1626.5	24.7
G54	96	262	0.37	0.3407	0.0015	5.3962	0.0202	0.1147	0.0008	1889.9	14.3	1884.2	14.1	1875.6	13.7	-0.3	-0.8	1875.6	13.7
G55	6	15	0.99	0.3079	0.0029	4.4180	0.0492	0.1055	0.0008	1730.3	28.5	1715.7	20.2	1723.4	14.6	-0.9	-0.4	1723.4	14.6
G56	31	76	1.63	0.2896	0.0040	4.0854	0.0812	0.1009	0.0010	1639.5	39.9	1651.4	27.3	1639.8	17.4	0.7	0.0	1639.8	17.4
G57	6	9	1.04	0.4795	0.0043	10.7268	0.1580	0.1719	0.0019	2525.2	37.5	2499.7	26.9	2575.9	22.8	-1.0	2.0	2575.9	22.8
G58	18	180	1.13	0.0772	0.0035	0.6374	0.0842	0.0583	0.0011	479.1	42.3	500.7	38.7	541.4	18.1	4.3	11.5	479.1	42.3
G59	85	146	0.52	0.5015	0.0071	12.5985	0.4785	0.1794	0.0029	2620.4	60.9	2650.1	40.7	2647.1	32.6	1.1	1.0	2647.1	32.6
G60	68	126	1.93	0.3543	0.0010	5.8330	0.0143	0.1203	0.0010	1954.9	9.3	1951.3	15.2	1961.3	16.2	-0.2	0.3	1961.3	16.2
G61	30	167	0.95	0.1484	0.0060	1.4638	0.2251	0.0701	0.0016	892.2	66.8	915.6	55.2	929.8	29.6	2.6	4.1	892.2	66.8
G62	164	466	0.32	0.3349	0.0042	5.6156	0.1025	0.1189	0.0012	1862.3	40.7	1918.5	27.2	1940.1	18.5	2.9	4.0	1940.1	18.5
G63	209	405	0.82	0.4270	0.0019	9.3800	0.0323	0.1593	0.0010	2292.3	16.7	2375.9	14.4	2447.9	13.8	3.5	6.4	2447.9	13.8
G64	71	179	0.79	0.3334	0.0050	5.2686	0.1417	0.1135	0.0014	1854.8	48.3	1863.8	32.7	1856.8	22.2	0.5	0.1	1856.8	22.2
G65	22	34	1.26	0.4812	0.0010	11.3997	0.0168	0.1702	0.0009	2532.3	8.8	2556.4	10.7	2560.0	11.7	0.9	1.1	2560.0	11.7
G66	8	209	0.23	0.0396	0.0039	0.2811	0.0833	0.0512	0.0010	250.5	48.6	251.5	44.8	249.4	10.6	0.4	-0.5	250.5	48.6
G67	23	215	0.37	0.1046	0.0062	0.8843	0.3330	0.0595	0.0021	641.2	71.9	643.3	64.2	584.3	32.8	0.3	-9.7	641.2	71.9
G68	17	211	0.88	0.0670	0.0005	0.4913	0.0064	0.0535	0.0010	418.2	6.2	405.8	13.3	350.1	12.6	-3.1	-19.5	418.2	6.2
G69	39	62	1.05	0.4780	0.0013	10.9160	0.0159	0.1659	0.0008	2518.7	11.0	2516.0	9.7	2516.8	10.1	-0.1	-0.1	2516.8	10.1
G70	20	58	0.50	0.3058	0.0008	4.4025	0.0096	0.1064	0.0008	1720.0	8.1	1712.8	13.3	1738.5	14.2	-0.4	1.1	1738.5	14.2
G71	7	253	1.18	0.0222	0.0058	0.1510	0.2292	0.0488	0.0017	141.7	72.9	142.8	69.3	137.8	10.6	0.7	-2.9	141.7	72.9
G72	34	56	0.60	0.5151	0.0037	12.5969	0.0936	0.1819	0.0013	2678.5	31.8	2650.0	18.8	2669.9	14.7	-1.1	-0.3	2669.9	14.7
G73	132	202	0.24	0.5644	0.0003	14.7021	0.0041	0.1857	0.0012	2884.7	2.5	2796.2	12.4	2704.2	14.0	-3.2	-6.7	2704.2	14.0
G74	5	94	0.76	0.0462	0.0062	0.3252	0.2533	0.0522	0.0018	291.0	76.3	285.9	70.1	295.1	19.3	-1.8	1.4	291.0	76.3
G75	138	448	0.37	0.2926	0.0066	4.5508	0.2483	0.1125	0.0017	1654.7	66.2	1740.3	45.3	1840.2	27.3	4.9	10.1	1840.2	27.3
G76	16	198	0.60	0.0748	0.0006	0.5784	0.0097	0.0564	0.0014	464.9	7.7	463.4	19.1	467.0	19.8	-0.3	0.4	464.9	7.7

Table 4

Gr. No.	Pb (ppm)	U (ppm)	Atomic Th/U	Ratios 206/238	± s.e.	207/235	± s.e.	207/206	± s.e.	Ages (Ma) 206/238	± 2s	207/235	± 2s	207/206	± 2s	% concord. (206/238 / 207/235)	% concord. (206/238 / 207/206)	Best Age (Ma)	±2s
G77	159	290	0.62	0.4668	0.0034	10.2672	0.0703	0.1602	0.0011	2469.6	30.1	2459.2	18.2	2457.2	13.9	-0.4	-0.5	2457.2	13.9
G78	137	829	0.43	0.1567	0.0009	1.5100	0.0120	0.0705	0.0009	938.5	10.4	934.5	17.1	942.7	17.2	-0.4	0.4	938.5	10.4
G79	8	91	0.66	0.0783	0.0055	0.6177	0.1570	0.0570	0.0015	485.7	65.3	488.4	57.4	489.6	21.5	0.6	0.8	485.7	65.3
G80	6	192	0.59	0.0300	0.0018	0.2105	0.0225	0.0503	0.0007	190.8	22.9	194.0	21.8	208.0	6.8	1.7	8.3	190.8	22.9
G81	34	893	0.19	0.0394	0.0010	0.2780	0.0144	0.0510	0.0010	249.2	12.4	249.0	14.3	240.8	10.5	-0.1	-3.5	249.2	12.4
G82	59	1507	0.19	0.0404	0.0004	0.2872	0.0059	0.0512	0.0013	255.2	5.1	256.4	12.0	250.3	12.6	0.5	-2.0	255.2	5.1
G83	29	492	0.29	0.0566	0.0005	0.4671	0.0044	0.0590	0.0006	355.1	5.7	389.2	8.3	565.2	10.4	8.8	37.2	355.1	5.7
G84	69	123	0.46	0.4951	0.0005	12.8926	0.0045	0.1825	0.0006	2592.8	4.1	2671.8	6.1	2675.8	7.6	3.0	3.1	2675.8	7.6
G85	94	163	0.74	0.4749	0.0007	10.5824	0.0085	0.1638	0.0008	2505.1	6.0	2487.2	9.6	2495.5	10.9	-0.7	-0.4	2495.5	10.9
G86	11	208	1.06	0.0436	0.0059	0.3278	0.2483	0.0543	0.0018	274.8	73.0	287.9	69.8	383.9	23.3	4.5	28.4	274.8	73.0
G87	100	326	0.23	0.3001	0.0056	4.7407	0.1852	0.1124	0.0016	1691.6	55.7	1774.5	39.3	1838.6	25.9	4.7	8.0	1838.6	25.9
G88	119	1278	0.44	0.0884	0.0005	0.7024	0.0069	0.0575	0.0009	545.9	6.4	540.2	14.5	511.9	14.7	-1.1	-6.6	545.9	6.4
G89	51	258	0.92	0.1630	0.0035	1.6251	0.0779	0.0711	0.0011	973.3	39.2	980.0	33.6	959.4	21.5	0.7	-1.4	973.3	39.2
G90	11	278	0.24	0.0396	0.0010	0.2786	0.0104	0.0509	0.0006	250.5	12.8	249.6	12.5	234.5	6.5	-0.4	-6.8	250.5	12.8
G91	61	308	0.48	0.1822	0.0019	1.9018	0.0273	0.0755	0.0008	1079.0	21.0	1081.7	19.9	1080.8	15.8	0.3	0.2	1079.0	21.0
G92	8	202	0.33	0.0381	0.0005	0.3147	0.0054	0.0584	0.0008	240.9	6.1	277.8	9.0	545.9	13.3	13.3	55.9	240.9	6.1
G93	15	81	0.71	0.1631	0.0022	1.6419	0.0307	0.0712	0.0008	973.8	23.8	986.5	21.7	963.4	15.7	1.3	-1.1	973.8	23.8
G94	74	115	0.83	0.5067	0.0005	11.9661	0.0085	0.1660	0.0014	2642.5	4.4	2601.8	15.7	2517.9	17.2	-1.6	-4.9	2517.9	17.2
G95	63	158	0.61	0.3546	0.0021	6.9770	0.0394	0.1394	0.0012	1956.6	19.6	2108.5	17.9	2220.0	16.6	7.2	11.9	2220.0	16.6
G96	206	556	0.68	0.3210	0.0061	4.9731	0.2441	0.1122	0.0018	1794.4	59.3	1814.8	41.8	1835.4	28.7	1.1	2.2	1835.4	28.7
G97	24	525	0.16	0.0479	0.0043	0.3553	0.1367	0.0532	0.0016	301.6	52.4	308.7	49.4	335.2	18.4	2.3	10.0	301.6	52.4
G98	357	646	0.17	0.5166	0.0038	13.1953	0.0774	0.1851	0.0011	2684.7	32.0	2693.7	17.9	2699.1	13.3	0.3	0.5	2699.1	13.3
G99	186	601	0.75	0.2647	0.0006	3.4640	0.0062	0.0944	0.0007	1513.7	5.8	1519.1	12.1	1516.9	13.4	0.4	0.2	1516.9	13.4
G100	45	116	1.05	0.3034	0.0060	4.3246	0.2021	0.1043	0.0018	1708.0	59.7	1698.1	43.7	1701.8	30.5	-0.6	-0.4	1701.8	30.5
G101	33	271	0.47	0.1153	0.0031	1.0220	0.0528	0.0642	0.0010	703.5	35.8	714.9	31.6	747.2	17.6	1.6	5.9	703.5	35.8
G102	115	322	0.40	0.3317	0.0036	5.2863	0.0791	0.1140	0.0012	1846.8	35.0	1866.6	25.6	1864.3	19.4	1.1	0.9	1864.3	19.4
G103	130	338	1.40	0.2827	0.0014	3.8520	0.0180	0.0986	0.0008	1604.8	13.9	1603.7	15.4	1597.6	15.0	-0.1	-0.4	1597.6	15.0
G104	16	185	0.52	0.0803	0.0036	0.6975	0.0791	0.0634	0.0012	497.9	43.2	537.3	40.8	720.3	20.9	7.3	30.9	497.9	43.2
G105	12	307	0.25	0.0401	0.0014	0.2866	0.0180	0.0514	0.0008	253.5	17.1	255.8	17.0	259.7	9.0	0.9	2.4	253.5	17.1
G106	7	214	0.99	0.0283	0.0039	0.1976	0.0910	0.0506	0.0012	180.1	49.3	183.1	47.2	221.7	11.4	1.6	18.8	180.1	49.3
G107	222	378	0.48	0.5072	0.0033	12.3334	0.0625	0.1776	0.0011	2644.5	28.5	2630.1	16.6	2630.2	12.8	-0.5	-0.5	2630.2	12.8
G108	33	87	0.66	0.3321	0.0010	5.1842	0.0131	0.1128	0.0009	1848.5	9.5	1850.0	14.3	1844.2	15.2	0.1	-0.2	1844.2	15.2
G109	14	34	0.92	0.3203	0.0005	4.8563	0.0060	0.1098	0.0009	1791.3	4.9	1794.7	13.7	1795.8	15.2	0.2	0.2	1795.8	15.2
G110	9	165	1.83	0.0365	0.0004	0.2543	0.0056	0.0507	0.0013	231.2	4.9	230.1	11.5	227.7	12.3	-0.5	-1.6	231.2	4.9
12061804 Terrace Song Trac																			
G1	248.1	1215.9	0.42	0.1926	0.0023	2.1147	0.0318	0.0791	0.0010	1135.6	24.8	1153.6	23.6	1174.6	17.2	1.6	3.3	1174.6	17.25
G2	67.8	884.0	0.51	0.0716	0.0009	0.5403	0.0101	0.0546	0.0009	445.7	10.5	438.6	14.4	395.1	11.3	-1.6	-12.8	445.7	10.47

Table 4

				Ratios						Ages (Ma)									
Gr. No.	Pb (ppm)	U (ppm)	Atomic Th/U	206/238	± s.e.	207/235	± s.e.	207/206	± s.e.	206/238	± 2s	207/235	± 2s	207/206	± 2s	% concord. (206/238 / 207/235)	% concord. (206/238 / 207/206)	Best Age (Ma)	±2s
G3	34.8	94.2	0.40	0.3414	0.0043	5.1182	0.1613	0.1123	0.0019	1893.4	41.6	1839.1	36.6	1837.0	30.1	-3.0	-3.1	1837.0	30.07
G4	139.2	401.9	0.47	0.3190	0.0038	4.8413	0.0825	0.1105	0.0014	1785.0	37.2	1792.1	29.2	1807.8	22.0	0.4	1.3	1807.8	21.97
G5	55.8	317.0	0.42	0.1667	0.0020	1.6610	0.0344	0.0716	0.0011	994.1	22.4	993.7	25.0	973.7	20.3	0.0	-2.1	973.7	20.33
G6	87.1	140.8	1.01	0.4804	0.0058	11.0598	0.2496	0.1684	0.0022	2529.1	50.8	2528.2	33.2	2541.6	25.1	0.0	0.5	2541.6	25.09
G7	81.0	1244.8	0.11	0.0687	0.0008	0.5097	0.0088	0.0542	0.0008	428.3	10.0	418.3	13.2	381.0	10.2	-2.4	-12.4	428.3	10.01
G8	7.5	295.6	0.58	0.0230	0.0004	0.1523	0.0082	0.0505	0.0026	146.8	4.7	143.9	15.2	219.9	21.2	-2.0	33.2	146.8	4.66
G9	57.5	274.1	0.21	0.6856	0.0083	22.8134	0.5376	0.2371	0.0030	3365.7	63.5	3219.0	33.9	3100.8	25.0	-4.6	-8.5	3100.8	24.97
G10	12.8	93.2	1.47	0.1003	0.0014	0.8081	0.0315	0.0592	0.0018	615.9	16.2	601.4	31.1	572.6	28.0	-2.4	-7.6	615.9	16.17
G11	57.5	209.8	0.68	0.2390	0.0029	2.9128	0.0651	0.0857	0.0013	1381.4	30.4	1385.2	29.4	1330.5	23.4	0.3	-3.8	1330.5	23.41
G12	37.7	217.3	0.44	0.1634	0.0020	1.5835	0.0361	0.0702	0.0012	975.8	22.3	963.7	26.1	932.7	21.4	-1.2	-4.6	932.7	21.43
G13	262.3	853.2	0.09	0.3128	0.0037	4.7722	0.0789	0.1106	0.0014	1754.4	36.7	1780.0	29.0	1808.5	21.8	1.4	3.0	1808.5	21.81
G14	45.6	79.3	0.61	0.4840	0.0061	10.7579	0.3567	0.1640	0.0025	2544.6	53.3	2502.4	37.1	2497.7	29.4	-1.7	-1.9	2497.7	29.38
G15	106.4	330.1	0.09	0.3279	0.0039	5.7442	0.1049	0.1287	0.0017	1828.2	38.3	1938.1	30.5	2079.6	23.4	5.7	12.1	2079.6	23.42
G16	11.4	97.9	1.20	0.0907	0.0013	0.7638	0.0344	0.0600	0.0022	559.9	15.6	576.2	34.1	604.7	33.8	2.8	7.4	559.9	15.60
G17	111.4	230.3	0.07	0.4688	0.0057	10.1262	0.2113	0.1588	0.0021	2478.3	49.8	2446.4	32.7	2442.5	24.6	-1.3	-1.5	2442.5	24.59
G18	2.4	72.7	0.50	0.0311	0.0005	0.2079	0.0136	0.0486	0.0030	197.6	6.8	191.8	22.5	128.1	15.6	-3.1	-54.3	197.6	6.75
G19	209.5	759.0	0.04	0.2871	0.0035	4.5825	0.0855	0.1136	0.0015	1627.2	34.7	1746.1	29.7	1857.0	23.2	6.8	12.4	1857.0	23.25
G20	16.5	237.8	0.29	0.0692	0.0009	0.5146	0.0143	0.0535	0.0013	431.1	10.7	421.5	18.5	347.9	14.7	-2.3	-23.9	431.1	10.73
G21	43.3	123.1	0.34	0.3310	0.0041	4.9716	0.1334	0.1094	0.0017	1843.0	39.9	1814.5	33.9	1788.8	27.2	-1.6	-3.0	1788.8	27.19
G22	50.0	93.2	0.34	0.4826	0.0062	10.8269	0.3920	0.1656	0.0027	2538.7	54.0	2508.4	38.5	2513.5	30.8	-1.2	-1.0	2513.5	30.84
G23	46.6	274.1	0.23	0.1705	0.0021	1.6681	0.0348	0.0724	0.0011	1014.6	22.9	996.5	25.5	996.6	20.7	-1.8	-1.8	996.6	20.73
G24	114.6	362.7	0.39	0.2955	0.0036	4.0650	0.0736	0.1022	0.0014	1669.0	35.4	1647.3	29.3	1663.9	22.4	-1.3	-0.3	1663.9	22.35
G25	76.5	416.8	0.44	0.1734	0.0021	1.8130	0.0337	0.0760	0.0011	1030.5	23.1	1050.2	24.6	1095.3	20.0	1.9	5.9	1095.3	19.95
G26	167.6	515.7	0.11	0.3273	0.0039	5.3035	0.0893	0.1168	0.0015	1825.4	38.1	1869.4	29.7	1908.0	22.4	2.4	4.3	1908.0	22.38
G27	81.3	428.0	0.31	0.1853	0.0022	1.8497	0.0341	0.0742	0.0011	1095.8	24.4	1063.3	24.9	1046.9	19.4	-3.1	-4.7	1046.9	19.40
G28	152.2	672.3	0.17	0.2283	0.0027	2.7040	0.0443	0.0865	0.0011	1325.6	28.8	1329.6	26.2	1348.7	20.1	0.3	1.7	1348.7	20.07
G29	27.1	579.1	0.08	0.0497	0.0006	0.3678	0.0084	0.0544	0.0011	312.8	7.6	318.1	13.2	386.0	13.8	1.7	19.0	312.8	7.61
G30	106.9	663.9	0.27	0.1595	0.0019	1.5334	0.0264	0.0702	0.0010	954.1	21.3	943.9	22.6	932.7	17.6	-1.1	-2.3	932.7	17.61
G31	75.2	1823.0	0.39	0.0401	0.0005	0.2864	0.0049	0.0517	0.0008	253.7	6.1	255.8	8.8	270.4	8.0	0.8	6.2	253.7	6.07
G32	125.8	873.7	0.09	0.1504	0.0018	1.4793	0.0242	0.0699	0.0009	903.2	20.3	921.9	21.7	924.8	17.1	2.0	2.3	924.8	17.06
G33	50.9	158.5	0.42	0.2984	0.0037	4.2163	0.0961	0.1046	0.0016	1683.2	36.3	1677.2	31.7	1707.6	25.2	-0.4	1.4	1707.6	25.22
G34	35.2	488.6	0.30	0.0715	0.0009	0.5523	0.0116	0.0558	0.0010	445.2	10.6	446.5	15.8	445.6	13.8	0.3	0.1	445.2	10.59
G35	101.1	576.3	0.12	0.1811	0.0022	1.9159	0.0330	0.0781	0.0011	1072.8	23.8	1086.6	24.5	1149.7	19.6	1.3	6.7	1149.7	19.58
G36	18.2	394.4	0.29	0.0461	0.0006	0.3388	0.0086	0.0533	0.0012	290.8	7.3	296.3	13.4	341.6	13.9	1.9	14.9	290.8	7.27
G37	139.9	307.7	0.37	0.4219	0.0052	9.9433	0.2320	0.1752	0.0024	2269.2	46.9	2429.5	33.9	2608.1	26.3	6.6	13.0	2608.1	26.31
G38	12.3	255.5	1.07	0.0389	0.0006	0.2801	0.0115	0.0526	0.0020	246.3	6.9	250.7	17.9	312.0	20.8	1.8	21.1	246.3	6.95
G39	30.7	97.0	0.46	0.2919	0.0038	4.3153	0.1462	0.1102	0.0021	1651.1	37.9	1696.3	38.4	1802.5	33.0	2.7	8.4	1802.5	33.03
G40	16.8	44.8	0.25	0.3613	0.0049	6.1926	0.2590	0.1239	0.0025	1988.5	46.0	2003.4	42.7	2013.7	36.5	0.7	1.3	2013.7	36.48
G41	23.3	500.7	0.52	0.0433	0.0006	0.2824	0.0069	0.0474	0.0011	273.5	6.8	252.5	11.4	66.9	3.6	-8.3	-308.7	273.5	6.80

Table 4

Gr. No.	Pb (ppm)	U (ppm)	Atomic Th/U	Ratios 206/238	± s.e.	207/235	± s.e.	207/206	± s.e.	Ages (Ma) 206/238	± 2s	207/235	± 2s	207/206	± 2s	% concord. (206/238 / 207/235)	% concord. (206/238 / 207/206)	Best Age (Ma)	±2s
G42	220.4	427.1	0.71	0.4369	0.0053	9.1600	0.1798	0.1537	0.0020	2336.6	47.5	2354.1	32.6	2387.1	24.6	0.7	2.1	2387.1	24.64
G43	36.5	176.2	4.48	0.0896	0.0012	0.7078	0.0202	0.0586	0.0014	552.9	13.6	543.5	22.9	552.3	20.8	-1.7	-0.1	552.9	13.61
G44	6.1	18.6	0.45	0.3014	0.0051	4.1108	0.3013	0.0999	0.0037	1698.2	50.2	1656.4	66.9	1622.0	61.1	-2.5	-4.7	1622.0	61.05
G45	52.4	160.4	0.56	0.2946	0.0037	4.6940	0.1386	0.1165	0.0020	1664.3	37.2	1766.2	35.8	1902.7	30.2	5.8	12.5	1902.7	30.25
G46	10.0	194.9	1.01	0.0426	0.0006	0.2904	0.0106	0.0508	0.0017	268.8	7.3	258.9	16.7	233.6	14.5	-3.8	-15.1	268.8	7.30
G47	16.7	281.6	0.62	0.0537	0.0007	0.3865	0.0110	0.0534	0.0013	337.0	8.6	331.8	16.3	344.6	15.4	-1.5	2.2	337.0	8.57
G48	19.8	188.4	0.21	0.1059	0.0014	0.8947	0.0239	0.0611	0.0013	649.0	15.7	648.9	23.9	642.8	21.2	0.0	-1.0	649.0	15.74
G49	112.3	1957.2	0.13	0.0602	0.0007	0.4946	0.0093	0.0598	0.0010	376.7	9.0	408.1	13.7	596.0	15.4	7.7	36.8	376.7	9.00
G50	19.4	36.4	0.76	0.4432	0.0058	9.6200	0.3714	0.1602	0.0028	2364.9	52.1	2399.1	40.4	2457.6	33.2	1.4	3.8	2457.6	33.19
G51	65.4	413.1	0.34	0.1540	0.0019	1.4520	0.0284	0.0687	0.0011	923.4	21.0	910.7	23.7	889.4	19.0	-1.4	-3.8	889.4	19.02
G52	108.2	750.6	0.26	0.1438	0.0017	1.3418	0.0232	0.0668	0.0010	866.3	19.6	864.0	21.6	831.9	16.9	-0.3	-4.1	866.3	19.61
G53	64.0	107.2	0.43	0.5246	0.0065	13.5604	0.3384	0.1921	0.0026	2718.6	54.7	2719.5	35.0	2760.6	26.8	0.0	1.5	2760.6	26.79
G54	107.5	230.3	0.22	0.4482	0.0055	10.6440	0.2477	0.1749	0.0024	2387.3	49.1	2492.5	34.3	2605.3	26.6	4.2	8.4	2605.3	26.56
G55	1.8	55.9	0.56	0.0300	0.0007	0.1949	0.0199	0.0480	0.0047	190.4	8.6	180.8	33.5	98.8	19.0	-5.3	-92.7	190.4	8.64
G56	13.4	105.4	0.44	0.1208	0.0017	1.0511	0.0442	0.0655	0.0021	735.1	19.8	729.4	37.2	791.7	36.0	-0.8	7.2	735.1	19.79
G57	237.2	586.5	0.99	0.3250	0.0039	5.0405	0.0865	0.1130	0.0015	1814.2	38.1	1826.1	30.2	1848.7	23.0	0.7	1.9	1848.7	23.02
G58	7.6	99.8	0.50	0.0715	0.0010	0.5575	0.0236	0.0572	0.0021	445.3	12.4	449.9	28.4	498.5	29.1	1.0	10.7	445.3	12.39
G59	19.2	115.6	0.47	0.1549	0.0020	1.4733	0.0479	0.0700	0.0017	928.4	22.8	919.5	32.9	927.8	29.4	-1.0	-0.1	927.8	29.41
G60	99.3	189.3	0.32	0.4736	0.0059	10.3123	0.2917	0.1605	0.0024	2499.3	51.9	2463.2	36.2	2461.3	28.4	-1.5	-1.5	2461.3	28.40
G61	103.4	270.4	0.44	0.3539	0.0044	6.1952	0.1499	0.1224	0.0018	1953.2	41.7	2003.8	33.7	1991.1	26.7	2.5	1.9	1991.1	26.68
G62	83.5	1124.6	0.11	0.0777	0.0010	0.7330	0.0142	0.0677	0.0011	482.1	11.5	558.3	17.5	858.2	19.7	13.6	43.8	482.1	11.49
G63	70.9	214.5	0.23	0.3222	0.0040	4.8550	0.1081	0.1130	0.0017	1800.2	38.7	1794.5	32.6	1848.7	25.9	-0.3	2.6	1848.7	25.88
G64	60.3	412.1	0.60	0.1324	0.0016	1.2094	0.0251	0.0677	0.0011	801.3	18.6	804.9	23.1	858.5	19.9	0.5	6.7	801.3	18.56
G65	107.4	486.7	0.36	0.2108	0.0026	2.2616	0.0436	0.0794	0.0012	1233.2	27.4	1200.4	27.1	1183.1	21.3	-2.7	-4.2	1183.1	21.31
G66	57.0	1812.7	0.37	0.0307	0.0004	0.2159	0.0042	0.0505	0.0009	194.9	4.8	198.5	7.7	219.4	7.7	1.8	11.2	194.9	4.75
G67	35.9	452.2	0.59	0.0726	0.0009	0.5337	0.0129	0.0544	0.0011	451.5	10.9	434.2	17.4	389.3	14.2	-4.0	-16.0	451.5	10.94
G68	32.6	253.6	0.29	0.1264	0.0016	1.1181	0.0307	0.0656	0.0014	767.3	18.5	762.1	26.8	793.6	24.1	-0.7	3.3	767.3	18.54
G69	14.7	326.4	0.24	0.0458	0.0006	0.3366	0.0095	0.0536	0.0014	288.7	7.4	294.6	14.6	354.3	15.8	2.0	18.5	288.7	7.40
G70	40.3	243.4	0.44	0.1560	0.0019	1.4719	0.0326	0.0706	0.0012	934.3	21.6	918.9	25.9	947.0	21.8	-1.7	1.3	947.0	21.83
G71	10.5	31.7	0.50	0.3014	0.0043	4.3010	0.2046	0.1038	0.0026	1698.3	42.3	1693.5	47.7	1693.5	42.3	-0.3	-0.3	1693.5	42.31
G72	36.7	315.2	0.20	0.1187	0.0015	0.9706	0.0220	0.0616	0.0011	723.2	17.1	688.8	22.6	660.3	18.5	-5.0	-9.5	723.2	17.06
G73	145.6	258.3	0.62	0.4760	0.0058	10.6259	0.2239	0.1637	0.0022	2509.9	50.8	2491.0	34.1	2494.3	26.1	-0.8	-0.6	2494.3	26.14
G74	11.3	103.5	0.94	0.0906	0.0012	0.7233	0.0258	0.0601	0.0018	559.1	14.7	552.6	28.0	606.1	27.3	-1.2	7.7	559.1	14.66
G75	13.4	204.2	0.25	0.0658	0.0009	0.5384	0.0169	0.0565	0.0015	410.9	10.5	437.4	20.5	470.9	20.9	6.0	12.7	410.9	10.52
G76	44.3	315.2	0.32	0.1375	0.0017	1.2650	0.0271	0.0686	0.0012	830.3	19.3	830.1	24.0	887.3	20.7	0.0	6.4	830.3	19.27
G77	9.8	149.2	0.67	0.0584	0.0008	0.4208	0.0143	0.0541	0.0016	365.7	9.6	356.6	20.2	373.5	19.5	-2.6	2.1	365.7	9.62
G78	25.6	213.5	0.42	0.1140	0.0015	1.0161	0.0301	0.0654	0.0015	695.6	17.2	712.0	27.4	786.3	26.2	2.3	11.5	695.6	17.25
G79	134.5	478.4	0.05	0.2915	0.0036	4.4978	0.0838	0.1124	0.0016	1649.1	35.4	1730.6	30.8	1838.1	24.5	4.7	10.3	1838.1	24.46
G80	100.7	309.6	0.17	0.3228	0.0039	4.9381	0.0954	0.1131	0.0016	1803.3	38.4	1808.8	31.7	1850.1	24.8	0.3	2.5	1850.1	24.81

Table 4

Gr. No.	Pb (ppm)	U (ppm)	Atomic Th/U	Ratios 206/238	± s.e.	207/235	± s.e.	207/206	± s.e.	Ages (Ma) 206/238	± 2s	207/235	± 2s	207/206	± 2s	% concord. (206/238 / 207/235)	% concord. (206/238 / 207/206)	Best Age (Ma)	±2s
G81	96.3	162.2	0.28	0.5411	0.0068	14.9183	0.4360	0.2057	0.0031	2788.2	57.1	2810.0	37.2	2872.2	29.2	0.8	2.9	2872.2	29.15
G82	10.2	378.6	0.56	0.0249	0.0003	0.1703	0.0055	0.0510	0.0015	158.5	4.3	159.7	10.0	239.0	13.6	0.7	33.7	158.5	4.28
G83	145.1	487.7	0.62	0.2630	0.0032	3.5513	0.0642	0.0979	0.0014	1505.0	32.7	1538.7	29.4	1584.3	23.2	2.2	5.0	1584.3	23.18
G84	66.6	205.1	0.12	0.3257	0.0040	5.1437	0.1095	0.1154	0.0017	1817.7	39.0	1843.3	32.7	1886.8	26.0	1.4	3.7	1886.8	25.97
G85	38.7	354.3	0.25	0.1093	0.0014	0.9865	0.0212	0.0659	0.0012	668.8	15.8	696.9	21.7	801.9	20.1	4.0	16.6	668.8	15.81
G86	106.8	209.8	0.60	0.4409	0.0055	9.3673	0.2288	0.1627	0.0024	2354.5	49.0	2374.6	35.6	2483.8	28.1	0.8	5.2	2483.8	28.09
G87	28.8	970.7	0.11	0.0313	0.0004	0.2430	0.0065	0.0556	0.0014	198.6	5.1	220.9	10.9	436.0	18.1	10.1	54.4	198.6	5.13
G88	17.2	377.6	0.37	0.0455	0.0006	0.3223	0.0090	0.0526	0.0013	286.5	7.3	283.6	14.1	310.3	14.1	-1.0	7.7	286.5	7.28
G89	30.9	167.8	0.62	0.1647	0.0022	1.5332	0.0478	0.0690	0.0016	983.0	23.8	943.8	32.5	899.6	27.9	-4.2	-9.3	899.6	27.88
G90	10.9	104.4	0.91	0.0868	0.0013	0.7997	0.0331	0.0673	0.0022	536.5	14.8	596.7	32.9	846.1	39.0	10.1	36.6	536.5	14.83
G91	22.7	59.7	0.47	0.3466	0.0047	5.8724	0.2303	0.1252	0.0026	1918.2	44.6	1957.2	42.5	2030.9	36.5	2.0	5.5	2030.9	36.51
G92	6.5	151.1	1.04	0.0346	0.0005	0.2489	0.0105	0.0517	0.0020	219.5	6.2	225.7	16.7	269.9	19.3	2.8	18.7	219.5	6.23
G93	27.6	173.4	0.66	0.1408	0.0018	1.3147	0.0335	0.0679	0.0013	849.1	20.2	852.2	27.0	865.8	23.5	0.4	1.9	849.1	20.23
G94	120.3	388.8	0.21	0.3047	0.0037	4.7234	0.0891	0.1141	0.0016	1714.7	36.9	1771.4	31.6	1865.2	25.1	3.2	8.1	1865.2	25.13
G95	159.4	1979.6	0.26	0.0809	0.0010	0.6426	0.0110	0.0577	0.0009	501.7	11.8	503.9	15.2	517.2	12.7	0.4	3.0	501.7	11.81
G96	119.4	392.6	0.12	0.3088	0.0038	4.9000	0.1017	0.1152	0.0017	1734.7	37.5	1802.3	32.6	1882.2	26.2	3.7	7.8	1882.2	26.16
G97	16.6	347.8	1.20	0.0373	0.0005	0.2578	0.0075	0.0517	0.0014	235.8	6.1	232.9	12.6	271.3	13.4	-1.3	13.1	235.8	6.09
G98	13.1	178.1	0.48	0.0687	0.0010	0.5664	0.0201	0.0600	0.0018	428.6	11.5	455.7	24.4	604.7	28.2	6.0	29.1	428.6	11.46
G99	66.8	456.0	0.62	0.1315	0.0016	1.2081	0.0256	0.0670	0.0011	796.2	18.6	804.3	23.5	836.2	20.1	1.0	4.8	796.2	18.57
G100	112.7	507.3	0.37	0.2119	0.0026	2.4473	0.0463	0.0833	0.0013	1239.0	27.7	1256.6	27.9	1276.3	22.5	1.4	2.9	1276.3	22.53
G101	26.8	365.5	0.55	0.0677	0.0009	0.5574	0.0134	0.0604	0.0013	422.0	10.4	449.8	17.8	619.4	19.9	6.2	31.9	422.0	10.39
G102	16.5	366.5	0.41	0.0433	0.0006	0.3292	0.0090	0.0565	0.0014	273.5	6.9	289.0	14.2	470.9	19.1	5.4	41.9	273.5	6.92
G103	57.7	332.0	0.42	0.1652	0.0021	1.6141	0.0348	0.0723	0.0012	985.5	22.7	975.7	26.5	993.0	22.1	-1.0	0.8	993.0	22.13
G104	172.2	484.9	0.17	0.3495	0.0043	5.7394	0.1067	0.1215	0.0018	1932.4	40.9	1937.3	32.8	1977.9	25.8	0.3	2.3	1977.9	25.82
G105	15.5	363.7	0.41	0.0410	0.0005	0.2786	0.0080	0.0511	0.0013	258.8	6.7	249.6	13.3	246.7	12.1	-3.7	-4.9	258.8	6.69
G106	251.7	436.4	0.28	0.5271	0.0065	14.2785	0.2696	0.1971	0.0028	2729.1	54.5	2768.4	35.4	2802.2	27.6	1.4	2.6	2802.2	27.56
G107	22.1	306.8	0.42	0.0691	0.0009	0.5338	0.0141	0.0573	0.0013	430.6	10.7	434.3	18.6	501.9	18.6	0.8	14.2	430.6	10.73
G108	92.7	687.2	0.06	0.1430	0.0018	1.3783	0.0264	0.0706	0.0011	861.4	19.9	879.7	23.6	944.4	20.1	2.1	8.8	861.4	19.85
G109	205.1	650.9	0.11	0.3182	0.0039	4.9401	0.0979	0.1130	0.0017	1781.0	38.3	1809.1	32.6	1847.6	26.0	1.6	3.6	1847.6	26.04
G110	77.1	398.2	0.39	0.1851	0.0023	1.9613	0.0418	0.0776	0.0013	1094.9	25.0	1102.3	27.9	1135.9	23.3	0.7	3.6	1135.9	23.29
G111	11.3	163.2	0.21	0.0699	0.0009	0.6472	0.0203	0.0709	0.0019	435.6	11.3	506.8	24.4	955.7	33.4	14.0	54.4	435.6	11.33
G112	77.8	400.0	0.68	0.1707	0.0021	1.6721	0.0355	0.0722	0.0012	1015.9	23.3	998.0	26.7	991.6	21.9	-1.8	-2.5	991.6	21.95
G113	28.8	691.0	0.37	0.0409	0.0005	0.3228	0.0085	0.0571	0.0013	258.3	6.6	284.0	13.3	494.2	19.1	9.1	47.7	258.3	6.56
G114	41.5	548.3	0.31	0.0748	0.0010	0.6020	0.0157	0.0584	0.0013	465.1	11.5	478.5	19.5	542.9	19.3	2.8	14.3	465.1	11.52
G115	48.9	749.7	0.20	0.0670	0.0009	0.5177	0.0126	0.0564	0.0012	418.1	10.3	423.6	17.0	468.1	16.4	1.3	10.7	418.1	10.27
G116	131.6	178.1	0.57	0.6173	0.0077	20.6797	0.4683	0.2464	0.0036	3099.2	61.0	3123.7	37.3	3161.7	29.2	0.8	2.0	3161.7	29.24
G117	26.3	43.8	1.16	0.4553	0.0060	9.9346	0.3703	0.1635	0.0030	2418.7	53.3	2428.7	41.9	2492.2	34.8	0.4	2.9	2492.2	34.79
G118	21.3	573.5	0.39	0.0360	0.0005	0.2618	0.0088	0.0526	0.0016	228.2	6.1	236.1	14.1	309.8	17.1	3.4	26.4	228.2	6.10
G119	14.4	364.6	0.29	0.0395	0.0005	0.2858	0.0084	0.0538	0.0014	249.5	6.4	255.2	13.7	362.7	17.1	2.3	31.2	249.5	6.45

Table 4

Gr. No.	Pb (ppm)	U (ppm)	Atomic Th/U	**Ratios**						**Ages (Ma)**						% concord. (206/238 / 207/235)	% concord. (206/238 / 207/206)	Best Age (Ma)	±2s
				206/238	**± s.e.**	**207/235**	**± s.e.**	**207/206**	**± s.e.**	**206/238**	**± 2s**	**207/235**	**± 2s**	**207/206**	**± 2s**				
G120	31.9	89.5	0.29	0.3410	0.0044	5.3732	0.1565	0.1184	0.0021	1891.3	42.0	1880.6	37.8	1932.1	31.5	-0.6	2.1	1932.1	31.53
G121	386.8	898.0	0.17	0.4202	0.0052	9.3923	0.1831	0.1621	0.0024	2261.5	47.0	2377.1	35.4	2477.9	28.2	4.9	8.7	2477.9	28.18
G122	85.0	197.7	0.39	0.3959	0.0049	7.3109	0.1679	0.1392	0.0022	2150.1	45.6	2150.1	35.9	2217.0	29.0	0.0	3.0	2217.0	28.96
G123	194.4	381.4	0.42	0.4577	0.0057	10.0576	0.2001	0.1636	0.0024	2429.5	50.0	2440.1	35.8	2493.6	28.4	0.4	2.6	2493.6	28.41
G124	189.0	347.8	0.54	0.4698	0.0059	10.3368	0.2362	0.1622	0.0025	2482.6	51.3	2465.4	36.7	2478.4	29.3	-0.7	-0.2	2478.4	29.31
G125	27.7	309.6	0.93	0.0748	0.0010	0.6080	0.0191	0.0596	0.0016	465.2	12.0	482.3	23.0	588.4	24.4	3.5	20.9	465.2	12.00
G126	8.3	168.8	0.21	0.0505	0.0008	0.3898	0.0205	0.0552	0.0026	317.3	9.9	334.3	27.8	419.9	32.9	5.1	24.4	317.3	9.94
G127	170.7	714.3	0.28	0.2339	0.0029	2.8092	0.0556	0.0879	0.0014	1354.6	30.3	1358.0	30.0	1380.3	24.4	0.2	1.9	1380.3	24.43
G128	10.8	68.1	1.12	0.1259	0.0018	1.1023	0.0443	0.0657	0.0020	764.4	20.4	754.5	36.6	797.2	34.7	-1.3	4.1	764.4	20.38
G129	71.6	537.1	0.29	0.1338	0.0017	1.3990	0.0316	0.0761	0.0014	809.5	19.2	888.5	26.1	1098.0	24.9	8.9	26.3	809.5	19.22
G130	3.8	69.9	0.31	0.0537	0.0011	0.3917	0.0326	0.0541	0.0040	337.1	13.5	335.6	44.6	374.4	47.1	-0.5	9.9	337.1	13.46
G131	85.6	271.3	0.30	0.3088	0.0039	4.7459	0.1263	0.1125	0.0020	1734.6	38.7	1775.4	36.5	1840.5	30.6	2.3	5.8	1840.5	30.63
G132	157.1	806.6	0.64	0.1738	0.0022	1.8451	0.0360	0.0757	0.0012	1033.0	23.6	1061.7	26.5	1087.9	22.1	2.7	5.0	1087.9	22.07
G133	13.4	356.2	0.16	0.0392	0.0005	0.2792	0.0088	0.0523	0.0015	247.6	6.6	250.0	14.2	298.1	15.6	0.9	16.9	247.6	6.58
G134	106.3	201.4	0.42	0.4703	0.0059	10.7807	0.2489	0.1678	0.0027	2484.9	51.6	2504.4	37.5	2536.1	30.2	0.8	2.0	2536.1	30.16
G135	117.7	232.2	0.35	0.4630	0.0059	10.1534	0.2624	0.1661	0.0027	2452.9	51.6	2448.8	38.4	2518.8	31.2	-0.2	2.6	2518.8	31.20
G136	63.1	586.5	0.25	0.1066	0.0014	1.0166	0.0280	0.0683	0.0015	653.0	16.2	712.2	26.1	876.2	26.7	8.3	25.5	653.0	16.19
G137	57.6	107.2	0.61	0.4590	0.0058	10.0419	0.2797	0.1602	0.0027	2434.9	51.6	2438.6	39.0	2458.2	31.9	0.2	0.9	2458.2	31.91
G138	12.4	208.9	0.51	0.0552	0.0008	0.4175	0.0174	0.0560	0.0021	346.6	9.8	354.3	24.0	453.6	27.6	2.2	23.6	346.6	9.77
G139	140.9	511.0	0.29	0.2667	0.0033	3.5364	0.0738	0.0991	0.0016	1523.9	33.8	1535.4	32.6	1606.3	27.0	0.7	5.1	1606.3	26.95
G140	68.0	428.9	0.28	0.1578	0.0022	1.5747	0.0574	0.0741	0.0020	944.5	24.1	960.3	37.3	1043.6	35.2	1.6	9.5	1043.6	35.24
12061703 Upper reaches mainstream																			
G2	67	541	0.06	0.1313	0.0015	1.2203	0.0166	0.0667	0.0005	795.3	17.2	809.9	15.4	827.2	10.2	1.8	3.8	795.3	17.2
G3	55	287	0.20	0.1919	0.0022	2.0321	0.0289	0.0763	0.0006	1131.4	24.0	1126.3	19.0	1102.2	12.0	-0.5	-2.7	1102.2	12.0
G6	71	174	0.63	0.3503	0.0041	5.6654	0.0854	0.1181	0.0009	1935.8	38.7	1926.1	23.7	1927.8	14.1	-0.5	-0.4	1927.8	14.1
G7	17	187	0.80	0.0763	0.0009	0.5945	0.0113	0.0568	0.0008	474.1	11.1	473.7	14.1	484.9	12.2	-0.1	2.2	474.1	11.1
G8	37	480	0.59	0.0705	0.0008	0.5389	0.0078	0.0555	0.0005	439.2	9.9	437.7	10.6	432.8	8.0	-0.4	-1.5	439.2	9.9
G10	53	97	0.40	0.4827	0.0056	11.2491	0.1897	0.1681	0.0012	2538.9	48.9	2544.0	25.6	2538.4	15.0	0.2	0.0	2538.4	15.0
G11	155	675	0.33	0.2205	0.0025	2.4727	0.0333	0.0814	0.0006	1284.3	26.7	1264.1	19.5	1230.6	11.5	-1.6	-4.4	1230.6	11.5
G14	51	76	1.37	0.4796	0.0057	10.7667	0.2035	0.1667	0.0013	2525.6	49.2	2503.2	26.5	2525.0	16.2	-0.9	0.0	2525.0	16.2
G15	123	320	0.73	0.3263	0.0037	4.9868	0.0673	0.1118	0.0008	1820.5	36.4	1817.1	22.6	1828.4	12.9	-0.2	0.4	1828.4	12.9
G16	82	147	0.52	0.4829	0.0056	11.1910	0.1780	0.1691	0.0012	2540.0	48.6	2539.2	25.3	2548.3	14.6	0.0	0.3	2548.3	14.6
G18	37	829	0.94	0.0369	0.0004	0.2768	0.0043	0.0547	0.0006	233.5	5.3	248.1	7.1	398.3	8.7	5.9	41.4	233.5	5.3
G19	423	1304	0.20	0.3198	0.0037	4.9834	0.0633	0.1122	0.0007	1788.7	35.7	1816.5	22.1	1835.0	12.3	1.5	2.5	1835.0	12.3
G20	517	1212	0.30	0.3999	0.0046	7.9008	0.0990	0.1416	0.0009	2168.6	42.0	2219.8	23.4	2247.1	12.7	2.3	3.5	2247.1	12.7
G21	128	435	0.16	0.2950	0.0034	4.4878	0.0647	0.1113	0.0008	1666.3	33.9	1728.7	22.7	1819.9	13.7	3.6	8.4	1819.9	13.7
G22	100	174	0.77	0.4686	0.0054	10.3861	0.1602	0.1618	0.0011	2477.6	47.6	2469.8	25.1	2474.6	14.4	-0.3	-0.1	2474.6	14.4
G23	17	378	0.05	0.0472	0.0006	0.3632	0.0071	0.0566	0.0009	297.4	7.1	314.6	10.8	476.4	13.1	5.5	37.6	297.4	7.1

Table 4

Gr. No.	Pb (ppm)	U (ppm)	Atomic Th/U	Ratios						Ages (Ma)						% concord.	% concord.		
				206/238	± s.e.	207/235	± s.e.	207/206	± s.e.	206/238	± 2s	207/235	± 2s	207/206	± 2s	(206/238 / 207/235)	(206/238 / 207/206)	Best Age (Ma)	±2s
G24	95	959	0.23	0.0986	0.0011	0.8646	0.0122	0.0637	0.0006	606.0	13.4	632.6	13.6	730.4	10.4	4.2	17.0	606.0	13.4
G25	6	181	0.53	0.0291	0.0004	0.2010	0.0062	0.0503	0.0014	185.0	5.1	186.0	10.8	207.0	12.0	0.5	10.7	185.0	5.1
G26	129	206	1.11	0.4860	0.0056	11.3947	0.1621	0.1714	0.0011	2553.4	48.4	2556.0	24.8	2571.4	13.8	0.1	0.7	2571.4	13.8
G27	29	982	0.54	0.0272	0.0003	0.1962	0.0033	0.0531	0.0007	172.7	4.0	181.9	6.0	331.4	8.8	5.1	47.9	172.7	4.0
G28	12	42	0.45	0.2725	0.0034	4.0420	0.0974	0.1061	0.0013	1553.4	34.2	1642.7	28.3	1733.3	21.7	5.4	10.4	1733.3	21.7
G29	22	795	0.41	0.0261	0.0003	0.1852	0.0033	0.0523	0.0007	166.2	3.9	172.5	5.9	297.7	8.7	3.7	44.2	166.2	3.9
G30	13	333	0.49	0.0363	0.0004	0.2530	0.0049	0.0510	0.0008	229.9	5.5	229.0	8.3	239.5	8.2	-0.4	4.0	229.9	5.5
G31	15	42	0.81	0.2950	0.0037	4.7245	0.1200	0.1135	0.0014	1666.6	36.7	1771.6	29.4	1855.6	22.5	5.9	10.2	1855.6	22.5
G32	19	311	1.01	0.0503	0.0006	0.3636	0.0062	0.0529	0.0007	316.2	7.4	314.9	9.6	325.8	8.5	-0.4	3.0	316.2	7.4
G33	75	363	1.01	0.1665	0.0019	1.6488	0.0231	0.0724	0.0006	992.5	21.2	989.1	17.8	996.1	11.5	-0.3	0.4	996.1	11.5
G34	36	60	0.87	0.4767	0.0056	10.7926	0.2060	0.1682	0.0014	2513.1	49.1	2505.4	26.6	2540.0	16.4	-0.3	1.1	2540.0	16.4
G35	217	630	0.26	0.3321	0.0038	5.2275	0.0692	0.1151	0.0008	1848.4	36.8	1857.1	22.7	1880.7	13.0	0.5	1.7	1880.7	13.0
G36	106	307	0.19	0.3374	0.0039	5.4038	0.0751	0.1147	0.0008	1874.1	37.3	1885.5	23.0	1874.5	13.3	0.6	0.0	1874.5	13.3
G37	123	346	0.22	0.3438	0.0039	5.4646	0.0741	0.1166	0.0008	1904.7	37.8	1895.1	23.0	1904.3	13.2	-0.5	0.0	1904.3	13.2
G38	23	589	0.16	0.0405	0.0005	0.2877	0.0047	0.0516	0.0006	255.7	5.9	256.8	7.8	269.5	7.2	0.4	5.1	255.7	5.9
G39	56	95	0.68	0.4894	0.0058	11.6346	0.2164	0.1784	0.0014	2567.9	49.8	2575.5	26.6	2638.2	16.2	0.3	2.7	2638.2	16.2
G40	120	767	0.13	0.1616	0.0019	1.5946	0.0209	0.0721	0.0005	965.7	20.5	968.1	17.0	989.3	10.7	0.2	2.4	989.3	10.7
G41	365	603	1.23	0.4806	0.0055	11.0826	0.1453	0.1677	0.0011	2530.1	47.8	2530.1	24.5	2535.0	13.5	0.0	0.2	2535.0	13.5
G46	17	320	1.09	0.0434	0.0005	0.3182	0.0059	0.0532	0.0008	274.1	6.5	280.5	9.4	338.6	9.8	2.3	19.1	274.1	6.5
G47	185	533	0.35	0.3260	0.0037	5.0902	0.0680	0.1133	0.0008	1819.1	36.3	1834.5	22.7	1853.6	13.1	0.8	1.9	1853.6	13.1
G48	88	177	0.38	0.4478	0.0052	9.4370	0.1496	0.1535	0.0011	2385.5	46.1	2381.4	25.2	2385.7	14.9	-0.2	0.0	2385.7	14.9
G49	102	260	0.41	0.3605	0.0042	5.9552	0.0898	0.1219	0.0009	1984.6	39.4	1969.3	24.0	1983.8	14.5	-0.8	0.0	1983.8	14.5
G50	78	213	0.39	0.3404	0.0039	5.3860	0.0780	0.1151	0.0009	1888.5	37.7	1882.6	23.4	1882.1	14.0	-0.3	-0.3	1882.1	14.0
G51	9	201	1.01	0.0364	0.0005	0.2854	0.0073	0.0579	0.0013	230.2	6.0	254.9	11.8	527.1	19.7	9.7	56.3	230.2	6.0
G52	30	55	0.38	0.4910	0.0058	11.4486	0.2271	0.1699	0.0014	2575.2	50.2	2560.4	27.1	2557.0	17.0	-0.6	-0.7	2557.0	17.0
G53	347	1055	0.11	0.3306	0.0038	5.1153	0.0652	0.1130	0.0008	1841.0	36.5	1838.6	22.5	1847.9	12.8	-0.1	0.4	1847.9	12.8
G54	149	435	0.20	0.3364	0.0039	5.3131	0.0705	0.1149	0.0008	1869.4	37.1	1871.0	22.9	1877.8	13.3	0.1	0.4	1877.8	13.3
G55	228	540	0.03	0.4222	0.0048	8.2920	0.1092	0.1436	0.0010	2270.4	43.7	2263.4	24.1	2270.6	13.6	-0.3	0.0	2270.6	13.6
G56	175	412	0.37	0.3936	0.0045	8.4202	0.1133	0.1564	0.0011	2139.7	41.7	2277.4	24.2	2416.8	14.0	6.0	11.5	2416.8	14.0
G57	123	273	0.40	0.4102	0.0047	7.9410	0.1113	0.1397	0.0010	2215.8	43.1	2224.3	24.3	2223.0	14.0	0.4	0.3	2223.0	14.0
G58	181	496	0.48	0.3325	0.0038	5.3718	0.0720	0.1178	0.0008	1850.6	36.9	1880.4	23.0	1923.7	13.5	1.6	3.8	1923.7	13.5
G60	92	126	0.44	0.6309	0.0073	22.7002	0.3958	0.2601	0.0019	3153.3	58.0	3214.2	26.7	3247.4	15.5	1.9	2.9	3247.4	15.5
G61	11	435	0.87	0.0221	0.0003	0.1566	0.0033	0.0513	0.0009	141.0	3.5	147.7	6.1	253.4	9.6	4.6	44.4	141.0	3.5
G62	85	220	0.40	0.3546	0.0041	5.8341	0.0855	0.1199	0.0009	1956.5	38.9	1951.5	23.9	1955.3	14.4	-0.3	-0.1	1955.3	14.4
G63	214	563	0.60	0.3342	0.0038	5.2543	0.0716	0.1137	0.0008	1858.7	37.0	1861.5	23.0	1859.5	13.5	0.1	0.0	1859.5	13.5
G64	117	314	0.18	0.3618	0.0042	6.0448	0.0899	0.1233	0.0009	1990.9	39.5	1982.3	24.1	2004.5	14.6	-0.4	0.7	2004.5	14.6
G65	28	363	0.48	0.0718	0.0008	0.5462	0.0088	0.0558	0.0006	446.8	10.1	442.5	11.8	444.4	9.6	-1.0	-0.5	446.8	10.1
G66	82	147	0.57	0.4772	0.0056	10.9195	0.1873	0.1678	0.0013	2515.2	48.5	2516.3	26.1	2535.6	15.9	0.0	0.8	2535.6	15.9
G67	156	432	0.43	0.3318	0.0038	5.1346	0.0740	0.1129	0.0009	1847.0	37.0	1841.9	23.4	1846.1	14.2	-0.3	0.0	1846.1	14.2

Table 4

Gr. No.	Pb (ppm)	U (ppm)	Atomic Th/U	Ratios 206/238	± s.e.	207/235	± s.e.	207/206	± s.e.	Ages (Ma) 206/238	± 2s	207/235	± 2s	207/206	± 2s	% concord. (206/238 / 207/235)	% concord. (206/238 / 207/206)	Best Age (Ma)	±2s
G68	62	92	0.97	0.5171	0.0061	13.2105	0.2540	0.1841	0.0015	2687.0	51.8	2694.8	27.1	2689.8	16.9	0.3	0.1	2689.8	16.9
G69	14	178	0.76	0.0699	0.0009	0.5301	0.0102	0.0569	0.0008	435.4	10.2	431.9	13.8	486.9	12.8	-0.8	10.6	435.4	10.2
G70	164	530	0.21	0.3039	0.0035	4.7631	0.0623	0.1142	0.0008	1710.7	34.3	1778.4	22.6	1867.1	13.5	3.8	8.4	1867.1	13.5
G71	26	65	0.30	0.3816	0.0045	6.6380	0.1310	0.1290	0.0012	2083.5	42.3	2064.4	26.8	2084.1	18.0	-0.9	0.0	2084.1	18.0
G72	160	297	0.40	0.4794	0.0055	11.0423	0.1626	0.1668	0.0012	2524.8	48.0	2526.7	25.3	2525.8	14.9	0.1	0.0	2525.8	14.9
G73	210	611	0.33	0.3252	0.0037	5.0867	0.0705	0.1133	0.0008	1814.8	36.3	1833.9	23.2	1853.3	14.0	1.0	2.1	1853.3	14.0
G74	320	999	0.10	0.3241	0.0037	5.1226	0.0656	0.1143	0.0008	1809.7	36.0	1839.9	22.7	1868.7	13.3	1.6	3.2	1868.7	13.3
G75	54	144	0.47	0.3370	0.0040	5.4380	0.0985	0.1145	0.0010	1872.4	38.2	1890.9	25.4	1871.4	16.9	1.0	-0.1	1871.4	16.9
G76	27	339	0.52	0.0727	0.0009	0.5536	0.0092	0.0559	0.0007	452.3	10.3	447.4	12.2	449.2	9.9	-1.1	-0.7	452.3	10.3
G77	48	604	0.59	0.0717	0.0008	0.5525	0.0081	0.0558	0.0005	446.1	10.0	446.7	10.9	444.8	8.3	0.1	-0.3	446.1	10.0
G78	42	132	0.37	0.2961	0.0035	4.1619	0.0688	0.1036	0.0009	1672.0	34.4	1666.6	24.0	1688.7	15.8	-0.3	1.0	1688.7	15.8
G79	140	412	0.31	0.3233	0.0037	4.9911	0.0702	0.1124	0.0009	1805.8	36.1	1817.8	23.3	1837.9	14.2	0.7	1.7	1837.9	14.2
G80	38	175	1.30	0.1650	0.0020	1.6640	0.0299	0.0733	0.0008	984.5	21.7	994.9	20.7	1021.7	15.8	1.0	3.6	1021.7	15.8
G81	218	614	0.28	0.3384	0.0039	5.3108	0.0706	0.1151	0.0008	1879.1	37.3	1870.6	23.1	1881.9	13.7	-0.5	0.2	1881.9	13.7
G82	420	798	0.53	0.4576	0.0052	10.2939	0.1376	0.1608	0.0011	2428.8	46.3	2461.6	24.9	2464.4	14.5	1.3	1.4	2464.4	14.5
G83	68	163	0.60	0.3715	0.0043	6.7949	0.1119	0.1324	0.0011	2036.3	40.6	2085.1	25.2	2129.8	16.0	2.3	4.4	2129.8	16.0
G85	348	1177	0.05	0.3060	0.0035	4.9994	0.0640	0.1179	0.0008	1720.8	34.5	1819.2	22.7	1924.0	13.7	5.4	10.6	1924.0	13.7
G86	73	396	0.53	0.1692	0.0020	1.6912	0.0245	0.0729	0.0006	1007.9	21.5	1005.2	18.4	1010.9	12.4	-0.3	0.3	1010.9	12.4
G87	92	234	0.70	0.3350	0.0039	5.1582	0.0826	0.1136	0.0010	1862.7	37.6	1845.7	24.5	1858.3	15.8	-0.9	-0.2	1858.3	15.8
G89	161	379	0.39	0.3963	0.0045	8.5621	0.1178	0.1601	0.0012	2152.0	41.9	2292.5	24.8	2456.4	15.0	6.1	12.4	2456.4	15.0
G92	32	94	0.54	0.3080	0.0037	4.5067	0.0971	0.1067	0.0012	1731.1	36.7	1732.2	27.4	1742.9	20.0	0.1	0.7	1742.9	20.0
G93	104	663	0.88	0.1331	0.0015	1.2921	0.0181	0.0714	0.0006	805.3	17.4	842.2	16.5	968.9	12.0	4.4	16.9	805.3	17.4
G94	23	471	0.16	0.0514	0.0006	0.3657	0.0065	0.0522	0.0007	323.0	7.6	316.4	10.0	294.6	8.4	-2.1	-9.7	323.0	7.6
G95	57	90	1.22	0.4710	0.0056	10.7888	0.2190	0.1632	0.0015	2487.7	49.0	2505.1	27.7	2489.4	18.2	0.7	0.1	2489.4	18.2
G96	21	498	0.41	0.0407	0.0005	0.2918	0.0057	0.0522	0.0008	257.1	6.2	260.0	9.2	292.9	9.4	1.1	12.2	257.1	6.2
G97	16	312	0.96	0.0415	0.0005	0.2982	0.0058	0.0527	0.0008	262.2	6.3	265.0	9.5	314.6	10.0	1.0	16.7	262.2	6.3
G98	460	1325	0.11	0.3505	0.0040	6.8748	0.0903	0.1429	0.0011	1936.8	38.2	2095.4	24.1	2263.0	14.7	7.6	14.4	2263.0	14.7
G99	134	392	0.33	0.3234	0.0037	5.0071	0.0738	0.1128	0.0009	1806.2	36.3	1820.5	23.8	1844.8	15.1	0.8	2.1	1844.8	15.1
G101	23	287	0.76	0.0708	0.0009	0.5633	0.0117	0.0590	0.0010	441.2	10.6	453.6	15.1	567.5	15.4	2.7	22.2	441.2	10.6
G104	135	394	0.20	0.3354	0.0039	5.2424	0.0771	0.1145	0.0009	1864.4	37.4	1859.5	24.1	1871.4	15.3	-0.3	0.4	1871.4	15.3
G105	15	210	1.19	0.0554	0.0007	0.4347	0.0098	0.0578	0.0011	347.7	8.6	366.5	13.9	523.7	16.4	5.1	33.6	347.7	8.6
G106	223	673	0.12	0.3311	0.0038	5.0941	0.0702	0.1129	0.0009	1843.6	36.8	1835.1	23.6	1846.0	14.6	-0.5	0.1	1846.0	14.6
G108	351	1017	0.40	0.3201	0.0037	4.9420	0.0663	0.1127	0.0009	1790.3	35.7	1809.5	23.3	1844.0	14.5	1.1	2.9	1844.0	14.5
G111	214	546	0.42	0.3596	0.0041	5.9245	0.0808	0.1216	0.0010	1980.4	39.1	1964.8	24.2	1979.5	15.0	-0.8	0.0	1979.5	15.0
G112	28	745	0.56	0.0350	0.0004	0.2484	0.0044	0.0518	0.0007	222.0	5.2	225.3	7.5	275.3	8.2	1.4	19.3	222.0	5.2
G113	167	358	0.84	0.3872	0.0041	8.1442	0.0808	0.1549	0.0010	2109.7	38.3	2247.2	22.3	2400.3	12.7	6.1	12.1	2400.3	12.7
G114	10	199	1.10	0.0405	0.0004	0.3217	0.0044	0.0578	0.0007	256.0	5.2	283.2	8.1	521.8	11.7	9.6	50.9	256.0	5.2
G115	176	533	0.22	0.3245	0.0045	5.8809	0.1244	0.1310	0.0013	1811.6	43.5	1958.4	29.2	2111.8	18.6	7.5	14.2	2111.8	18.6
G116	153	900	0.48	0.1575	0.0006	1.6573	0.0087	0.0751	0.0014	942.8	6.1	992.4	23.2	1070.6	25.3	5.0	11.9	1070.6	25.3

Table 4

Gr. No.	Pb (ppm)	U (ppm)	Atomic Th/U	Ratios						Ages (Ma)						% concord. (206/238 / 207/235)	% concord. (206/238 / 207/206)	Best Age (Ma)	±2s
				206/238	± s.e.	207/235	± s.e.	207/206	± s.e.	206/238	± 2s	207/235	± 2s	207/206	± 2s				
G117	135	216	1.28	0.4593	0.0038	9.9574	0.0894	0.1583	0.0011	2436.6	33.1	2430.8	19.8	2437.4	14.2	-0.2	0.0	2437.4	14.2
G119	113	312	0.13	0.3596	0.0053	6.3433	0.1575	0.1306	0.0013	1980.5	50.4	2024.5	31.5	2105.6	19.3	2.2	5.9	2105.6	19.3
G120	105	572	0.65	0.1627	0.0006	1.5883	0.0142	0.0715	0.0019	971.6	6.2	965.6	33.7	972.9	34.8	-0.6	0.1	972.9	34.8
G121	1	16	0.84	0.0628	0.0042	0.4973	0.0982	0.0568	0.0011	392.4	50.5	409.9	46.2	483.4	16.4	4.3	18.8	392.4	50.5
G124	57	87	0.53	0.5617	0.0030	17.6672	0.0668	0.2230	0.0011	2873.5	24.4	2971.8	14.0	3002.7	11.0	3.3	4.3	3002.7	11.0
G125	9	207	0.78	0.0391	0.0024	0.2736	0.0604	0.0511	0.0013	247.1	29.2	245.6	28.6	244.9	12.4	-0.6	-0.9	247.1	29.2
G126	199	549	0.36	0.3388	0.0067	5.4759	0.3680	0.1180	0.0020	1880.9	64.1	1896.8	44.9	1925.7	31.1	0.8	2.3	1925.7	31.1
G127	77	340	0.66	0.2000	0.0005	2.1579	0.0070	0.0793	0.0011	1175.5	5.5	1167.6	20.4	1178.6	21.4	-0.7	0.3	1178.6	21.4
G128	107	293	0.51	0.3318	0.0039	5.9841	0.0818	0.1312	0.0010	1847.2	37.9	1973.5	24.5	2114.6	15.1	6.4	12.6	2114.6	15.1
G129	31	170	1.53	0.1308	0.0023	1.2288	0.0324	0.0676	0.0007	792.6	26.5	813.8	23.2	854.8	13.9	2.6	7.3	792.6	26.5
G130	283	664	0.48	0.3840	0.0039	6.9625	0.1011	0.1316	0.0012	2094.9	36.1	2106.7	24.3	2119.0	17.7	0.6	1.1	2119.0	17.7
G131	294	652	0.48	0.4147	0.0016	9.4565	0.0230	0.1687	0.0009	2236.5	14.3	2383.3	11.7	2544.6	10.9	6.2	12.1	2544.6	10.9
G132	17	36	1.29	0.3553	0.0044	5.9255	0.1013	0.1208	0.0011	1960.0	42.0	1965.0	26.8	1967.5	17.2	0.3	0.4	1967.5	17.2
G133	144	4010	0.64	0.0321	0.0048	0.2546	0.1345	0.0573	0.0014	203.6	59.6	230.3	61.9	504.3	20.6	11.6	59.6	203.6	59.6
G134	214	638	0.27	0.3229	0.0045	4.9141	0.1632	0.1131	0.0016	1803.9	43.8	1804.7	33.7	1849.0	25.6	0.0	2.4	1849.0	25.6
G135	63	121	0.29	0.4742	0.0004	10.4823	0.0035	0.1654	0.0005	2501.8	3.2	2478.4	6.0	2512.0	7.2	-0.9	0.4	2512.0	7.2
G137	117	215	1.19	0.4143	0.0056	8.3435	0.1947	0.1509	0.0015	2234.6	50.9	2269.1	30.7	2356.0	20.1	1.5	5.2	2356.0	20.1
G138	20	350	1.51	0.0407	0.0034	0.3041	0.0735	0.0543	0.0011	257.2	42.0	269.6	40.7	385.2	14.3	4.6	33.2	257.2	42.0
G139	65	274	0.11	0.2444	0.0049	2.9931	0.1474	0.0894	0.0014	1409.7	50.4	1405.9	38.6	1411.7	25.3	-0.3	0.1	1411.7	25.3
G140	378	771	0.45	0.4400	0.0005	9.4163	0.0066	0.1565	0.0010	2350.4	4.6	2379.4	11.8	2418.2	13.0	1.2	2.8	2418.2	13.0
G141	24	350	1.29	0.0533	0.0029	0.4226	0.0492	0.0567	0.0009	334.8	35.0	357.9	33.4	480.7	13.4	6.5	30.3	334.8	35.0
G142	328	1053	0.08	0.3171	0.0050	4.9796	0.1300	0.1128	0.0013	1775.6	49.3	1815.9	33.1	1845.0	21.0	2.2	3.8	1845.0	21.0
G143	88	315	0.62	0.2477	0.0007	2.9764	0.0088	0.0900	0.0010	1426.7	6.8	1401.6	16.7	1425.7	17.5	-1.8	-0.1	1425.7	17.5
G144	27	633	0.80	0.0360	0.0036	0.2779	0.0692	0.0561	0.0010	228.1	45.3	249.0	45.3	454.7	13.9	8.4	49.9	228.1	45.3
G146	50	82	1.22	0.4567	0.0004	9.8590	0.0049	0.1601	0.0008	2424.9	3.8	2421.7	9.1	2456.4	10.3	-0.1	1.3	2456.4	10.3
G147	253	412	0.95	0.4828	0.0029	11.1006	0.0538	0.1688	0.0010	2539.6	24.9	2531.6	15.4	2546.1	12.1	-0.3	0.3	2546.1	12.1
G149	172	475	0.43	0.3353	0.0055	5.8376	0.2183	0.1305	0.0017	1864.1	53.1	1952.0	36.3	2105.1	24.2	4.5	11.5	2105.1	24.2
G150	140	357	0.36	0.3650	0.0056	6.1940	0.1630	0.1233	0.0015	2005.6	52.5	2003.6	33.7	2004.1	21.9	-0.1	-0.1	2004.1	21.9
14052705 Song Trac																			
G1	33	324	1.58	0.0721	0.0009	0.5224	0.0104	0.0543	0.0008	449.0	10.8	426.8	13.9	384.3	9.7	-5.2	-16.8	449.0	10.8
G2	46	183	1.03	0.2001	0.0025	2.1439	0.0412	0.0788	0.0009	1176.0	26.3	1163.1	23.4	1166.1	20.7	-1.1	-0.8	1166.1	20.7
G3	182	357	0.41	0.4592	0.0054	9.9951	0.1486	0.1577	0.0012	2435.9	47.7	2434.3	25.7	2430.8	18.5	-0.1	-0.2	2430.8	18.5
G4	106	276	0.62	0.3343	0.0040	5.2041	0.0862	0.1142	0.0010	1859.0	38.5	1853.3	25.0	1867.8	19.3	-0.3	0.5	1867.8	19.3
G5	247	2139	0.26	0.1146	0.0014	1.1862	0.0178	0.0759	0.0007	699.3	15.7	794.2	16.6	1092.2	17.0	11.9	36.0	699.3	15.7
G6	212	585	0.33	0.3422	0.0040	6.1505	0.0869	0.1293	0.0010	1897.3	38.5	1997.4	24.3	2088.6	17.9	5.0	9.2	2088.6	17.9
G7	279	1034	0.06	0.2799	0.0033	4.4119	0.0600	0.1129	0.0008	1591.1	32.9	1714.6	22.9	1846.8	17.3	7.2	13.8	1846.8	17.3
G8	6	94	0.72	0.0551	0.0009	0.3996	0.0165	0.0518	0.0019	346.0	10.9	341.3	22.9	278.4	22.4	-1.4	-24.3	346.0	10.9
G9	100	92	2.05	0.3096	0.0039	4.5377	0.1102	0.1101	0.0014	1738.8	38.5	1737.9	29.7	1800.9	25.6	-0.1	3.4	1800.9	25.6

Table 4

Gr. No.	Pb (ppm)	U (ppm)	Atomic Th/U	Ratios 206/238	± s.e.	207/235	± s.e.	207/206	± s.e.	Ages (Ma) 206/238	± 2s	207/235	± 2s	207/206	± 2s	% concord. (206/238 207/235)	% concord. (206/238 207/206)	Best Age (Ma)	±2s
G10	28	365	1.50	0.0556	0.0007	0.4113	0.0100	0.0534	0.0011	348.8	8.9	349.8	14.1	344.1	16.4	0.3	-1.4	348.8	8.9
G11	30	393	0.56	0.0685	0.0009	0.5489	0.0114	0.0573	0.0009	426.9	10.4	444.3	14.5	503.9	17.4	3.9	15.3	426.9	10.4
G12	258	566	0.59	0.3920	0.0046	7.4881	0.1140	0.1359	0.0011	2132.3	42.7	2171.6	25.2	2175.0	18.6	1.8	2.0	2175.0	18.6
G13	46	77	1.03	0.4601	0.0059	10.7850	0.3011	0.1606	0.0018	2439.8	51.7	2504.8	31.4	2462.2	25.5	2.6	0.9	2462.2	25.5
G14	90	59	1.74	0.3253	0.0042	4.9219	0.1347	0.1116	0.0015	1815.8	40.9	1806.0	31.8	1824.8	27.7	-0.5	0.5	1824.8	27.7
G15	48	82	0.57	0.4910	0.0061	11.3532	0.2737	0.1693	0.0017	2575.0	52.7	2552.6	29.8	2550.9	23.4	-0.9	-0.9	2550.9	23.4
G16	44	284	0.32	0.1523	0.0018	1.4149	0.0247	0.0694	0.0008	913.6	20.5	895.2	19.7	910.4	18.0	-2.1	-0.4	910.4	18.0
G17	99	244	0.78	0.3374	0.0040	5.2768	0.0948	0.1127	0.0010	1874.1	38.9	1865.1	25.8	1843.2	20.4	-0.5	-1.7	1843.2	20.4
G18	15	78	1.26	0.1417	0.0019	1.3124	0.0382	0.0652	0.0013	854.0	21.6	851.2	27.7	781.1	26.7	-0.3	-9.3	854.0	21.6
G19	16	80	2.30	0.1237	0.0017	1.0960	0.0323	0.0619	0.0013	751.9	19.3	751.4	26.4	668.9	25.6	-0.1	-12.4	751.9	19.3
G20	78	473	1.21	0.1278	0.0015	1.1464	0.0184	0.0652	0.0007	775.5	17.4	775.5	17.1	779.5	15.8	0.0	0.5	775.5	17.4
G21	32	81	1.14	0.3077	0.0038	4.5361	0.0985	0.1062	0.0012	1729.3	37.4	1737.6	27.7	1734.8	23.3	0.5	0.3	1734.8	23.3
G22	159	518	0.44	0.2846	0.0033	4.4251	0.0648	0.1122	0.0009	1614.2	33.5	1717.1	23.5	1835.7	18.3	6.0	12.1	1835.7	18.3
G23	86	204	1.15	0.3237	0.0039	4.9081	0.0865	0.1100	0.0010	1807.6	37.6	1803.6	25.5	1799.1	20.3	-0.2	-0.5	1799.1	20.3
G24	245	724	0.17	0.3333	0.0039	5.2270	0.0751	0.1130	0.0009	1854.6	37.7	1857.0	23.9	1848.5	17.9	0.1	-0.3	1848.5	17.9
G25	137	347	0.85	0.3271	0.0039	5.1015	0.0848	0.1134	0.0010	1824.5	37.7	1836.4	25.1	1854.0	19.7	0.6	1.6	1854.0	19.7
G26	23	149	0.44	0.1442	0.0019	1.5336	0.0387	0.0763	0.0013	868.4	21.2	943.9	26.1	1102.2	27.4	8.0	21.2	868.4	21.2
G27	194	382	0.30	0.4630	0.0055	9.8546	0.1569	0.1524	0.0012	2452.9	48.0	2421.3	26.2	2373.3	19.3	-1.3	-3.4	2373.3	19.3
G28	24	475	0.65	0.0454	0.0006	0.3516	0.0077	0.0548	0.0010	286.3	7.2	305.9	11.5	404.1	16.7	6.4	29.1	286.3	7.2
G29	179	297	1.17	0.4503	0.0053	9.6780	0.1624	0.1550	0.0013	2396.7	47.3	2404.6	26.6	2402.1	20.0	0.3	0.2	2402.1	20.0
G30	111	770	0.15	0.1493	0.0018	1.4254	0.0217	0.0686	0.0006	897.1	19.7	899.6	17.9	887.9	15.7	0.3	-1.0	897.1	19.7
G31	73	387	0.58	0.1699	0.0021	1.7236	0.0316	0.0731	0.0008	1011.3	22.6	1017.4	21.4	1015.3	19.4	0.6	0.4	1015.3	19.4
G32	386	1909	0.73	0.1744	0.0020	1.9209	0.0261	0.0793	0.0006	1036.3	22.3	1088.4	18.8	1180.1	15.7	4.8	12.2	1180.1	15.7
G33	89	249	1.10	0.2802	0.0033	3.7033	0.0625	0.0983	0.0009	1592.5	33.5	1572.1	24.3	1591.7	19.7	-1.3	0.0	1591.7	19.7
G34	155	429	0.27	0.3479	0.0041	5.9070	0.0956	0.1222	0.0011	1924.6	39.2	1962.3	25.3	1989.2	19.6	1.9	3.2	1989.2	19.6
G35	252	497	0.37	0.4660	0.0055	11.6162	0.1839	0.1820	0.0015	2465.8	48.2	2574.0	26.7	2671.3	19.9	4.2	7.7	2671.3	19.9
G36	363	739	0.20	0.4633	0.0054	10.3518	0.1639	0.1591	0.0013	2454.0	47.9	2466.8	26.4	2446.3	19.8	0.5	-0.3	2446.3	19.8
G37	19	418	0.74	0.0401	0.0005	0.3148	0.0070	0.0561	0.0010	253.1	6.3	277.9	10.7	456.7	18.2	8.9	44.6	253.1	6.3
G38	14	220	0.41	0.0613	0.0008	0.4591	0.0107	0.0544	0.0010	383.3	9.6	383.6	14.6	388.5	16.9	0.1	1.3	383.3	9.6
G39	42	410	0.57	0.0903	0.0011	0.7605	0.0157	0.0617	0.0009	557.5	13.4	574.3	17.4	664.8	19.5	2.9	16.1	557.5	13.4
G40	19	143	0.83	0.1109	0.0014	0.9610	0.0237	0.0621	0.0011	678.0	16.6	683.8	21.9	675.8	22.5	0.9	-0.3	678.0	16.6
G41	218	691	0.07	0.3229	0.0038	4.9618	0.0763	0.1123	0.0010	1804.1	36.9	1812.8	24.6	1836.3	19.2	0.5	1.8	1836.3	19.2
G42	89	1209	0.43	0.0699	0.0008	0.5355	0.0084	0.0556	0.0006	435.7	10.0	435.4	11.4	434.4	12.3	-0.1	-0.3	435.7	10.0
G43	15	290	1.07	0.0424	0.0006	0.3060	0.0085	0.0523	0.0013	267.8	7.2	271.1	13.3	299.9	17.3	1.2	10.7	267.8	7.2
G44	28	352	0.71	0.0704	0.0009	0.5412	0.0099	0.0559	0.0008	438.6	10.4	439.2	13.1	449.2	14.5	0.1	2.4	438.6	10.4
G45	27	334	0.76	0.0709	0.0009	0.5658	0.0105	0.0572	0.0008	441.5	10.4	455.3	13.4	500.4	15.6	3.0	11.8	441.5	10.4
G46	9	201	1.31	0.0351	0.0005	0.2481	0.0078	0.0518	0.0015	222.1	6.2	225.0	12.8	276.1	18.3	1.3	19.6	222.1	6.2
G47	51	160	0.56	0.2852	0.0035	4.3427	0.0935	0.1125	0.0013	1617.7	35.1	1701.5	28.0	1840.2	24.4	4.9	12.1	1840.2	24.4
G48	92	251	0.57	0.3265	0.0039	5.0711	0.0922	0.1126	0.0011	1821.5	37.9	1831.3	26.3	1842.1	21.4	0.5	1.1	1842.1	21.4

Table 4

Gr. No.	Pb (ppm)	U (ppm)	Atomic Th/U	Ratios 206/238	± s.e.	207/235	± s.e.	207/206	± s.e.	Ages (Ma) 206/238	± 2s	207/235	± 2s	207/206	± 2s	% concord. (206/238 / 207/235)	% concord. (206/238 / 207/206)	Best Age (Ma)	±2s
G49	126	370	0.26	0.3278	0.0039	5.0573	0.0795	0.1125	0.0010	1827.6	37.4	1829.0	25.0	1840.8	19.8	0.1	0.7	1840.8	19.8
G50	43	594	0.44	0.0682	0.0008	0.5491	0.0105	0.0573	0.0008	425.3	10.1	444.4	13.5	504.3	16.2	4.3	15.7	425.3	10.1
G51	34	443	0.73	0.0672	0.0008	0.5102	0.0105	0.0547	0.0009	419.1	10.0	418.6	13.9	400.8	15.3	-0.1	-4.6	419.1	10.0
G52	78	191	0.93	0.3303	0.0040	4.9561	0.1003	0.1118	0.0012	1839.7	38.8	1811.9	27.6	1829.2	23.0	-1.5	-0.6	1829.2	23.0
G53	10	87	0.75	0.0975	0.0014	0.9181	0.0298	0.0671	0.0017	599.6	16.3	661.3	27.5	839.3	32.9	9.3	28.6	599.6	16.3
G54	161	352	0.25	0.4295	0.0051	8.5510	0.1444	0.1450	0.0013	2303.4	45.6	2291.4	26.9	2287.8	21.0	-0.5	-0.7	2287.8	21.0
G55	87	173	0.73	0.4230	0.0050	8.9755	0.1683	0.1501	0.0014	2274.2	45.7	2335.5	27.8	2347.1	22.1	2.6	3.1	2347.1	22.1
G56	55	142	0.82	0.3217	0.0039	4.8314	0.0941	0.1113	0.0012	1797.9	37.8	1790.4	27.1	1819.9	22.6	-0.4	1.2	1819.9	22.6
G57	21	59	0.65	0.3032	0.0039	4.3692	0.1234	0.1032	0.0015	1707.4	38.8	1706.5	32.4	1682.6	29.0	0.0	-1.5	1682.6	29.0
G58	47	1399	0.40	0.0325	0.0004	0.2337	0.0043	0.0520	0.0008	206.4	5.0	213.3	7.3	283.2	11.8	3.2	27.1	206.4	5.0
G59	16	46	0.71	0.2947	0.0041	4.8635	0.1704	0.1127	0.0020	1665.0	40.4	1796.0	37.2	1843.6	34.5	7.3	9.7	1843.6	34.5
G60	101	590	0.32	0.1672	0.0020	1.6286	0.0271	0.0704	0.0008	996.5	21.9	981.3	20.0	941.2	17.7	-1.5	-5.9	941.2	17.7
G61	24	641	0.26	0.0378	0.0005	0.2924	0.0069	0.0563	0.0011	239.1	6.1	260.4	11.0	465.0	19.6	8.2	48.6	239.1	6.1
G62	32	375	0.86	0.0713	0.0009	0.5524	0.0111	0.0565	0.0009	444.2	10.6	446.5	14.3	472.9	16.3	0.5	6.1	444.2	10.6
G63	127	375	0.56	0.3036	0.0036	4.7007	0.0814	0.1127	0.0011	1709.2	35.6	1767.4	25.8	1843.4	21.4	3.3	7.3	1843.4	21.4
G64	21	413	1.06	0.0401	0.0005	0.2675	0.0061	0.0484	0.0009	253.6	6.3	240.7	10.0	117.4	9.0	-5.4	-116.0	253.6	6.3
G65	47	134	0.54	0.3157	0.0038	4.6705	0.0959	0.1086	0.0012	1768.5	37.4	1762.0	27.8	1776.7	23.7	-0.4	0.5	1776.7	23.7
G66	166	362	1.06	0.3630	0.0043	6.5222	0.1153	0.1307	0.0013	1996.5	40.7	2048.9	27.1	2107.5	22.1	2.6	5.3	2107.5	22.1
G67	6	88	0.76	0.0573	0.0008	0.4135	0.0144	0.0530	0.0016	359.4	10.2	351.4	20.0	330.5	21.6	-2.3	-8.7	359.4	10.2
G68	44	105	1.24	0.3138	0.0039	5.4832	0.1346	0.1251	0.0016	1759.2	38.6	1898.0	30.6	2030.2	27.0	7.3	13.3	2030.2	27.0
G69	297	709	0.10	0.4156	0.0049	9.0499	0.1396	0.1584	0.0014	2240.5	44.2	2343.1	27.0	2438.5	21.3	4.4	8.1	2438.5	21.3
G70	143	516	0.21	0.2764	0.0033	4.1846	0.0689	0.1095	0.0011	1573.0	32.9	1671.0	25.2	1790.4	21.3	5.9	12.1	1790.4	21.3
G71	3	9	0.82	0.3122	0.0061	4.5825	0.3215	0.1077	0.0037	1751.3	60.0	1746.1	66.3	1760.2	62.4	-0.3	0.5	1760.2	62.4
G72	13	34	0.66	0.3235	0.0045	4.4345	0.1614	0.1027	0.0019	1806.7	43.9	1718.8	38.9	1673.8	35.3	-5.1	-7.9	1673.8	35.3
G73	4	125	0.53	0.0273	0.0005	0.1811	0.0091	0.0501	0.0024	173.3	6.3	169.0	16.4	197.3	21.8	-2.5	12.2	173.3	6.3
G74	213	666	0.53	0.2895	0.0034	4.5916	0.0744	0.1155	0.0011	1639.2	34.0	1747.8	25.5	1888.3	21.4	6.2	13.2	1888.3	21.4
G75	22	350	1.18	0.0480	0.0006	0.3810	0.0099	0.0570	0.0013	302.5	7.9	327.8	14.3	490.8	21.7	7.7	38.4	302.5	7.9
G76	248	446	1.65	0.3872	0.0046	8.0550	0.1378	0.1540	0.0015	2109.7	42.5	2237.2	27.7	2390.5	22.6	5.7	11.7	2390.5	22.6
G77	23	284	0.99	0.0671	0.0009	0.6149	0.0153	0.0657	0.0013	418.8	10.6	486.7	18.3	795.9	26.7	13.9	47.4	418.8	10.6
G78	113	301	0.63	0.3337	0.0041	5.7620	0.1227	0.1225	0.0014	1856.1	39.2	1940.7	28.8	1993.5	24.7	4.4	6.9	1993.5	24.7
G79	122	348	0.35	0.3303	0.0039	4.9608	0.0919	0.1129	0.0012	1839.8	38.2	1812.7	27.3	1846.6	22.9	-1.5	0.4	1846.6	22.9
G80	175	359	0.93	0.3950	0.0047	8.2028	0.1411	0.1518	0.0015	2146.0	43.1	2253.7	27.9	2366.3	22.8	4.8	9.3	2366.3	22.8
G81	57	2018	0.52	0.0264	0.0003	0.1872	0.0034	0.0503	0.0007	167.9	4.0	174.2	5.9	206.6	10.1	3.6	18.7	167.9	4.0
G82	11	221	1.17	0.0390	0.0006	0.2909	0.0099	0.0549	0.0017	246.3	7.2	259.2	15.7	409.8	25.3	5.0	39.9	246.3	7.2
G83	4	66	2.12	0.0413	0.0007	0.2950	0.0144	0.0504	0.0023	260.9	9.0	262.5	21.8	212.1	21.8	0.6	-23.0	260.9	9.0
G84	711	1444	0.06	0.4816	0.0056	11.5347	0.1733	0.1735	0.0016	2534.1	48.7	2567.4	27.9	2591.8	22.3	1.3	2.2	2591.8	22.3
G85	20	50	1.46	0.2892	0.0039	4.5106	0.1467	0.1045	0.0018	1637.4	38.7	1732.9	35.6	1704.7	33.0	5.5	3.9	1704.7	33.0
G86	5	124	1.06	0.0342	0.0005	0.2441	0.0087	0.0504	0.0017	217.0	6.4	221.8	14.0	213.0	17.2	2.2	-1.9	217.0	6.4
G87	28	44	1.17	0.4713	0.0063	10.3851	0.3511	0.1644	0.0024	2489.2	54.9	2469.7	36.4	2501.5	31.4	-0.8	0.5	2501.5	31.4

Table 4

				Ratios						Ages (Ma)									
Gr. No.	**Pb (ppm)**	**U (ppm)**	**Atomic Th/U**	**206/238**	**± s.e.**	**207/235**	**± s.e.**	**207/206**	**± s.e.**	**206/238**	**± 2s**	**207/235**	**± 2s**	**207/206**	**± 2s**	**% concord. (206/238 / 207/235)**	**% concord. (206/238 / 207/206)**	**Best Age (Ma)**	**±2s**
G88	137	913	0.26	0.1485	0.0018	1.4363	0.0237	0.0707	0.0008	892.6	19.6	904.2	19.5	949.6	18.4	1.3	6.0	892.6	19.6
G89	3	69	0.35	0.0431	0.0007	0.3068	0.0146	0.0500	0.0022	272.0	9.1	271.7	21.8	194.1	20.1	-0.1	-40.2	272.0	9.1
G90	22	331	0.36	0.0660	0.0008	0.5192	0.0110	0.0573	0.0010	412.0	9.9	424.6	14.4	503.9	17.8	3.0	18.2	412.0	9.9
G91	6	126	1.18	0.0374	0.0006	0.2639	0.0091	0.0504	0.0016	236.4	6.8	237.8	14.4	212.1	16.6	0.6	-11.5	236.4	6.8
G92	248	614	0.43	0.3665	0.0043	6.6381	0.1179	0.1333	0.0014	2013.1	40.9	2064.4	28.1	2142.2	23.7	2.5	6.0	2142.2	23.7
G93	34	107	0.63	0.2827	0.0036	4.4576	0.1162	0.1127	0.0016	1604.8	36.1	1723.1	31.9	1843.6	29.4	6.9	12.9	1843.6	29.4
G94	5	148	0.94	0.0271	0.0005	0.1935	0.0091	0.0527	0.0024	172.2	6.0	179.6	16.1	317.2	29.0	4.1	45.7	172.2	6.0
G95	76	275	0.72	0.2371	0.0029	2.8324	0.0550	0.0867	0.0011	1371.8	29.7	1364.2	25.9	1353.4	23.1	-0.6	-1.4	1353.4	23.1
G96	35	1242	0.56	0.0257	0.0003	0.1766	0.0040	0.0495	0.0010	163.7	4.1	165.1	7.1	173.0	10.8	0.9	5.4	163.7	4.1
G97	173	489	0.34	0.3325	0.0039	5.2130	0.0903	0.1130	0.0012	1850.3	37.9	1854.7	27.3	1848.2	23.2	0.2	-0.1	1848.2	23.2
G98	101	265	0.73	0.3223	0.0039	4.9236	0.1022	0.1112	0.0014	1801.1	37.9	1806.3	29.0	1819.8	25.4	0.3	1.0	1819.8	25.4
G99	10	195	1.44	0.0366	0.0006	0.2654	0.0094	0.0536	0.0017	232.0	6.8	239.0	15.3	354.3	23.9	2.9	34.5	232.0	6.8
G100	28	399	0.37	0.0663	0.0008	0.5772	0.0122	0.0617	0.0010	413.7	9.9	462.7	15.1	664.8	20.8	10.6	37.8	413.7	9.9
G101	53	702	0.56	0.0694	0.0006	0.5326	0.0094	0.0558	0.0017	432.6	6.6	433.5	22.5	446.0	26.9	0.2	3.0	432.6	6.6
G102	24	561	0.27	0.0420	0.0008	0.3207	0.0122	0.0547	0.0010	265.3	10.1	282.4	13.2	400.8	17.0	6.1	33.8	265.3	10.1
G103	344	574	1.01	0.4656	0.0008	10.3107	0.0096	0.1621	0.0008	2464.4	7.3	2463.1	9.3	2477.7	13.4	-0.1	0.5	2477.7	13.4
G104	53	178	1.33	0.2212	0.0005	2.6080	0.0071	0.0870	0.0010	1288.0	5.6	1302.9	17.5	1360.9	22.1	1.1	5.4	1360.9	22.1
G105	18	632	0.40	0.0268	0.0055	0.1840	0.1786	0.0499	0.0018	170.6	68.7	171.5	65.4	188.0	16.7	0.5	9.2	170.6	68.7
G106	44	83	0.73	0.4477	0.0027	9.6369	0.0583	0.1597	0.0013	2385.1	24.3	2400.7	18.3	2452.9	19.1	0.6	2.8	2452.9	19.1
G107	83	148	0.63	0.4710	0.0004	10.4066	0.0045	0.1632	0.0011	2487.9	3.1	2471.6	12.1	2488.6	16.7	-0.7	0.0	2488.6	16.7
G108	10	142	1.49	0.0539	0.0057	0.4366	0.2692	0.0588	0.0022	338.5	69.2	367.8	68.6	558.2	36.1	8.0	39.4	338.5	69.2
G109	70	1238	0.48	0.0524	0.0056	0.4182	0.2100	0.0575	0.0019	329.1	69.0	354.7	67.0	511.5	30.9	7.2	35.7	329.1	69.0
G110	32	176	1.27	0.1366	0.0008	1.2595	0.0153	0.0669	0.0019	825.2	8.7	827.7	31.9	835.0	36.1	0.3	1.2	825.2	8.7
G111	29	101	4.40	0.1270	0.0006	1.1444	0.0077	0.0669	0.0008	770.7	7.2	774.6	14.5	833.4	18.6	0.5	7.5	770.7	7.2
G112	347	1085	0.15	0.3186	0.0017	4.8972	0.0348	0.1109	0.0015	1782.8	16.9	1801.8	24.6	1813.6	27.5	1.1	1.7	1813.6	27.5
G113	39	95	0.98	0.3252	0.0031	4.9755	0.1752	0.1109	0.0031	1814.9	29.9	1815.2	50.5	1813.7	52.5	0.0	-0.1	1813.7	52.5
G114	163	400	1.23	0.3088	0.0037	4.6821	0.0810	0.1112	0.0012	1734.8	36.7	1764.1	27.6	1819.3	23.5	1.7	4.6	1819.3	23.5
G115	70	633	1.26	0.0834	0.0037	0.6718	0.0859	0.0580	0.0013	516.4	43.6	521.8	40.2	527.9	23.6	1.0	2.2	516.4	43.6
G116	117	355	0.43	0.3043	0.0014	4.7421	0.0249	0.1143	0.0011	1712.7	13.9	1774.7	17.7	1868.6	20.8	3.5	8.3	1868.6	20.8
G117	157	1058	0.33	0.1447	0.0010	1.3816	0.0122	0.0699	0.0008	871.0	11.3	881.1	15.7	924.2	18.4	1.1	5.8	871.0	11.3
G118	56	814	0.38	0.0665	0.0036	0.5047	0.0885	0.0550	0.0014	415.0	43.8	414.9	40.9	412.6	21.8	0.0	-0.6	415.0	43.8
G119	58	156	0.69	0.3193	0.0008	4.7309	0.0091	0.1099	0.0008	1786.2	7.7	1772.7	12.4	1797.6	16.3	-0.8	0.6	1797.6	16.3
G120	326	783	0.61	0.3645	0.0027	7.1833	0.0538	0.1412	0.0012	2003.5	25.1	2134.4	19.8	2242.2	19.9	6.1	10.6	2242.2	19.9
G121	164	960	1.20	0.1318	0.0039	1.2032	0.1100	0.0664	0.0015	797.8	44.8	802.0	41.9	820.0	30.6	0.5	2.7	797.8	44.8
G122	15	169	0.85	0.0743	0.0043	0.5949	0.1268	0.0566	0.0017	461.8	51.6	474.0	48.4	475.2	26.9	2.6	2.8	461.8	51.6
G123	25	416	0.57	0.0550	0.0016	0.4102	0.0216	0.0541	0.0009	345.4	19.1	349.0	19.3	376.9	14.8	1.0	8.4	345.4	19.1
G124	42	1039	0.47	0.0377	0.0010	0.3022	0.0177	0.0579	0.0014	238.4	12.5	268.1	17.0	526.0	24.5	11.1	54.7	238.4	12.5
G125	67	115	0.78	0.4690	0.0007	10.1266	0.0100	0.1617	0.0011	2479.2	6.2	2446.4	12.9	2473.1	17.3	-1.3	-0.2	2473.1	17.3
G126	11	40	1.35	0.2103	0.0005	2.3135	0.0064	0.0816	0.0010	1230.3	5.0	1216.4	18.1	1235.5	22.5	-1.1	0.4	1235.5	22.5

Table 4

Gr. No.	Pb (ppm)	U (ppm)	Atomic Th/U	Ratios 206/238	± s.e.	207/235	± s.e.	207/206	± s.e.	Ages (Ma) 206/238	± 2s	207/235	± 2s	207/206	± 2s	% concord. (206/238 / 207/235)	% concord. (206/238 / 207/206)	Best Age (Ma)	±2s
G127	30	1077	0.34	0.0273	0.0030	0.1864	0.0870	0.0495	0.0020	173.5	38.2	173.6	37.7	172.1	17.1	0.0	-0.8	173.5	38.2
G128	29	75	0.83	0.3228	0.0008	4.7380	0.0218	0.1108	0.0019	1803.5	8.1	1774.0	29.9	1812.7	34.2	-1.7	0.5	1812.7	34.2
G129	42	118	0.81	0.2955	0.0040	4.3169	0.1190	0.1037	0.0017	1669.1	40.2	1696.6	34.6	1692.1	31.0	1.6	1.4	1692.1	31.0
G130	8	137	1.21	0.0436	0.0028	0.2998	0.0888	0.0519	0.0019	275.2	34.8	266.3	35.7	282.3	22.2	-3.3	2.5	275.2	34.8
G131	406	700	0.56	0.4953	0.0007	12.0336	0.0115	0.1758	0.0018	2593.5	5.9	2607.0	19.4	2613.4	23.9	0.5	0.8	2613.4	23.9
G132	95	336	0.36	0.2677	0.0022	3.9575	0.0499	0.1043	0.0014	1529.0	22.6	1625.5	25.3	1702.2	26.7	5.9	10.2	1702.2	26.7
G133	228	337	1.60	0.4666	0.0058	10.3557	0.2067	0.1620	0.0021	2468.7	51.1	2467.1	33.6	2476.7	29.0	-0.1	0.3	2476.7	29.0
12061807 River Mouth																			
G1	27	341	0.27	0.0793	0.0010	0.7433	0.0117	0.0659	0.0007	491.8	11.3	564.3	13.3	803.2	11.1	12.9	38.8	491.8	11.3
G2	25	581	0.58	0.0399	0.0005	0.2844	0.0044	0.0519	0.0006	252.2	6.0	254.1	7.3	282.8	7.7	0.8	10.8	252.2	6.0
G3	36	152	0.93	0.1923	0.0023	2.2006	0.0368	0.0809	0.0008	1134.0	24.9	1181.2	21.0	1219.3	15.5	4.0	7.0	1219.3	15.5
G4	8	210	0.42	0.0361	0.0005	0.2939	0.0079	0.0570	0.0013	228.4	6.1	261.6	12.1	490.4	20.5	12.7	53.4	228.4	6.1
G5	16	370	0.33	0.0415	0.0005	0.3473	0.0066	0.0586	0.0009	262.2	6.4	302.7	9.8	553.8	14.9	13.4	52.6	262.2	6.4
G6	39	252	0.77	0.1325	0.0016	1.2368	0.0209	0.0673	0.0007	802.3	18.1	817.4	17.8	847.4	14.3	1.8	5.3	802.3	18.1
G7	36	979	0.24	0.0374	0.0005	0.2735	0.0043	0.0530	0.0006	236.8	5.6	245.5	7.0	327.5	8.4	3.6	27.7	236.8	5.6
G8	38	504	0.63	0.0677	0.0008	0.5400	0.0087	0.0574	0.0006	422.0	9.8	438.4	11.4	507.7	11.0	3.7	16.9	422.0	9.8
G9	55	510	0.56	0.0987	0.0012	0.9467	0.0142	0.0695	0.0006	606.8	13.7	676.4	14.7	912.1	13.3	10.3	33.5	606.8	13.7
G10	15	354	0.37	0.0414	0.0005	0.3004	0.0058	0.0522	0.0008	261.3	6.3	266.7	9.2	295.1	10.2	2.1	11.5	261.3	6.3
G11	12	300	0.44	0.0380	0.0005	0.2789	0.0058	0.0519	0.0009	240.7	6.0	249.8	9.3	281.4	10.8	3.7	14.5	240.7	6.0
G12	22	200	0.42	0.1063	0.0013	1.0576	0.0221	0.0692	0.0010	650.9	15.5	732.6	19.5	905.9	19.7	11.2	28.1	650.9	15.5
G13	22	78	0.64	0.2429	0.0030	3.0321	0.0663	0.0877	0.0011	1401.7	31.2	1415.7	26.1	1374.8	20.4	1.0	-2.0	1374.8	20.4
G14	13	295	0.50	0.0402	0.0005	0.3049	0.0066	0.0532	0.0010	253.8	6.3	270.2	10.1	335.6	12.6	6.1	24.4	253.8	6.3
G15	12	311	0.21	0.0397	0.0005	0.3145	0.0062	0.0562	0.0009	251.2	6.2	277.6	9.6	460.3	13.9	9.5	45.4	251.2	6.2
G16	26	343	0.28	0.0716	0.0009	0.6498	0.0116	0.0642	0.0008	446.0	10.5	508.3	13.7	747.9	15.6	12.3	40.4	446.0	10.5
G17	49	305	0.74	0.1380	0.0016	1.2683	0.0193	0.0658	0.0006	833.6	18.5	831.6	16.6	799.4	12.1	-0.2	-4.3	833.6	18.5
G18	11	125	0.70	0.0767	0.0010	0.6655	0.0137	0.0627	0.0010	476.3	11.5	518.0	16.0	698.8	17.8	8.1	31.8	476.3	11.5
G19	51	122	0.45	0.3799	0.0045	6.7401	0.1110	0.1294	0.0010	2075.8	42.0	2077.9	25.0	2089.8	15.9	0.1	0.7	2089.8	15.9
G20	253	515	0.72	0.4118	0.0048	7.9111	0.1031	0.1382	0.0009	2223.1	43.7	2220.9	23.8	2205.1	13.6	-0.1	-0.8	2205.1	13.6
G21	131	535	0.34	0.2343	0.0027	2.7977	0.0372	0.0854	0.0006	1357.2	28.5	1354.9	20.0	1325.5	12.2	-0.2	-2.4	1325.5	12.2
G22	34	740	0.35	0.0451	0.0005	0.3382	0.0050	0.0542	0.0005	284.6	6.5	295.8	7.8	378.5	8.4	3.8	24.8	284.6	6.5
G23	98	178	0.56	0.4730	0.0056	11.1118	0.1786	0.1655	0.0012	2496.8	48.8	2532.5	25.6	2513.0	15.5	1.4	0.6	2513.0	15.5
G24	30	238	0.84	0.1071	0.0013	0.9326	0.0170	0.0621	0.0008	655.9	15.1	669.0	16.7	678.2	14.5	2.0	3.3	655.9	15.1
G25	168	350	0.61	0.4106	0.0048	7.8631	0.1092	0.1362	0.0009	2217.7	43.8	2215.5	24.1	2178.9	14.2	-0.1	-1.8	2178.9	14.2
G26	26	639	0.26	0.0401	0.0005	0.3116	0.0052	0.0566	0.0007	253.3	6.0	275.4	8.2	476.0	11.5	8.0	46.8	253.3	6.0
G27	28	329	0.89	0.0718	0.0009	0.6321	0.0114	0.0622	0.0008	446.7	10.6	497.4	13.7	682.4	15.1	10.2	34.5	446.7	10.6
G28	14	215	0.36	0.0627	0.0008	0.4863	0.0104	0.0559	0.0009	392.0	9.6	402.4	13.8	448.8	14.4	2.6	12.7	392.0	9.6
G29	16	429	0.24	0.0382	0.0005	0.2943	0.0057	0.0556	0.0009	241.5	6.0	262.0	9.2	434.4	13.3	7.8	44.4	241.5	6.0
G30	20	492	0.22	0.0414	0.0005	0.2927	0.0050	0.0507	0.0006	261.2	6.2	260.7	7.9	227.7	7.4	-0.2	-14.7	261.2	6.2

Table 4

Gr. No.	Pb (ppm)	U (ppm)	Atomic Th/U	Ratios 206/238	± s.e.	207/235	± s.e.	207/206	± s.e.	Ages (Ma) 206/238	± 2s	207/235	± 2s	207/206	± 2s	% concord. (206/238 / 207/235)	% concord. (206/238 / 207/206)	Best Age (Ma)	±2s
G31	43	483	0.38	0.0868	0.0010	0.7953	0.0127	0.0656	0.0007	536.4	12.3	594.2	14.2	794.6	13.8	9.7	32.5	536.4	12.3
G32	36	334	0.40	0.1028	0.0013	0.9584	0.0168	0.0673	0.0008	630.9	14.6	682.5	16.7	847.4	15.7	7.6	25.6	630.9	14.6
G33	159	798	0.45	0.1857	0.0022	2.0667	0.0288	0.0799	0.0006	1098.3	23.7	1137.8	18.9	1194.0	12.7	3.5	8.0	1194.0	12.7
G34	104	821	0.35	0.1212	0.0014	1.1835	0.0168	0.0705	0.0006	737.4	16.3	793.0	15.6	941.8	12.3	7.0	21.7	737.4	16.3
G35	55	309	0.63	0.1584	0.0019	1.5798	0.0245	0.0712	0.0006	948.0	20.9	962.3	18.4	961.7	13.5	1.5	1.4	961.7	13.5
G36	13	325	0.23	0.0415	0.0005	0.3511	0.0061	0.0617	0.0008	262.2	6.3	305.6	9.5	663.7	15.0	14.2	60.5	262.2	6.3
G37	102	632	0.37	0.1557	0.0018	1.5137	0.0211	0.0710	0.0006	932.6	20.3	935.9	17.2	956.5	12.0	0.4	2.5	956.5	12.0
G38	83	137	0.95	0.4761	0.0056	10.8531	0.1762	0.1642	0.0012	2510.4	49.1	2510.6	25.7	2499.7	15.7	0.0	-0.4	2499.7	15.7
G39	29	379	0.45	0.0689	0.0008	0.6199	0.0103	0.0637	0.0007	429.3	10.0	489.8	12.6	731.7	14.1	12.3	41.3	429.3	10.0
G40	19	450	0.53	0.0392	0.0005	0.2889	0.0047	0.0531	0.0006	247.7	5.8	257.7	7.6	330.9	9.1	3.9	25.2	247.7	5.8
G41	58	287	1.04	0.1621	0.0019	1.6191	0.0246	0.0716	0.0006	968.5	21.3	977.6	18.4	973.7	13.4	0.9	0.5	973.7	13.4
G42	23	485	0.71	0.0416	0.0005	0.3012	0.0055	0.0512	0.0007	262.5	6.3	267.3	8.6	251.2	8.6	1.8	-4.5	262.5	6.3
G43	111	701	0.09	0.1664	0.0019	1.6636	0.0220	0.0719	0.0005	992.1	21.4	994.7	17.2	984.2	11.1	0.3	-0.8	984.2	11.1
G44	69	362	0.48	0.1768	0.0021	1.8127	0.0274	0.0746	0.0006	1049.7	22.9	1050.1	19.1	1056.4	13.6	0.0	0.6	1056.4	13.6
G45	192	1096	0.22	0.1755	0.0020	1.8680	0.0244	0.0768	0.0005	1042.6	22.4	1069.8	17.8	1115.0	11.7	2.5	6.5	1115.0	11.7
G46	14	478	0.28	0.0289	0.0004	0.2164	0.0045	0.0538	0.0009	183.5	4.5	198.9	7.6	361.0	12.8	7.8	49.2	183.5	4.5
G47	118	1072	1.38	0.0807	0.0009	0.6474	0.0088	0.0579	0.0005	500.0	11.2	506.9	11.2	527.1	8.9	1.4	5.1	500.0	11.2
G48	86	462	0.08	0.1958	0.0023	2.3063	0.0348	0.0836	0.0007	1152.6	24.9	1214.2	20.3	1282.3	14.4	5.1	10.1	1282.3	14.4
G49	79	520	0.40	0.1446	0.0017	1.4490	0.0224	0.0729	0.0007	870.7	19.4	909.5	18.0	1010.9	14.0	4.3	13.9	870.7	19.4
G50	33	744	0.36	0.0437	0.0005	0.3039	0.0046	0.0509	0.0005	275.7	6.4	269.4	7.5	235.9	6.7	-2.3	-16.9	275.7	6.4
G51	13	338	0.24	0.0396	0.0005	0.3036	0.0063	0.0561	0.0010	250.5	6.2	269.2	10.1	454.3	14.8	7.0	44.9	250.5	6.2
G52	15	367	0.43	0.0395	0.0005	0.2905	0.0060	0.0525	0.0009	250.0	6.2	258.9	9.5	308.5	11.3	3.4	19.0	250.0	6.2
G53	210	728	0.24	0.2849	0.0033	4.4170	0.0578	0.1123	0.0008	1616.1	33.3	1715.5	22.2	1837.6	13.7	5.8	12.1	1837.6	13.7
G54	90	346	0.62	0.2319	0.0027	3.1385	0.0469	0.0960	0.0008	1344.2	28.6	1442.2	21.7	1548.6	14.9	6.8	13.2	1548.6	14.9
G55	55	489	0.29	0.1113	0.0013	1.0117	0.0143	0.0653	0.0005	680.0	15.2	709.7	14.6	782.7	11.4	4.2	13.1	680.0	15.2
G56	82	208	0.73	0.3325	0.0039	5.2158	0.0786	0.1128	0.0009	1850.6	37.8	1855.2	23.8	1845.0	15.2	0.2	-0.3	1845.0	15.2
G57	15	267	1.47	0.0401	0.0005	0.2999	0.0060	0.0535	0.0009	253.6	6.2	266.3	9.4	350.9	11.9	4.8	27.7	253.6	6.2
G58	169	762	0.79	0.1886	0.0022	2.0015	0.0272	0.0769	0.0006	1113.8	23.9	1116.0	18.7	1118.6	12.4	0.2	0.4	1118.6	12.4
G59	99	248	0.19	0.3873	0.0046	7.1539	0.1114	0.1345	0.0010	2110.1	42.5	2130.8	25.0	2156.9	15.9	1.0	2.2	2156.9	15.9
G60	113	801	0.16	0.1444	0.0017	1.4711	0.0212	0.0742	0.0006	869.6	19.2	918.6	17.4	1045.6	13.1	5.3	16.8	869.6	19.2
G61	108	1566	0.17	0.0713	0.0008	0.5550	0.0077	0.0569	0.0005	443.7	10.1	448.2	10.6	488.8	8.9	1.0	9.2	443.7	10.1
G62	18	413	0.45	0.0405	0.0005	0.2956	0.0061	0.0520	0.0009	256.2	6.3	262.9	9.6	283.2	10.6	2.6	9.5	256.2	6.3
G63	56	325	0.32	0.1666	0.0020	1.7057	0.0263	0.0731	0.0007	993.5	21.8	1010.7	18.9	1016.7	14.0	1.7	2.3	1016.7	14.0
G64	19	500	0.32	0.0383	0.0005	0.2818	0.0058	0.0523	0.0009	242.4	6.0	252.1	9.2	299.0	11.1	3.8	18.9	242.4	6.0
G65	138	484	0.27	0.2793	0.0033	4.0706	0.0550	0.1054	0.0008	1587.8	32.9	1648.4	22.3	1721.8	14.2	3.7	7.8	1721.8	14.2
G66	19	323	0.37	0.0566	0.0007	0.4194	0.0081	0.0542	0.0008	354.8	8.5	355.6	11.6	377.7	11.7	0.2	6.1	354.8	8.5
G67	11	239	0.35	0.0439	0.0005	0.3172	0.0062	0.0525	0.0008	277.0	6.7	279.8	9.7	308.1	10.6	1.0	10.1	277.0	6.7
G68	22	106	1.36	0.1518	0.0019	1.5235	0.0317	0.0725	0.0010	911.0	21.2	939.9	22.5	1001.1	19.6	3.1	9.0	1001.1	19.6
G69	14	358	0.29	0.0396	0.0005	0.2874	0.0055	0.0520	0.0008	250.2	6.1	256.5	8.8	285.8	9.9	2.5	12.5	250.2	6.1

Table 4

Gr. No.	Pb (ppm)	U (ppm)	Atomic Th/U	Ratios						Ages (Ma)						% concord. (206/238 207/235)	% concord. (206/238 207/206)	Best Age (Ma)	±2s
				206/238	± s.e.	207/235	± s.e.	207/206	± s.e.	206/238	± 2s	207/235	± 2s	207/206	± 2s				
G70	130	357	0.27	0.3474	0.0041	5.6408	0.0796	0.1165	0.0009	1922.0	38.9	1922.4	23.8	1902.4	14.9	0.0	-1.0	1902.4	14.9
G71	95	609	0.11	0.1621	0.0019	1.5374	0.0216	0.0695	0.0006	968.7	21.1	945.5	17.6	912.1	12.1	-2.5	-6.2	912.1	12.1
G72	76	476	0.83	0.1349	0.0016	1.2444	0.0182	0.0667	0.0006	815.6	18.1	820.9	16.5	826.9	12.2	0.6	1.4	815.6	18.1
G73	29	736	0.16	0.0403	0.0005	0.2896	0.0044	0.0519	0.0006	254.4	5.9	258.3	7.2	281.9	7.6	1.5	9.7	254.4	5.9
G74	16	397	0.52	0.0377	0.0005	0.2865	0.0061	0.0545	0.0010	238.6	6.0	255.8	9.7	392.2	13.8	6.7	39.2	238.6	6.0
G75	20	481	0.42	0.0394	0.0005	0.3152	0.0055	0.0574	0.0008	248.9	6.0	278.2	8.7	506.6	12.9	10.5	50.9	248.9	6.0
G76	239	484	0.49	0.4406	0.0052	10.2452	0.1468	0.1672	0.0012	2353.1	46.2	2457.2	25.4	2529.8	15.7	4.2	7.0	2529.8	15.7
G77	26	561	0.81	0.0391	0.0005	0.3143	0.0053	0.0576	0.0007	247.3	5.8	277.5	8.4	512.7	12.6	10.9	51.8	247.3	5.8
G78	12	278	0.43	0.0426	0.0005	0.3330	0.0065	0.0562	0.0009	268.9	6.6	291.9	10.0	461.1	13.8	7.9	41.7	268.9	6.6
G79	16	360	0.52	0.0402	0.0005	0.3143	0.0061	0.0560	0.0009	253.8	6.2	277.5	9.5	452.8	13.6	8.5	43.9	253.8	6.2
G80	43	543	0.53	0.0727	0.0009	0.5674	0.0087	0.0563	0.0006	452.2	10.3	456.3	11.4	465.8	9.9	0.9	2.9	452.2	10.3
G81	204	3415	1.80	0.0412	0.0005	0.3177	0.0043	0.0559	0.0005	260.1	5.9	280.1	6.9	449.6	8.2	7.2	42.2	260.1	5.9
G82	22	527	0.27	0.0415	0.0005	0.3032	0.0054	0.0516	0.0007	262.3	6.3	268.9	8.5	269.5	8.8	2.4	2.7	262.3	6.3
G83	17	409	0.28	0.0419	0.0005	0.3356	0.0067	0.0573	0.0009	264.7	6.6	293.9	10.3	503.1	15.0	9.9	47.4	264.7	6.6
G84	28	664	0.18	0.0433	0.0005	0.3420	0.0058	0.0574	0.0007	273.2	6.5	298.7	9.1	505.4	12.5	8.5	45.9	273.2	6.5
G85	85	435	0.17	0.1987	0.0023	2.1605	0.0302	0.0791	0.0006	1168.4	25.1	1168.4	19.7	1175.1	13.4	0.0	0.6	1175.1	13.4
G86	34	434	0.81	0.0678	0.0008	0.5533	0.0100	0.0597	0.0008	422.7	10.0	447.2	13.1	592.7	14.2	5.5	28.7	422.7	10.0
G87	16	381	0.28	0.0398	0.0005	0.2865	0.0059	0.0527	0.0009	251.8	6.2	255.8	9.6	315.5	11.5	1.6	20.2	251.8	6.2
G88	88	642	0.11	0.1423	0.0005	1.4041	0.0059	0.0723	0.0009	857.4	5.6	890.6	15.2	994.4	18.0	3.7	13.8	857.4	5.6
G89	47	416	0.12	0.1178	0.0035	1.0971	0.0941	0.0661	0.0012	717.9	40.0	751.9	36.5	808.3	22.8	4.5	11.2	717.9	40.0
G90	49	1100	0.76	0.0385	0.0017	0.2931	0.0209	0.0549	0.0007	243.7	20.9	261.0	20.7	407.3	10.3	6.6	40.2	243.7	20.9
G91	174	243	0.14	0.6420	0.0005	22.5163	0.0046	0.2536	0.0006	3197.0	3.6	3206.3	5.0	3207.3	7.1	0.3	0.3	3207.3	7.1
G92	126	857	0.09	0.1542	0.0030	1.4932	0.0811	0.0709	0.0013	924.2	33.2	927.6	32.0	953.4	24.3	0.4	3.1	953.4	24.3
G93	26	497	0.21	0.0539	0.0007	0.4097	0.0337	0.0555	0.0034	338.5	8.2	348.6	37.1	432.8	45.5	2.9	21.8	338.5	8.2
G94	30	180	0.97	0.1350	0.0018	1.4083	0.0211	0.0736	0.0006	816.4	20.6	892.5	18.3	1031.3	12.7	8.5	20.8	816.4	20.6
G95	75	238	0.63	0.2758	0.0007	3.6922	0.0071	0.0984	0.0007	1570.3	6.6	1569.7	12.2	1593.1	14.0	0.0	1.4	1593.1	14.0
G96	22	133	0.47	0.1535	0.0016	1.5877	0.0250	0.0747	0.0008	920.7	18.3	965.4	19.3	1061.2	17.2	4.6	13.2	1061.2	17.2
G97	357	627	0.67	0.4756	0.0033	11.0497	0.0546	0.1653	0.0008	2508.2	28.4	2527.3	15.6	2510.2	11.5	0.8	0.1	2510.2	11.5
G98	142	878	0.24	0.1625	0.0019	1.6113	0.0319	0.0730	0.0010	970.7	21.1	974.6	22.3	1015.1	19.4	0.4	4.4	1015.1	19.4
G99	17	226	0.57	0.0693	0.0056	0.5732	0.1499	0.0601	0.0012	431.8	66.9	460.1	61.2	607.5	21.1	6.1	28.9	431.8	66.9
G100	17	389	0.38	0.0429	0.0009	0.3526	0.0112	0.0593	0.0009	270.6	10.6	306.7	13.2	577.8	15.6	11.8	53.2	270.6	10.6
G101	105	279	0.37	0.3520	0.0034	6.4326	0.0845	0.1333	0.0012	1944.2	32.8	2036.7	23.3	2141.5	18.3	4.5	9.2	2141.5	18.3
G102	46	519	0.16	0.0926	0.0006	0.9261	0.0074	0.0714	0.0009	570.7	6.5	665.6	13.9	969.7	18.6	14.3	41.1	570.7	6.5
G103	76	1764	0.45	0.0409	0.0041	0.3041	0.0957	0.0541	0.0011	258.2	51.3	269.6	49.0	373.1	15.0	4.2	30.8	258.2	51.3
G104	157	443	0.34	0.3337	0.0011	5.2176	0.0150	0.1129	0.0008	1856.4	10.7	1855.5	12.9	1846.9	14.0	-0.1	-0.5	1846.9	14.0
G105	36	764	0.91	0.0390	0.0005	0.2960	0.0043	0.0547	0.0005	246.3	6.0	263.2	7.0	398.3	8.3	6.4	38.2	246.3	6.0
G106	14	165	0.74	0.0730	0.0039	0.6171	0.0741	0.0618	0.0009	454.3	47.1	488.0	43.4	668.6	16.8	6.9	32.0	454.3	47.1
G107	15	357	0.38	0.0421	0.0009	0.3270	0.0139	0.0565	0.0011	266.0	11.6	287.2	14.7	472.5	16.8	7.4	43.7	266.0	11.6
G108	71	348	0.65	0.1806	0.0020	1.9957	0.0478	0.0801	0.0012	1070.3	21.8	1114.0	25.2	1199.2	23.4	3.9	10.7	1199.2	23.4

Table 4

				Ratios						Ages (Ma)									
Gr. No.	Pb (ppm)	U (ppm)	Atomic Th/U	206/238	± s.e.	207/235	± s.e.	207/206	± s.e.	206/238	± 2s	207/235	± 2s	207/206	± 2s	% concord. (206/238 / 207/235)	% concord. (206/238 / 207/206)	Best Age (Ma)	±2s
G109	313	619	0.34	0.4595	0.0005	9.9962	0.0069	0.1593	0.0010	2437.5	4.8	2434.4	11.6	2447.9	13.7	-0.1	0.4	2447.9	13.7
G110	307	768	0.50	0.3607	0.0022	6.3038	0.0320	0.1287	0.0008	1985.7	20.4	2019.0	15.0	2079.6	13.2	1.6	4.5	2079.6	13.2
G111	176	478	0.97	0.2987	0.0054	4.2748	0.1399	0.1054	0.0013	1685.0	53.4	1688.5	35.7	1720.8	22.2	0.2	2.1	1720.8	22.2
12061712 Rao Tro																			
G1	38.5	863.5	0.77	0.0392	0.0005	0.2899	0.0061	0.0538	0.0010	247.6	6.0	258.5	10.4	362.3	15.1	4.2	31.7	247.6	5.96
G2	15.5	418.2	0.22	0.0378	0.0006	0.2714	0.0115	0.0538	0.0021	239.1	6.8	243.8	18.5	361.8	27.2	1.9	33.9	239.1	6.83
G3	18.6	485.8	0.24	0.0387	0.0005	0.2688	0.0082	0.0508	0.0014	244.8	6.3	241.7	13.4	231.3	15.0	-1.3	-5.8	244.8	6.33
G4	13.6	329.1	0.31	0.0410	0.0005	0.2848	0.0086	0.0514	0.0014	259.2	6.6	254.4	13.9	257.9	15.9	-1.9	-0.5	259.2	6.56
G5	12.5	306.4	0.36	0.0395	0.0005	0.2702	0.0098	0.0504	0.0017	249.4	6.7	242.9	15.7	213.0	16.1	-2.7	-17.1	249.4	6.70
G6	16.2	373.9	0.33	0.0430	0.0006	0.2971	0.0098	0.0511	0.0015	271.2	7.0	264.2	15.5	244.9	16.5	-2.6	-10.7	271.2	7.05
G7	15.3	386.6	0.23	0.0402	0.0005	0.2838	0.0078	0.0521	0.0013	254.3	6.4	253.6	12.8	289.4	16.0	-0.2	12.1	254.3	6.44
G8	65.7	328.5	0.66	0.1781	0.0022	1.7612	0.0446	0.0743	0.0014	1056.5	24.3	1031.3	29.0	1050.4	27.4	-2.4	-0.6	1050.4	27.35
G9	11.3	267.2	0.31	0.0415	0.0006	0.3098	0.0098	0.0545	0.0016	262.2	6.8	274.0	15.2	392.2	22.0	4.3	33.1	262.2	6.81
G10	12.3	328.5	0.28	0.0374	0.0005	0.2407	0.0095	0.0508	0.0019	236.5	6.6	219.0	16.5	233.1	18.6	-8.0	-1.5	236.5	6.59
G11	51.6	553.3	1.14	0.0731	0.0009	0.5732	0.0116	0.0568	0.0010	454.5	10.7	460.1	15.6	483.8	16.7	1.2	6.1	454.5	10.69
G12	24.9	659.5	0.19	0.0390	0.0005	0.2732	0.0082	0.0514	0.0014	246.3	6.3	245.2	13.3	259.3	15.9	-0.5	5.0	246.3	6.33
G13	29.4	495.9	0.61	0.0535	0.0007	0.3845	0.0087	0.0533	0.0011	335.7	8.1	330.3	13.5	340.3	15.0	-1.6	1.3	335.7	8.08
G14	15.1	355.0	0.31	0.0421	0.0005	0.2934	0.0084	0.0516	0.0013	266.0	6.7	261.2	13.6	266.8	15.6	-1.8	0.3	266.0	6.68
G15	9.2	212.2	0.47	0.0411	0.0006	0.2767	0.0143	0.0497	0.0024	259.3	7.9	248.0	22.3	181.5	19.2	-4.6	-42.9	259.3	7.93
G16	128.0	763.1	0.56	0.1523	0.0018	1.5033	0.0266	0.0714	0.0010	914.0	20.5	931.7	22.7	968.9	21.2	1.9	5.7	968.9	21.24
G17	22.7	598.2	0.34	0.0372	0.0005	0.2786	0.0079	0.0539	0.0014	235.3	6.0	249.6	12.8	367.7	19.4	5.7	36.0	235.3	5.97
G18	14.2	334.8	0.32	0.0419	0.0005	0.2971	0.0084	0.0528	0.0014	264.4	6.7	264.1	13.7	318.5	17.5	-0.1	17.0	264.4	6.68
G19	169.3	1238.1	0.14	0.1412	0.0017	1.3738	0.0227	0.0712	0.0010	851.6	19.1	877.8	21.4	962.9	20.3	3.0	11.6	851.6	19.09
G20	19.0	442.8	0.23	0.0435	0.0006	0.3030	0.0110	0.0521	0.0017	274.4	7.4	268.7	17.2	287.6	19.9	-2.1	4.6	274.4	7.41
G21	1455.1	2587.3	0.26	0.5117	0.0061	12.8844	0.1871	0.1793	0.0022	2663.7	51.9	2671.2	31.8	2646.4	26.0	0.3	-0.7	2646.4	25.95
G22	13.5	292.5	0.27	0.0466	0.0006	0.3773	0.0131	0.0599	0.0019	293.5	7.9	325.1	19.1	599.6	31.4	9.7	51.1	293.5	7.88
G23	13.7	289.3	0.33	0.0466	0.0006	0.3436	0.0117	0.0544	0.0017	293.6	7.8	299.9	17.6	386.4	23.0	2.1	24.0	293.6	7.76
G24	49.6	78.3	0.04	0.6043	0.0076	19.9798	0.6606	0.2411	0.0034	3047.0	61.3	3090.4	36.9	3127.4	31.0	1.4	2.6	3127.4	31.04
G25	16.3	389.1	0.32	0.0417	0.0005	0.2983	0.0081	0.0534	0.0013	263.4	6.7	265.0	13.2	346.3	17.8	0.6	23.9	263.4	6.68
G26	75.4	113.7	0.73	0.5371	0.0069	14.5178	0.5419	0.1975	0.0031	2771.3	58.2	2784.2	38.8	2805.7	33.5	0.5	1.2	2805.7	33.45
G27	242.4	583.0	0.41	0.3869	0.0047	8.2790	0.1537	0.1585	0.0020	2108.2	43.4	2262.0	32.0	2439.5	27.2	6.8	13.6	2439.5	27.17
G28	23.4	547.0	0.38	0.0416	0.0005	0.3544	0.0100	0.0620	0.0016	262.7	6.7	308.0	15.2	675.1	28.4	14.7	61.1	262.7	6.68
G29	10.9	259.0	0.26	0.0424	0.0006	0.3302	0.0122	0.0577	0.0019	267.7	7.3	289.7	18.5	519.1	30.4	7.6	48.4	267.7	7.30
G30	65.7	648.7	0.80	0.0851	0.0011	0.7797	0.0172	0.0663	0.0012	526.2	12.6	585.3	19.6	814.3	23.9	10.1	35.4	526.2	12.60
G31	11.7	279.2	0.34	0.0412	0.0005	0.2977	0.0087	0.0546	0.0014	260.0	6.7	264.6	14.1	395.9	20.7	1.8	34.3	260.0	6.69
G32	12.8	308.3	0.38	0.0404	0.0005	0.2821	0.0080	0.0528	0.0014	255.1	6.4	252.3	13.3	321.1	17.6	-1.1	20.6	255.1	6.44
G33	12.9	325.9	0.29	0.0396	0.0005	0.2829	0.0084	0.0529	0.0014	250.1	6.4	252.9	13.7	322.4	18.3	1.1	22.4	250.1	6.45
G34	13.3	312.7	0.47	0.0401	0.0005	0.2885	0.0083	0.0538	0.0014	253.7	6.4	257.3	13.6	361.0	19.3	1.4	29.7	253.7	6.45

Table 4

				Ratios						Ages (Ma)									
Gr. No.	Pb (ppm)	U (ppm)	Atomic Th/U	206/238	± s.e.	207/235	± s.e.	207/206	± s.e.	206/238	± 2s	207/235	± 2s	207/206	± 2s	% concord. (206/238 / 207/235)	% concord. (206/238 / 207/206)	Best Age (Ma)	±2s
G35	17.6	444.7	0.35	0.0387	0.0005	0.2710	0.0098	0.0517	0.0017	244.9	6.6	243.5	15.8	271.7	19.3	-0.6	9.9	244.9	6.58
G36	14.3	337.3	0.28	0.0426	0.0006	0.2968	0.0084	0.0524	0.0014	269.2	6.8	263.9	13.8	302.0	16.9	-2.0	10.9	269.2	6.80
G37	247.9	668.9	0.49	0.3360	0.0041	5.3614	0.0942	0.1159	0.0015	1867.3	39.2	1878.7	30.5	1893.1	25.9	0.6	1.4	1893.1	25.91
G38	14.1	319.6	0.31	0.0438	0.0006	0.3455	0.0128	0.0587	0.0020	276.5	7.7	301.3	19.2	557.1	31.9	8.2	50.4	276.5	7.66
G39	14.9	332.9	0.64	0.0406	0.0005	0.2835	0.0085	0.0524	0.0014	256.6	6.6	253.4	13.9	304.6	17.8	-1.3	15.8	256.6	6.57
G40	16.2	398.6	0.24	0.0414	0.0006	0.3094	0.0100	0.0567	0.0017	261.3	6.9	273.7	16.1	481.1	26.0	4.5	45.7	261.3	6.93
G41	28.3	626.6	0.31	0.0452	0.0006	0.3148	0.0094	0.0512	0.0014	284.7	7.3	277.9	14.8	251.2	15.5	-2.4	-13.3	284.7	7.28
G42	18.2	441.5	0.21	0.0423	0.0005	0.2842	0.0076	0.0502	0.0012	266.9	6.7	254.0	12.5	203.8	12.3	-5.1	-31.0	266.9	6.68
G43	14.2	341.1	0.29	0.0416	0.0006	0.2829	0.0085	0.0514	0.0014	262.5	6.8	252.9	14.0	260.6	15.9	-3.8	-0.7	262.5	6.81
G44	25.7	668.3	0.59	0.0351	0.0005	0.2496	0.0071	0.0524	0.0014	222.1	5.7	226.2	11.9	300.7	16.9	1.8	26.2	222.1	5.73
G45	15.6	347.4	0.58	0.0413	0.0006	0.3013	0.0109	0.0539	0.0018	261.1	7.1	267.4	17.1	368.1	23.8	2.3	29.1	261.1	7.06
G46	16.4	410.0	0.21	0.0410	0.0005	0.2911	0.0076	0.0527	0.0012	258.8	6.6	259.4	12.5	316.3	16.2	0.2	18.2	258.8	6.56
G47	10.6	243.8	0.45	0.0413	0.0006	0.2872	0.0097	0.0518	0.0016	260.9	6.9	256.3	15.6	274.4	18.3	-1.8	4.9	260.9	6.93
G48	116.7	1234.9	0.07	0.1006	0.0012	0.9261	0.0181	0.0665	0.0011	618.1	14.5	665.6	19.9	822.8	21.7	7.1	24.9	618.1	14.53
G49	12.0	326.6	0.25	0.0372	0.0005	0.2559	0.0108	0.0520	0.0020	235.7	6.7	231.4	17.7	283.2	22.6	-1.9	16.8	235.7	6.71
G50	12.5	283.0	0.27	0.0443	0.0006	0.3312	0.0133	0.0544	0.0020	279.1	7.9	290.5	19.8	388.5	26.9	3.9	28.1	279.1	7.90
G51	41.6	341.1	0.33	0.1194	0.0015	1.0701	0.0262	0.0680	0.0013	727.0	17.4	738.8	24.7	867.9	25.9	1.6	16.2	727.0	17.39
G52	488.0	790.2	0.69	0.5184	0.0063	14.0648	0.2253	0.1951	0.0025	2692.6	53.2	2754.1	33.2	2785.8	27.5	2.2	3.3	2785.8	27.55
G53	13.0	310.8	0.10	0.0446	0.0006	0.3767	0.0108	0.0640	0.0016	281.4	7.3	324.6	16.5	742.3	30.4	13.3	62.1	281.4	7.28
G54	39.2	253.3	0.95	0.1285	0.0017	1.2317	0.0384	0.0709	0.0017	779.4	19.3	815.1	30.5	954.8	32.5	4.4	18.4	779.4	19.31
G55	14.5	271.6	0.34	0.0531	0.0007	0.4181	0.0130	0.0581	0.0016	333.6	8.7	354.7	18.5	531.6	26.1	5.9	37.3	333.6	8.69
G56	20.5	232.5	0.88	0.0746	0.0010	0.5514	0.0158	0.0574	0.0014	463.8	11.6	445.9	20.8	505.0	22.8	-4.0	8.2	463.8	11.64
G57	25.0	38.5	1.49	0.4622	0.0067	10.1142	0.5421	0.1675	0.0037	2449.4	58.7	2445.3	48.5	2533.0	44.0	-0.2	3.3	2533.0	43.99
G58	18.6	432.7	0.56	0.0396	0.0005	0.2799	0.0074	0.0524	0.0013	250.4	6.3	250.6	12.3	300.7	15.9	0.1	16.7	250.4	6.32
G59	104.7	572.9	0.65	0.1623	0.0020	1.5780	0.0294	0.0712	0.0011	969.7	22.1	961.6	24.1	962.0	21.9	-0.8	-0.8	962.0	21.92
G60	12.5	303.2	0.28	0.0414	0.0006	0.2817	0.0086	0.0521	0.0015	261.4	6.8	252.0	14.4	290.2	17.4	-3.7	9.9	261.4	6.81
G61	213.5	1476.2	0.05	0.1533	0.0019	1.4744	0.0239	0.0692	0.0009	919.5	20.8	919.9	22.0	903.2	19.7	0.0	-1.8	903.2	19.66
G62	20.2	509.8	0.29	0.0396	0.0005	0.2776	0.0070	0.0518	0.0012	250.4	6.3	248.7	11.8	277.0	14.5	-0.7	9.6	250.4	6.32
G63	23.1	575.5	0.27	0.0404	0.0005	0.2838	0.0069	0.0511	0.0011	255.1	6.3	253.7	11.3	244.9	12.9	-0.6	-4.2	255.1	6.32
G64	37.1	974.7	0.14	0.0399	0.0005	0.2804	0.0060	0.0509	0.0010	252.2	6.2	251.0	10.1	237.7	11.5	-0.5	-6.1	252.2	6.20
G65	54.3	500.9	0.17	0.1130	0.0014	1.0624	0.0251	0.0703	0.0013	690.2	16.6	735.0	24.2	937.7	26.6	6.1	26.4	690.2	16.56
G66	10.3	263.4	0.42	0.0373	0.0005	0.2501	0.0092	0.0503	0.0017	236.1	6.5	226.7	15.3	210.3	16.2	-4.2	-12.3	236.1	6.46
G67	56.4	1401.0	0.07	0.0432	0.0005	0.3007	0.0056	0.0504	0.0008	272.4	6.6	266.9	9.6	212.6	9.7	-2.1	-28.1	272.4	6.55
G68	16.1	312.7	1.26	0.0445	0.0006	0.3616	0.0127	0.0611	0.0019	280.5	7.7	313.4	19.0	643.1	33.3	10.5	56.4	280.5	7.65
G69	12.4	305.7	0.29	0.0407	0.0006	0.2717	0.0103	0.0510	0.0018	256.9	7.1	244.0	16.8	239.0	18.1	-5.3	-7.5	256.9	7.06
G70	11.0	245.1	0.48	0.0422	0.0006	0.2746	0.0110	0.0507	0.0019	266.7	7.4	246.3	18.2	226.3	18.3	-8.3	-17.9	266.7	7.42
G71	46.5	1016.4	0.16	0.0469	0.0006	0.4020	0.0093	0.0626	0.0013	295.2	7.4	343.1	14.0	694.7	23.8	14.0	57.5	295.2	7.39
G72	73.9	1213.4	0.36	0.0588	0.0007	0.4527	0.0100	0.0549	0.0011	368.1	9.0	379.2	14.4	409.4	16.4	2.9	10.1	368.1	9.01
G73	28.6	728.3	0.39	0.0379	0.0005	0.2658	0.0062	0.0505	0.0011	239.9	6.0	239.3	10.4	219.4	11.7	-0.2	-9.3	239.9	5.96

Table 4

Gr. No.	Pb (ppm)	U (ppm)	Atomic Th/U	Ratios						Ages (Ma)						% concord. (206/238 / 207/235)	% concord. (206/238 / 207/206)	Best Age (Ma)	±2s
				206/238	± s.e.	207/235	± s.e.	207/206	± s.e.	206/238	± 2s	207/235	± 2s	207/206	± 2s				
G74	10.9	274.1	0.28	0.0398	0.0005	0.2724	0.0082	0.0518	0.0014	251.8	6.6	244.6	13.7	274.8	16.6	-2.9	8.4	251.8	6.57
G75	11.9	132.0	0.70	0.0797	0.0012	0.5897	0.0246	0.0575	0.0020	494.0	13.7	470.7	29.9	509.6	31.6	-5.0	3.1	494.0	13.73
G76	12.3	299.4	0.31	0.0406	0.0005	0.2678	0.0083	0.0502	0.0014	256.7	6.7	240.9	13.9	202.4	13.8	-6.6	-26.8	256.7	6.69
G77	60.0	1244.4	1.01	0.0390	0.0005	0.2785	0.0055	0.0524	0.0009	246.7	6.0	249.4	9.6	303.3	12.6	1.1	18.7	246.7	5.96
G78	14.0	85.9	0.44	0.1535	0.0020	1.4266	0.0430	0.0709	0.0016	920.6	22.5	900.1	31.5	955.1	31.0	-2.3	3.6	955.1	30.98
G79	10.1	264.0	0.22	0.0391	0.0005	0.2584	0.0083	0.0504	0.0015	247.3	6.6	233.4	14.0	212.6	14.6	-6.0	-16.3	247.3	6.58
G80	129.7	1090.3	0.28	0.1173	0.0015	1.2099	0.0223	0.0743	0.0011	714.8	16.7	805.1	21.7	1049.1	23.3	11.2	31.9	714.8	16.73
G81	11.7	293.1	0.32	0.0394	0.0005	0.2743	0.0078	0.0520	0.0014	248.8	6.5	246.1	13.0	286.7	16.4	-1.1	13.2	248.8	6.45
G82	12.8	320.3	0.21	0.0409	0.0005	0.2879	0.0084	0.0531	0.0014	258.3	6.7	256.9	13.9	330.9	18.4	-0.5	21.9	258.3	6.69
G83	8.4	191.4	0.46	0.0412	0.0006	0.2919	0.0096	0.0532	0.0016	260.0	6.9	260.0	15.5	335.6	20.5	0.0	22.5	260.0	6.93
G84	19.4	484.5	0.18	0.0411	0.0006	0.3017	0.0095	0.0543	0.0015	259.7	6.8	267.7	15.0	385.2	21.6	3.0	32.6	259.7	6.81
G85	37.2	267.8	0.47	0.1298	0.0017	1.1432	0.0316	0.0657	0.0014	786.6	19.2	774.0	27.5	795.2	27.1	-1.6	1.1	786.6	19.17
G86	9.9	140.2	0.70	0.0623	0.0009	0.4596	0.0217	0.0544	0.0022	389.5	11.4	384.0	28.2	388.5	29.9	-1.5	-0.3	389.5	11.41
G87	17.2	416.3	0.32	0.0408	0.0005	0.2718	0.0074	0.0505	0.0013	257.9	6.6	244.1	12.6	219.9	13.2	-5.6	-17.3	257.9	6.57
G88	13.6	354.4	0.25	0.0389	0.0005	0.2627	0.0082	0.0507	0.0014	245.7	6.5	236.8	13.6	227.2	15.0	-3.7	-8.1	245.7	6.45
G89	21.5	546.4	0.13	0.0413	0.0005	0.2880	0.0069	0.0521	0.0011	261.1	6.6	257.0	11.6	290.2	14.3	-1.6	10.0	261.1	6.56
G90	50.0	1151.5	0.75	0.0379	0.0005	0.2703	0.0059	0.0510	0.0010	239.7	6.0	242.9	10.0	240.4	11.8	1.3	0.3	239.7	5.96
G91	156.4	935.5	0.41	0.1579	0.0020	1.6517	0.0343	0.0758	0.0012	945.3	21.9	990.2	26.0	1088.7	25.3	4.5	13.2	1088.7	25.26
G92	17.6	332.3	0.21	0.0542	0.0007	0.4234	0.0133	0.0587	0.0016	340.4	8.9	358.5	19.0	557.1	27.1	5.0	38.9	340.4	8.93
G93	12.7	251.4	0.33	0.0493	0.0007	0.3488	0.0108	0.0540	0.0015	310.0	8.1	303.8	16.8	371.5	20.7	-2.0	16.6	310.0	8.11
G94	11.5	297.5	0.26	0.0389	0.0005	0.2735	0.0080	0.0525	0.0014	246.3	6.5	245.5	13.2	305.1	17.4	-0.3	19.3	246.3	6.45
G95	13.8	348.7	0.31	0.0394	0.0005	0.2633	0.0078	0.0500	0.0014	248.9	6.5	237.3	13.0	195.9	13.0	-4.9	-27.1	248.9	6.45
G96	18.9	522.4	0.19	0.0373	0.0005	0.2655	0.0076	0.0521	0.0014	236.0	6.1	239.1	12.5	288.9	16.5	1.3	18.3	236.0	6.09
G97	20.1	236.2	0.43	0.0805	0.0010	0.6786	0.0174	0.0656	0.0014	499.1	12.4	525.9	21.6	793.0	27.2	5.1	37.1	499.1	12.41
G98	7.3	179.4	0.57	0.0368	0.0005	0.2614	0.0107	0.0520	0.0020	233.2	6.7	235.8	17.2	284.1	22.1	1.1	17.9	233.2	6.71
G99	18.3	145.9	0.75	0.1089	0.0015	0.9525	0.0364	0.0653	0.0020	666.5	17.8	679.4	33.3	784.3	36.2	1.9	15.0	666.5	17.79
G100	13.5	343.0	0.21	0.0401	0.0006	0.2725	0.0116	0.0514	0.0020	253.5	7.3	244.7	18.7	260.1	21.2	-3.6	2.6	253.5	7.31
G101	14.2	332.9	0.32	0.0421	0.0006	0.2886	0.0088	0.0514	0.0014	265.7	6.9	257.4	14.2	258.4	15.9	-3.2	-2.8	265.7	6.93
G102	18.6	463.6	0.37	0.0391	0.0005	0.2648	0.0072	0.0509	0.0013	247.4	6.3	238.5	12.2	234.5	13.8	-3.7	-5.5	247.4	6.33
G103	33.0	450.4	0.44	0.0696	0.0009	0.5394	0.0126	0.0561	0.0011	433.7	10.7	438.0	17.0	455.1	18.2	1.0	4.7	433.7	10.73
G104	57.6	379.6	0.61	0.1367	0.0018	1.2147	0.0297	0.0665	0.0013	825.7	19.8	807.4	26.1	820.9	25.1	-2.3	-0.6	825.7	19.85
G105	13.4	307.6	0.31	0.0430	0.0006	0.3122	0.0122	0.0559	0.0020	271.5	7.7	275.9	19.3	449.6	29.0	1.6	39.6	271.5	7.66
G106	29.6	738.4	0.65	0.0358	0.0005	0.2543	0.0058	0.0512	0.0011	226.5	5.7	230.0	10.0	251.6	12.6	1.5	10.0	226.5	5.73
G107	50.7	327.8	0.19	0.1569	0.0020	1.5034	0.0319	0.0720	0.0012	939.7	22.0	931.8	26.1	986.8	24.8	-0.8	4.8	986.8	24.78
G108	14.3	352.5	0.27	0.0408	0.0005	0.2805	0.0078	0.0519	0.0013	257.8	6.7	251.1	13.0	280.1	15.7	-2.7	8.0	257.8	6.69
G109	78.3	621.6	2.02	0.0814	0.0010	0.6406	0.0131	0.0575	0.0010	504.4	12.2	502.7	17.2	511.1	17.5	-0.3	1.3	504.4	12.16
G110	10.2	252.0	0.48	0.0379	0.0005	0.2557	0.0081	0.0512	0.0015	239.9	6.3	231.2	13.7	250.7	16.2	-3.8	4.3	239.9	6.34
G111	179.7	1006.9	0.36	0.1714	0.0022	1.7733	0.0372	0.0766	0.0013	1019.7	23.8	1035.7	27.2	1109.5	25.8	1.5	8.1	1109.5	25.79
G112	86.7	694.8	0.10	0.1306	0.0017	1.2171	0.0270	0.0686	0.0012	791.3	18.8	808.5	24.6	887.0	24.6	2.1	10.8	791.3	18.82

Table 4

Gr. No.	Pb (ppm)	U (ppm)	Atomic Th/U	Ratios 206/238	± s.e.	207/235	± s.e.	207/206	± s.e.	Ages (Ma) 206/238	± 2s	207/235	± 2s	207/206	± 2s	% concord. (206/238 / 207/235)	% concord. (206/238 / 207/206)	Best Age (Ma)	±2s
G113	11.8	298.1	0.28	0.0397	0.0005	0.2742	0.0080	0.0519	0.0014	250.7	6.6	246.1	13.3	278.8	16.3	-1.9	10.1	250.7	6.57
G114	37.2	408.7	0.26	0.0912	0.0012	0.7708	0.0204	0.0665	0.0015	562.7	14.1	580.2	23.6	821.2	28.1	3.0	31.5	562.7	14.06
G115	18.4	333.5	0.40	0.0539	0.0007	0.3908	0.0116	0.0558	0.0015	338.2	8.8	334.9	17.5	443.2	22.2	-1.0	23.7	338.2	8.81
G116	11.1	283.6	0.27	0.0392	0.0005	0.2697	0.0082	0.0520	0.0014	248.1	6.6	242.4	13.7	286.7	17.2	-2.3	13.5	248.1	6.58
G117	44.6	739.7	0.48	0.0566	0.0007	0.4169	0.0089	0.0534	0.0010	354.7	8.8	353.8	13.5	346.3	14.4	-0.2	-2.4	354.7	8.79
G118	38.5	875.5	0.74	0.0383	0.0005	0.2705	0.0065	0.0510	0.0011	242.2	6.1	243.1	10.7	242.6	12.6	0.4	0.2	242.2	6.08
G119	12.0	291.8	0.43	0.0392	0.0005	0.2643	0.0079	0.0509	0.0014	247.6	6.5	238.1	13.2	234.0	14.7	-4.0	-5.8	247.6	6.45
G120	86.1	644.9	0.17	0.1373	0.0017	1.3682	0.0265	0.0725	0.0012	829.2	19.5	875.4	24.0	1000.8	23.9	5.3	17.1	829.2	19.50
G121	46.3	410.0	0.21	0.1129	0.0015	1.0675	0.0272	0.0719	0.0015	689.8	17.0	737.5	26.0	982.8	29.1	6.5	29.8	689.8	17.03
G122	58.1	1706.1	0.15	0.0355	0.0005	0.2535	0.0050	0.0518	0.0009	225.0	5.6	229.4	8.9	274.4	11.9	1.9	18.0	225.0	5.60
G123	12.7	309.5	0.33	0.0405	0.0005	0.2704	0.0077	0.0509	0.0013	255.7	6.7	243.0	13.0	234.0	14.2	-5.2	-9.3	255.7	6.69
G124	23.7	214.1	1.50	0.0795	0.0011	0.5911	0.0179	0.0567	0.0015	492.9	12.7	471.6	22.4	479.5	22.9	-4.5	-2.8	492.9	12.66
G125	10.8	251.4	0.31	0.0426	0.0006	0.3192	0.0125	0.0582	0.0021	268.8	7.7	281.3	19.8	536.2	32.9	4.4	49.9	268.8	7.67
G126	14.0	352.5	0.25	0.0402	0.0005	0.2749	0.0078	0.0513	0.0013	254.1	6.6	246.6	13.0	254.3	15.0	-3.1	0.1	254.1	6.57
G127	55.0	1168.6	0.85	0.0399	0.0005	0.2816	0.0062	0.0512	0.0010	252.0	6.3	251.9	10.4	248.5	12.0	0.0	-1.4	252.0	6.32
G128	22.3	581.1	0.13	0.0401	0.0005	0.2859	0.0070	0.0522	0.0011	253.1	6.4	255.3	11.5	294.2	14.6	0.9	13.9	253.1	6.45
G129	22.0	590.0	0.24	0.0377	0.0005	0.2653	0.0067	0.0517	0.0012	238.7	6.1	238.9	11.2	272.2	14.1	0.1	12.3	238.7	6.09
14052705 Song Trac																			
G1	84.6	529.3	0.48	0.1498	0.0018	1.4734	0.0229	0.0714	0.0011	899.6	19.6	919.5	22.9	968.3	18.5	2.2	7.1	899.6	19.6
G10	44.0	104.2	0.16	0.4173	0.0050	9.7687	0.1505	0.1698	0.0025	2248.2	45.7	2413.2	34.9	2556.1	27.4	6.8	12.0	2556.1	27.4
G100	40.4	560.9	0.42	0.0685	0.0009	0.5289	0.0128	0.0560	0.0013	426.9	10.6	431.1	18.9	454.0	17.2	1.0	6.0	426.9	10.6
G101	45.7	256.5	0.56	0.1608	0.0021	1.5372	0.0333	0.0693	0.0015	961.4	22.8	945.4	30.1	908.9	25.1	-1.7	-5.8	908.9	25.1
G102	18.8	406.8	0.90	0.0383	0.0005	0.2734	0.0083	0.0518	0.0016	242.2	6.5	245.4	14.4	277.5	14.6	1.3	12.7	242.2	6.5
G103	231.6	447.2	0.49	0.4533	0.0056	9.8865	0.1758	0.1582	0.0026	2410.0	49.8	2424.3	38.1	2436.8	30.6	0.6	1.1	2436.8	30.6
G104	27.3	339.2	0.91	0.0661	0.0009	0.5125	0.0151	0.0563	0.0016	412.6	10.8	420.1	22.1	462.6	21.7	1.8	10.8	412.6	10.8
G105	86.3	411.2	0.69	0.1818	0.0023	2.0005	0.0396	0.0798	0.0015	1076.9	25.0	1115.7	30.6	1192.8	26.4	3.5	9.7	1192.8	26.4
G106	23.2	445.3	0.49	0.0485	0.0006	0.3565	0.0096	0.0533	0.0014	305.3	7.9	309.6	15.9	342.9	15.5	1.4	11.0	305.3	7.9
G107	21.4	393.5	0.32	0.0517	0.0007	0.3911	0.0105	0.0548	0.0015	325.2	8.3	335.2	16.9	405.7	17.7	3.0	19.8	325.2	8.3
G108	47.4	257.1	0.44	0.1726	0.0022	1.8343	0.0388	0.0771	0.0016	1026.2	24.2	1057.8	31.6	1124.3	27.7	3.0	8.7	1124.3	27.7
G109	129.3	219.2	0.99	0.4576	0.0057	10.2183	0.1889	0.1620	0.0028	2428.9	50.8	2454.7	39.5	2476.9	32.0	1.1	1.9	2476.9	32.0
G11	8.3	328.5	0.44	0.0240	0.0003	0.1655	0.0056	0.0499	0.0017	153.1	4.0	155.5	10.5	192.2	11.9	1.5	20.3	153.1	4.0
G110	41.3	224.9	0.49	0.1689	0.0022	1.8344	0.0399	0.0788	0.0017	1006.3	23.9	1057.8	32.3	1166.6	29.1	4.9	13.7	1166.6	29.1
G111	35.1	277.3	0.34	0.1208	0.0016	1.0569	0.0254	0.0635	0.0015	735.1	17.9	732.3	27.8	724.4	24.1	-0.4	-1.5	735.1	17.9
G112	22.6	530.0	0.63	0.0382	0.0005	0.2739	0.0076	0.0520	0.0014	241.7	6.3	245.8	13.3	285.4	13.6	1.6	15.3	241.7	6.3
G113	147.6	1020.8	0.13	0.1498	0.0019	1.4492	0.0292	0.0702	0.0013	899.6	21.2	909.5	27.5	934.2	23.3	1.1	3.7	899.6	21.2
G114	20.9	134.5	0.94	0.1279	0.0018	1.1675	0.0370	0.0662	0.0021	775.7	20.7	785.5	37.8	814.0	35.3	1.2	4.7	775.7	20.7
G115	2.4	37.9	1.15	0.0487	0.0013	0.3595	0.0385	0.0536	0.0058	306.2	15.4	311.8	60.1	354.7	65.2	1.8	13.7	306.2	15.4

Table 4

Gr. No.	Pb (ppm)	U (ppm)	Atomic Th/U	Ratios 206/238	± s.e.	207/235	± s.e.	207/206	± s.e.	Ages (Ma) 206/238	± 2s	207/235	± 2s	207/206	± 2s	% concord. (206/238 207/235)	% concord. (206/238 207/206)	Best Age (Ma)	±2s
G116	35.5	313.9	1.06	0.0894	0.0012	0.7374	0.0219	0.0598	0.0018	552.1	14.6	560.9	28.0	597.4	26.6	1.6	7.6	552.1	14.6
G117	33.5	416.3	0.85	0.0679	0.0009	0.5306	0.0162	0.0567	0.0017	423.2	11.2	432.2	23.3	481.1	23.1	2.1	12.0	423.2	11.2
G118	11.7	212.2	0.74	0.0477	0.0008	0.3445	0.0161	0.0524	0.0025	300.3	9.2	300.6	25.9	303.8	24.7	0.1	1.2	300.3	9.2
G119	15.4	272.2	1.97	0.0364	0.0006	0.2548	0.0112	0.0507	0.0023	230.7	7.0	230.5	19.4	228.1	18.1	-0.1	-1.1	230.7	7.0
G12	43.7	413.1	0.92	0.0880	0.0011	0.7215	0.0138	0.0595	0.0011	543.9	12.6	551.6	18.9	584.0	16.6	1.4	6.9	543.9	12.6
G120	67.4	468.7	0.04	0.1535	0.0020	1.5021	0.0352	0.0710	0.0016	920.6	22.5	931.3	31.8	957.4	27.9	1.1	3.8	957.4	27.9
G121	10.8	274.8	0.59	0.0356	0.0005	0.2558	0.0100	0.0522	0.0021	225.3	6.5	231.2	17.3	292.9	20.0	2.6	23.1	225.3	6.5
G122	19.1	125.7	0.98	0.1242	0.0018	1.1064	0.0378	0.0647	0.0022	754.5	20.8	756.4	39.5	763.0	36.5	0.3	1.1	754.5	20.8
G123	12.4	202.8	0.96	0.0498	0.0008	0.3860	0.0161	0.0562	0.0024	313.5	9.3	331.5	25.2	460.7	31.0	5.4	32.0	313.5	9.3
G124	40.5	483.2	0.87	0.0702	0.0010	0.5495	0.0166	0.0568	0.0017	437.1	11.6	444.7	23.6	484.9	22.9	1.7	9.9	437.1	11.6
G125	25.9	158.5	0.96	0.1341	0.0020	1.1914	0.0440	0.0645	0.0024	810.9	23.0	796.6	44.0	757.4	39.4	-1.8	-7.1	810.9	23.0
G13	43.5	668.9	0.39	0.0626	0.0008	0.4770	0.0088	0.0553	0.0010	391.2	9.1	396.0	14.1	424.8	12.4	1.2	7.9	391.2	9.1
G14	11.9	304.5	0.58	0.0358	0.0005	0.2577	0.0076	0.0523	0.0015	226.6	5.7	232.8	13.4	297.7	15.2	2.7	23.9	226.6	5.7
G15	283.7	560.9	0.63	0.4425	0.0052	10.9587	0.1571	0.1797	0.0024	2361.7	46.6	2519.6	33.2	2650.0	25.2	6.3	10.9	2650.0	25.2
G16	107.5	741.6	0.18	0.1479	0.0017	1.3996	0.0216	0.0687	0.0010	889.2	19.5	888.8	22.2	888.5	17.2	0.0	-0.1	889.2	19.5
G17	19.8	61.9	1.44	0.2372	0.0031	2.9256	0.0651	0.0895	0.0020	1372.3	31.9	1388.6	38.8	1414.2	33.8	1.2	3.0	1414.2	33.8
G18	35.5	445.3	0.06	0.0850	0.0011	0.6919	0.0190	0.0591	0.0016	525.9	13.2	534.0	25.2	569.3	23.9	1.5	7.6	525.9	13.2
G19	96.4	528.1	1.16	0.1446	0.0017	1.4607	0.0259	0.0733	0.0013	870.6	19.6	914.3	25.2	1022.3	22.0	4.8	14.8	870.6	19.6
G2	112.9	181.9	1.33	0.4608	0.0054	10.5946	0.1525	0.1668	0.0023	2442.9	47.7	2488.2	33.3	2526.0	25.2	1.8	3.3	2526.0	25.2
G20	36.0	135.2	0.61	0.2395	0.0031	3.1196	0.0674	0.0945	0.0020	1384.3	32.0	1437.5	38.4	1517.7	33.7	3.7	8.8	1517.7	33.7
G21	16.4	195.2	0.96	0.0701	0.0009	0.5330	0.0144	0.0552	0.0015	436.8	10.8	433.8	21.0	418.7	18.4	-0.7	-4.3	436.8	10.8
G22	187.5	317.7	0.82	0.4785	0.0056	11.0734	0.1588	0.1679	0.0022	2520.6	49.1	2529.3	33.1	2536.8	24.9	0.3	0.6	2536.8	24.9
G23	24.8	229.3	1.34	0.0816	0.0010	0.6504	0.0158	0.0578	0.0014	505.8	12.3	508.7	21.7	522.6	19.6	0.6	3.2	505.8	12.3
G24	267.0	1094.1	0.02	0.2571	0.0030	3.6097	0.0542	0.1019	0.0014	1475.1	31.1	1551.7	29.3	1658.3	23.1	4.9	11.0	1658.3	23.1
G25	65.7	708.7	0.08	0.0978	0.0012	0.8590	0.0176	0.0637	0.0013	601.3	14.1	629.6	22.1	733.0	21.0	4.5	18.0	601.3	14.1
G26	160.7	451.6	0.46	0.3275	0.0039	5.0671	0.0797	0.1122	0.0017	1826.3	38.1	1830.6	32.4	1836.0	25.3	0.2	0.5	1836.0	25.3
G27	86.4	245.1	0.37	0.3307	0.0040	5.2437	0.0884	0.1151	0.0019	1841.7	39.0	1859.7	34.5	1880.7	27.7	1.0	2.1	1880.7	27.7
G28	72.4	533.8	0.61	0.1228	0.0015	1.1052	0.0188	0.0653	0.0011	746.8	16.9	755.9	21.5	783.4	17.7	1.2	4.7	746.8	16.9
G29	124.9	357.5	0.35	0.3298	0.0040	5.2103	0.0832	0.1146	0.0017	1837.2	38.4	1854.3	33.0	1874.1	26.0	0.9	2.0	1874.1	26.0
G3	16.8	334.8	0.79	0.0436	0.0005	0.3230	0.0081	0.0538	0.0014	275.0	6.7	284.2	13.9	361.4	15.3	3.3	23.9	275.0	6.7
G30	43.8	610.8	0.65	0.0645	0.0008	0.4949	0.0098	0.0557	0.0011	402.8	9.4	408.2	15.4	439.6	13.8	1.3	8.4	402.8	9.4
G31	8.7	347.4	0.30	0.0248	0.0003	0.1676	0.0061	0.0491	0.0018	157.8	4.3	157.3	11.4	150.2	10.2	-0.3	-5.0	157.8	4.3
G32	280.6	750.4	0.88	0.3121	0.0037	4.9166	0.0740	0.1143	0.0016	1750.9	36.4	1805.1	31.1	1868.9	24.1	3.0	6.3	1868.9	24.1
G33	195.8	891.3	1.23	0.1708	0.0021	1.7749	0.0299	0.0754	0.0012	1016.7	22.6	1036.3	26.0	1078.4	21.3	1.9	5.7	1078.4	21.3
G34	55.2	314.6	0.87	0.1485	0.0019	1.4272	0.0327	0.0697	0.0016	892.7	21.2	900.4	31.0	919.8	27.4	0.9	3.0	892.7	21.2
G35	49.4	778.2	0.39	0.0614	0.0007	0.4741	0.0090	0.0560	0.0010	384.2	9.0	394.0	14.4	452.8	13.4	2.5	15.1	384.2	9.0
G36	102.3	737.8	0.31	0.1358	0.0016	1.2980	0.0210	0.0694	0.0011	820.6	18.3	844.9	22.2	909.8	18.4	2.9	9.8	820.6	18.3
G37	42.1	85.9	1.17	0.3814	0.0051	7.9631	0.1640	0.1515	0.0031	2083.0	47.5	2226.9	43.9	2362.6	37.3	6.5	11.8	2362.6	37.3
G38	58.3	708.7	1.10	0.0656	0.0008	0.5017	0.0096	0.0555	0.0010	409.7	9.6	412.9	15.0	431.6	13.1	0.8	5.1	409.7	9.6

Table 4

Gr. No.	Pb (ppm)	U (ppm)	Atomic Th/U	Ratios 206/238	± s.e.	207/235	± s.e.	207/206	± s.e.	Ages (Ma) 206/238	± 2s	207/235	± 2s	207/206	± 2s	% concord. (206/238 / 207/235)	% concord. (206/238 / 207/206)	Best Age (Ma)	±2s
G39	18.8	53.7	1.13	0.2736	0.0039	4.1530	0.1130	0.1101	0.0030	1558.9	39.9	1664.8	50.7	1801.7	46.2	6.4	13.5	1801.7	46.2
G4	34.6	190.1	0.80	0.1571	0.0020	1.5207	0.0344	0.0702	0.0016	940.9	22.1	938.8	31.6	934.5	27.5	-0.2	-0.7	934.5	27.5
G40	133.1	252.0	0.51	0.4634	0.0055	10.4233	0.1560	0.1632	0.0023	2454.7	48.6	2473.1	33.9	2488.9	25.8	0.7	1.4	2488.9	25.8
G41	260.2	761.2	0.51	0.3113	0.0037	4.8975	0.0757	0.1141	0.0017	1747.2	36.6	1801.8	31.6	1866.2	24.7	3.0	6.4	1866.2	24.7
G42	130.1	341.7	0.74	0.3290	0.0040	5.1501	0.0841	0.1136	0.0018	1833.6	38.6	1844.4	33.4	1857.3	26.4	0.6	1.3	1857.3	26.4
G43	75.5	1142.7	0.37	0.0639	0.0008	0.4888	0.0088	0.0555	0.0010	399.5	9.3	404.1	14.0	431.2	12.0	1.1	7.4	399.5	9.3
G44	152.0	349.3	0.34	0.4103	0.0049	9.4762	0.1430	0.1676	0.0024	2216.1	44.8	2385.2	33.8	2533.6	26.1	7.1	12.5	2533.6	26.1
G45	14.4	43.0	0.77	0.2872	0.0039	4.2132	0.1013	0.1064	0.0026	1627.5	39.2	1676.6	45.2	1739.3	39.9	2.9	6.4	1739.3	39.9
G46	11.8	137.7	0.54	0.0788	0.0011	0.6224	0.0192	0.0573	0.0018	488.8	12.7	491.4	26.2	503.9	24.5	0.5	3.0	488.8	12.7
G47	65.5	439.0	0.25	0.1478	0.0019	1.5507	0.0339	0.0761	0.0016	888.4	21.1	950.8	30.9	1098.8	28.9	6.6	19.1	888.4	21.1
G48	48.3	538.2	0.72	0.0787	0.0010	0.6143	0.0121	0.0566	0.0011	488.2	11.5	486.3	17.5	477.5	14.5	-0.4	-2.2	488.2	11.5
G49	14.3	70.7	0.78	0.1718	0.0026	1.7597	0.0640	0.0743	0.0027	1021.7	28.7	1030.7	51.6	1050.4	48.3	0.9	2.7	1050.4	48.3
G5	42.3	328.5	0.16	0.1329	0.0016	1.2644	0.0241	0.0690	0.0013	804.4	18.3	829.9	25.3	899.3	22.3	3.1	10.6	804.4	18.3
G50	9.9	200.2	1.13	0.0390	0.0006	0.2749	0.0102	0.0512	0.0019	246.6	6.8	246.6	17.6	247.6	16.5	0.0	0.4	246.6	6.8
G51	56.3	1308.2	0.87	0.0362	0.0005	0.2864	0.0063	0.0574	0.0012	229.3	5.6	255.7	11.3	506.2	17.2	10.3	54.7	229.3	5.6
G52	44.2	241.3	0.62	0.1645	0.0020	1.6107	0.0313	0.0710	0.0013	981.6	22.5	974.4	28.1	958.6	23.2	-0.7	-2.4	958.6	23.2
G53	55.9	826.2	0.35	0.0661	0.0008	0.5060	0.0120	0.0556	0.0013	412.3	10.0	415.8	18.1	435.6	16.6	0.8	5.4	412.3	10.0
G54	35.5	398.0	1.22	0.0693	0.0009	0.5184	0.0119	0.0543	0.0012	431.6	10.5	424.1	18.0	383.9	14.5	-1.8	-12.4	431.6	10.5
G55	21.8	507.2	0.84	0.0367	0.0005	0.2539	0.0069	0.0502	0.0013	232.5	5.8	229.7	12.2	202.4	9.8	-1.2	-14.8	232.5	5.8
G56	174.5	1271.5	0.05	0.1461	0.0018	1.4540	0.0253	0.0722	0.0012	879.0	19.9	911.5	24.7	991.9	21.0	3.6	11.4	879.0	19.9
G57	8.1	274.1	0.30	0.0292	0.0004	0.2289	0.0099	0.0568	0.0025	185.7	5.5	209.3	17.5	484.6	33.8	11.3	61.7	185.7	5.5
G58	20.1	420.1	0.93	0.0398	0.0005	0.2831	0.0077	0.0517	0.0014	251.3	6.3	253.1	13.4	271.3	12.9	0.7	7.4	251.3	6.3
G59	58.2	399.8	0.69	0.1282	0.0016	1.1498	0.0218	0.0651	0.0012	777.8	17.9	777.1	23.8	776.0	19.7	-0.1	-0.2	777.8	17.9
G6	33.5	193.9	0.64	0.1546	0.0020	1.5122	0.0346	0.0710	0.0016	926.7	21.8	935.3	31.7	956.5	28.1	0.9	3.1	956.5	28.1
G60	26.9	575.5	0.81	0.0401	0.0005	0.2866	0.0070	0.0519	0.0013	253.1	6.3	255.9	12.4	281.9	11.9	1.1	10.2	253.1	6.3
G61	197.8	935.5	0.46	0.1969	0.0024	2.1938	0.0354	0.0808	0.0012	1158.5	25.4	1179.1	26.9	1217.6	21.4	1.7	4.8	1217.6	21.4
G62	81.2	282.4	0.94	0.2329	0.0030	2.7114	0.0561	0.0845	0.0017	1349.8	30.8	1331.6	35.3	1302.9	29.6	-1.4	-3.6	1302.9	29.6
G63	82.1	1039.1	0.29	0.0785	0.0010	0.6245	0.0113	0.0577	0.0010	487.0	11.4	492.7	16.4	519.9	14.0	1.2	6.3	487.0	11.4
G64	216.4	380.3	0.59	0.4863	0.0059	11.3799	0.1840	0.1698	0.0026	2554.7	51.4	2554.8	36.2	2555.4	28.2	0.0	0.0	2555.4	28.2
G65	22.2	300.0	0.30	0.0735	0.0009	0.5800	0.0143	0.0573	0.0014	457.1	11.3	464.5	20.5	501.9	19.2	1.6	8.9	457.1	11.3
G66	67.3	343.0	2.15	0.1243	0.0016	1.1078	0.0240	0.0647	0.0014	755.4	18.0	757.1	26.2	763.0	22.6	0.2	1.0	755.4	18.0
G67	81.9	186.3	0.40	0.4087	0.0053	9.2510	0.1718	0.1642	0.0029	2209.1	48.0	2363.2	40.4	2499.5	33.3	6.5	11.6	2499.5	33.3
G68	66.8	2613.8	0.53	0.0236	0.0003	0.1620	0.0031	0.0498	0.0009	150.4	3.7	152.5	6.3	185.7	6.3	1.3	19.0	150.4	3.7
G69	12.1	329.1	1.67	0.0647	0.0008	0.4994	0.0122	0.0560	0.0013	404.4	10.1	411.3	18.4	450.8	17.4	1.7	10.3	404.4	10.1
G7	32.0	656.9	0.80	0.0421	0.0005	0.3218	0.0082	0.0555	0.0014	265.8	6.6	283.3	14.0	430.8	17.7	6.2	38.3	265.8	6.6
G70	23.4	159.8	1.00	0.1200	0.0016	1.1217	0.0293	0.0678	0.0018	730.7	18.3	763.8	31.3	862.4	30.2	4.3	15.3	730.7	18.3
G71	19.7	157.9	0.28	0.1236	0.0017	1.2937	0.0357	0.0760	0.0021	751.1	19.4	842.9	35.2	1093.8	36.9	10.9	31.3	751.1	19.4
G72	86.9	180.7	0.44	0.4339	0.0053	9.8587	0.1645	0.1649	0.0026	2323.1	47.8	2421.7	36.7	2506.0	29.1	4.1	7.3	2506.0	29.1
G73	60.0	362.6	0.82	0.1409	0.0017	1.3360	0.0254	0.0688	0.0013	849.7	19.7	861.5	25.5	892.4	21.6	1.4	4.8	849.7	19.7

Table 4

				Ratios						Ages (Ma)									
Gr. No.	Pb (ppm)	U (ppm)	Atomic Th/U	206/238	± s.e.	207/235	± s.e.	207/206	± s.e.	206/238	± 2s	207/235	± 2s	207/206	± 2s	% concord. (206/238 207/235)	% concord. (206/238 207/206)	Best Age (Ma)	±2s
G74	132.0	326.6	0.69	0.3515	0.0044	6.6105	0.1164	0.1364	0.0023	1941.8	41.7	2060.8	36.7	2182.5	30.0	5.8	11.0	2182.5	30.0
G75	264.3	802.2	0.54	0.2982	0.0036	4.6669	0.0781	0.1135	0.0018	1682.4	36.1	1761.3	33.2	1856.8	26.7	4.5	9.4	1856.8	26.7
G76	31.9	98.5	0.54	0.2909	0.0040	4.1971	0.1001	0.1047	0.0025	1645.9	39.5	1673.5	44.7	1708.7	39.0	1.6	3.7	1708.7	39.0
G77	11.0	137.1	0.75	0.0695	0.0010	0.5372	0.0179	0.0561	0.0019	433.3	11.6	436.6	25.6	454.7	24.5	0.8	4.7	433.3	11.6
G78	44.0	81.5	0.94	0.4292	0.0059	10.2591	0.2180	0.1734	0.0036	2302.0	53.1	2458.4	46.1	2591.0	39.0	6.4	11.2	2591.0	39.0
G79	44.2	578.6	0.76	0.0657	0.0008	0.5050	0.0110	0.0558	0.0012	410.0	9.9	415.1	16.7	444.0	15.2	1.2	7.7	410.0	9.9
G8	85.2	534.4	0.66	0.1419	0.0017	1.3865	0.0243	0.0709	0.0012	855.6	19.1	883.2	24.4	954.0	20.9	3.1	10.3	855.6	19.1
G80	116.6	230.6	0.71	0.4280	0.0053	9.7711	0.1651	0.1656	0.0026	2296.9	47.5	2413.4	36.9	2513.8	29.4	4.8	8.6	2513.8	29.4
G81	40.9	546.4	0.61	0.0675	0.0009	0.6053	0.0142	0.0651	0.0015	421.1	10.5	480.6	20.2	776.3	25.0	12.4	45.8	421.1	10.5
G82	92.3	445.3	0.68	0.1817	0.0023	1.9363	0.0394	0.0773	0.0015	1076.4	25.0	1093.7	31.3	1128.9	26.8	1.6	4.7	1128.9	26.8
G83	232.5	675.9	0.35	0.3227	0.0039	5.0779	0.0855	0.1142	0.0018	1803.0	38.3	1832.4	33.7	1866.7	26.8	1.6	3.4	1866.7	26.8
G84	2.7	54.3	0.71	0.0436	0.0009	0.3610	0.0275	0.0601	0.0047	275.0	11.4	312.9	43.3	606.8	70.9	12.1	54.7	275.0	11.4
G85	27.4	138.3	0.97	0.1611	0.0021	1.6127	0.0382	0.0726	0.0017	963.0	23.3	975.2	33.3	1003.4	29.5	1.2	4.0	1003.4	29.5
G86	49.1	698.0	0.45	0.0663	0.0008	0.5066	0.0108	0.0554	0.0011	413.8	10.0	416.1	16.4	429.6	14.4	0.6	3.7	413.8	10.0
G87	45.1	520.5	0.87	0.0728	0.0010	0.6280	0.0158	0.0626	0.0016	453.1	11.4	494.9	21.9	693.6	24.9	8.4	34.7	453.1	11.4
G88	127.5	350.6	0.35	0.3405	0.0042	5.5299	0.0963	0.1178	0.0019	1889.1	40.3	1905.2	35.1	1923.4	28.1	0.8	1.8	1923.4	28.1
G89	396.4	1399.8	0.91	0.2325	0.0029	2.9163	0.0505	0.0910	0.0015	1347.7	29.8	1386.2	30.7	1446.4	24.9	2.8	6.8	1446.4	24.9
G9	82.4	442.8	0.23	0.1854	0.0022	2.0916	0.0366	0.0819	0.0014	1096.2	24.3	1146.1	28.6	1242.4	24.3	4.4	11.8	1242.4	24.3
G90	96.6	581.1	0.36	0.1592	0.0020	1.5653	0.0305	0.0713	0.0013	952.2	22.1	956.6	27.8	967.2	23.3	0.5	1.5	967.2	23.3
G91	52.8	264.0	1.60	0.1396	0.0020	1.2373	0.0385	0.0643	0.0020	842.6	22.2	817.7	38.3	751.2	33.0	-3.0	-12.2	842.6	22.2
G92	22.6	299.4	0.58	0.0685	0.0009	0.5269	0.0137	0.0558	0.0014	427.1	10.7	429.7	20.0	444.4	18.3	0.6	3.9	427.1	10.7
G93	37.5	251.4	1.03	0.1194	0.0015	1.0511	0.0239	0.0639	0.0014	726.9	17.6	729.4	26.6	738.0	23.2	0.3	1.5	726.9	17.6
G94	67.8	172.4	1.13	0.3044	0.0039	4.8036	0.0980	0.1145	0.0023	1712.9	38.8	1785.5	39.5	1872.0	33.6	4.1	8.5	1872.0	33.6
G95	27.7	87.8	0.40	0.2946	0.0038	4.2830	0.0904	0.1055	0.0022	1664.2	38.1	1690.1	39.8	1722.9	33.8	1.5	3.4	1722.9	33.8
G96	73.6	1074.5	0.33	0.0670	0.0008	0.5009	0.0101	0.0542	0.0010	418.3	10.1	412.3	15.5	379.4	12.1	-1.5	-10.3	418.3	10.1
G97	251.8	825.6	0.02	0.3162	0.0039	4.9694	0.0909	0.1140	0.0020	1771.1	38.6	1814.1	35.9	1864.5	29.3	2.4	5.0	1864.5	29.3
G98	6.8	151.0	0.65	0.0402	0.0006	0.3001	0.0123	0.0542	0.0022	253.9	7.4	266.5	20.6	379.0	26.1	4.7	33.0	253.9	7.4
G99	47.1	879.3	0.07	0.0571	0.0007	0.4339	0.0091	0.0551	0.0011	357.9	8.8	365.9	14.6	417.5	13.8	2.2	14.3	357.9	8.8
14052801 Song Nan																			
G01	125.2	757.0	0.44	0.1569	0.0019	1.5051	0.0230	0.0696	0.0010	939.2	20.6	932.5	22.7	916.6	17.3	-0.7	-2.5	916.6	17.35
G02	22.2	212.7	1.04	0.0851	0.0011	0.6522	0.0158	0.0556	0.0013	526.3	12.8	509.8	21.8	436.8	17.1	-3.2	-20.5	526.3	12.83
G03	82.5	252.3	0.86	0.2792	0.0034	4.1836	0.0704	0.1087	0.0018	1587.2	34.3	1670.8	33.2	1777.6	27.2	5.0	10.7	1777.6	27.17
G04	226.1	440.1	0.37	0.4663	0.0055	10.4786	0.1500	0.1630	0.0022	2467.4	48.4	2478.0	33.0	2486.9	24.7	0.4	0.8	2486.9	24.70
G05	54.5	582.6	1.15	0.0744	0.0009	0.5699	0.0104	0.0556	0.0010	462.7	10.8	458.0	15.8	434.8	12.5	-1.0	-6.4	462.7	10.80
G06	19.5	94.3	1.27	0.1599	0.0020	1.6066	0.0363	0.0729	0.0016	956.1	22.7	972.8	32.2	1010.9	28.6	1.7	5.4	1010.9	28.63
G07	66.3	189.6	0.70	0.3034	0.0036	4.3550	0.0691	0.1041	0.0016	1708.0	36.0	1703.8	31.8	1698.8	24.9	-0.2	-0.5	1698.8	24.87
G08	70.0	197.2	0.51	0.3218	0.0039	4.7377	0.0747	0.1068	0.0016	1798.5	37.6	1773.9	32.2	1745.3	25.0	-1.4	-3.0	1745.3	24.97
G09	240.6	700.0	0.41	0.3192	0.0038	4.7827	0.0692	0.1087	0.0015	1785.7	36.7	1781.9	30.1	1777.4	22.7	-0.2	-0.5	1777.4	22.70

Table 4

Gr. No.	Pb (ppm)	U (ppm)	Atomic Th/U	Ratios 206/238	± s.e.	207/235	± s.e.	207/206	± s.e.	Ages (Ma) 206/238	± 2s	207/235	± 2s	207/206	± 2s	% concord. (206/238 / 207/235)	% concord. (206/238 / 207/206)	Best Age (Ma)	±2s
G10	12.2	69.9	0.48	0.1635	0.0021	1.5787	0.0386	0.0701	0.0017	975.9	23.5	961.9	34.2	930.1	29.6	-1.5	-4.9	930.1	29.56
G100	12.0	297.3	0.34	0.0395	0.0005	0.2772	0.0076	0.0509	0.0014	249.8	6.3	248.5	13.3	236.8	11.5	-0.5	-5.5	249.8	6.33
G101	13.7	67.6	0.81	0.1736	0.0023	1.7413	0.0441	0.0728	0.0018	1031.6	24.9	1024.0	36.7	1008.4	32.3	-0.8	-2.3	1008.4	32.31
G102	25.0	129.5	1.95	0.1271	0.0016	1.1370	0.0268	0.0649	0.0015	771.5	18.4	771.1	28.8	770.4	25.3	-0.1	-0.1	771.5	18.42
G103	145.2	192.3	2.28	0.4609	0.0056	10.2327	0.1805	0.1611	0.0027	2443.5	49.2	2456.0	38.6	2467.0	31.5	0.5	1.0	2467.0	31.50
G104	75.9	210.1	0.82	0.3032	0.0037	4.3412	0.0795	0.1039	0.0018	1707.1	36.4	1701.2	35.4	1694.6	29.2	-0.3	-0.7	1694.6	29.19
G105	30.9	374.7	0.70	0.0728	0.0009	0.5525	0.0122	0.0550	0.0012	453.2	10.8	446.6	18.0	413.4	14.7	-1.5	-9.6	453.2	10.82
G106	43.8	523.4	0.47	0.0791	0.0010	0.6330	0.0128	0.0580	0.0012	490.9	11.6	498.0	18.3	531.3	16.4	1.4	7.6	490.9	11.59
G107	24.5	147.8	1.05	0.1330	0.0017	1.2036	0.0273	0.0657	0.0015	804.9	19.0	802.3	28.5	795.6	24.7	-0.3	-1.2	804.9	19.00
G108	113.1	652.4	0.12	0.1791	0.0022	1.8725	0.0340	0.0759	0.0013	1061.8	23.6	1071.4	28.2	1091.6	23.5	0.9	2.7	1091.6	23.45
G109	14.7	158.4	0.87	0.0783	0.0010	0.5994	0.0159	0.0555	0.0015	486.1	12.1	476.9	22.4	433.6	18.7	-1.9	-12.1	486.1	12.08
G11	64.3	398.3	0.72	0.1423	0.0018	1.3163	0.0259	0.0671	0.0013	857.4	19.8	852.9	26.3	841.2	22.0	-0.5	-1.9	857.4	19.75
G110	146.5	232.3	0.16	0.5878	0.0071	18.8884	0.3332	0.2331	0.0040	2980.5	57.6	3036.1	40.2	3073.7	32.8	1.8	3.0	3073.7	32.82
G111	108.9	573.7	0.77	0.1626	0.0020	1.6045	0.0298	0.0716	0.0013	971.1	21.7	971.9	27.1	974.6	22.6	0.1	0.4	974.6	22.58
G112	57.8	116.6	0.85	0.4027	0.0049	7.2287	0.1356	0.1302	0.0024	2181.6	45.4	2140.1	39.2	2101.1	32.3	-1.9	-3.8	2101.1	32.29
G113	62.4	309.3	1.12	0.1611	0.0021	1.6456	0.0390	0.0741	0.0017	962.7	22.9	987.9	33.8	1044.7	30.6	2.5	7.9	1044.7	30.63
G114	9.3	51.2	0.30	0.1767	0.0024	1.8737	0.0536	0.0769	0.0022	1048.8	26.5	1071.8	42.1	1119.6	39.0	2.1	6.3	1119.6	38.97
G115	149.1	606.1	0.09	0.2538	0.0031	3.3998	0.0616	0.0972	0.0017	1457.9	31.5	1504.3	33.3	1571.1	28.0	3.1	7.2	1571.1	27.96
G116	56.6	119.3	0.80	0.3920	0.0048	7.2177	0.1366	0.1336	0.0025	2132.1	44.6	2138.7	39.5	2145.7	32.9	0.3	0.6	2145.7	32.88
G117	68.6	381.4	0.53	0.1654	0.0020	1.6606	0.0321	0.0728	0.0014	986.9	22.2	993.6	28.4	1009.2	24.1	0.7	2.2	1009.2	24.06
G118	134.0	231.4	0.71	0.4777	0.0058	10.7900	0.1972	0.1639	0.0029	2517.2	50.4	2505.2	39.7	2496.2	32.7	-0.5	-0.8	2496.2	32.75
G119	10.3	117.0	0.95	0.0723	0.0010	0.6248	0.0188	0.0627	0.0019	449.9	11.7	492.8	25.9	698.4	30.6	8.7	35.6	449.9	11.66
G12	24.5	320.4	0.58	0.0701	0.0009	0.5335	0.0113	0.0552	0.0012	436.9	10.4	434.1	17.1	419.5	14.3	-0.6	-4.1	436.9	10.36
G120	16.2	206.5	0.41	0.0746	0.0010	0.6117	0.0172	0.0595	0.0017	463.5	11.8	484.6	24.0	586.9	25.2	4.4	21.0	463.5	11.76
G121	84.0	441.5	0.45	0.1788	0.0022	1.8441	0.0355	0.0748	0.0014	1060.3	23.7	1061.3	29.4	1064.2	24.7	0.1	0.4	1064.2	24.67
G122	10.6	108.6	1.41	0.0727	0.0010	0.5756	0.0176	0.0575	0.0018	452.2	11.7	461.6	24.9	509.6	24.7	2.0	11.3	452.2	11.66
G123	37.4	453.0	0.74	0.0720	0.0009	0.5484	0.0120	0.0553	0.0012	448.0	10.7	443.9	17.9	423.6	14.9	-0.9	-5.8	448.0	10.70
G124	12.9	87.2	0.89	0.1235	0.0016	1.0981	0.0294	0.0645	0.0017	750.8	18.6	752.4	31.7	757.7	28.6	0.2	0.9	750.8	18.59
G125	32.3	388.1	0.82	0.0711	0.0009	0.5530	0.0125	0.0564	0.0013	442.7	10.6	447.0	18.4	469.7	16.7	1.0	5.7	442.7	10.59
G126	24.1	85.9	0.55	0.2533	0.0032	3.2175	0.0703	0.0922	0.0020	1455.5	32.9	1461.4	38.8	1470.7	33.5	0.4	1.0	1470.7	33.55
G127	48.2	88.1	0.57	0.4760	0.0061	11.8463	0.2400	0.1806	0.0036	2510.0	52.8	2592.3	44.2	2658.0	37.4	3.2	5.6	2658.0	37.43
G128	10.7	118.4	0.84	0.0772	0.0011	0.6050	0.0215	0.0569	0.0021	479.3	13.0	480.4	29.6	486.5	27.9	0.2	1.5	479.3	13.05
G129	10.2	96.6	1.68	0.1312	0.0017	1.1879	0.0303	0.0657	0.0017	794.9	19.4	795.0	31.5	796.2	28.1	0.0	0.2	794.9	19.38
G13	150.1	212.7	0.36	0.6346	0.0075	23.6373	0.3397	0.2702	0.0036	3167.9	59.3	3253.6	34.9	3307.0	26.2	2.6	4.2	3307.0	26.16
G130	18.8	230.5	0.64	0.0730	0.0010	0.5806	0.0161	0.0577	0.0016	454.4	11.4	464.8	22.9	517.6	22.5	2.2	12.2	454.4	11.41
G131	26.2	172.7	0.58	0.1389	0.0017	1.4004	0.0313	0.0732	0.0016	838.2	19.7	889.1	30.1	1018.9	28.5	5.7	17.7	838.2	19.70
G132	21.9	122.8	0.96	0.1473	0.0019	1.4304	0.0338	0.0705	0.0017	885.7	21.0	901.7	31.8	942.1	28.7	1.8	6.0	885.7	21.01
G133	59.0	96.6	1.29	0.4553	0.0058	10.4010	0.2135	0.1658	0.0033	2418.7	51.1	2471.1	44.1	2515.3	37.5	2.1	3.8	2515.3	37.48
G134	35.2	206.9	0.35	0.1643	0.0020	1.6294	0.0348	0.0720	0.0015	980.7	22.6	981.6	30.7	984.5	26.5	0.1	0.4	984.5	26.46

Table 4

Gr. No.	Pb (ppm)	U (ppm)	Atomic Th/U	Ratios						Ages (Ma)						% concord. (206/238 / 207/235)	% concord. (206/238 / 207/206)	Best Age (Ma)	±2s
				206/238	± s.e.	207/235	± s.e.	207/206	± s.e.	206/238	± 2s	207/235	± 2s	207/206	± 2s				
G135	70.6	360.5	0.48	0.1819	0.0023	1.8813	0.0394	0.0750	0.0015	1077.5	24.5	1074.5	31.8	1069.6	27.1	-0.3	-0.7	1069.6	27.14
G136	43.1	178.0	0.55	0.2188	0.0027	2.5771	0.0536	0.0855	0.0017	1275.7	28.7	1294.2	34.9	1325.8	30.1	1.4	3.8	1325.8	30.15
G137	66.2	271.5	1.20	0.1873	0.0023	2.0189	0.0413	0.0782	0.0016	1106.6	25.0	1121.9	32.0	1152.5	27.7	1.4	4.0	1152.5	27.66
G14	11.9	76.5	1.12	0.1245	0.0018	1.2084	0.0403	0.0704	0.0024	756.2	20.5	804.5	40.8	940.9	41.5	6.0	19.6	756.2	20.52
G15	128.1	1235.9	0.15	0.1072	0.0013	1.0132	0.0154	0.0685	0.0010	656.6	14.8	710.5	19.0	884.9	16.9	7.6	25.8	656.6	14.79
G16	23.4	331.1	0.30	0.0703	0.0009	0.5436	0.0115	0.0561	0.0012	438.1	10.5	440.8	17.2	455.1	15.2	0.6	3.7	438.1	10.48
G17	105.4	551.0	1.15	0.1514	0.0018	1.4735	0.0233	0.0706	0.0011	908.8	20.2	919.6	23.2	945.9	18.5	1.2	3.9	945.9	18.48
G18	76.8	107.7	2.30	0.4394	0.0054	9.7428	0.1575	0.1608	0.0025	2348.0	48.3	2410.8	36.4	2464.4	28.7	2.6	4.7	2464.4	28.66
G19	34.7	217.6	1.10	0.1275	0.0016	1.1619	0.0224	0.0661	0.0012	773.6	17.8	782.8	24.4	809.5	20.9	1.2	4.4	773.6	17.84
G20	39.5	529.6	0.56	0.0688	0.0008	0.5123	0.0097	0.0540	0.0010	428.7	10.0	420.0	15.2	372.7	11.5	-2.1	-15.0	428.7	10.01
G21	43.6	259.9	0.64	0.1501	0.0018	1.4570	0.0260	0.0704	0.0012	901.5	20.4	912.8	25.5	940.3	21.2	1.2	4.1	940.3	21.25
G22	12.1	145.5	0.91	0.0697	0.0009	0.5219	0.0153	0.0543	0.0016	434.4	11.1	426.4	22.5	383.9	18.8	-1.9	-13.1	434.4	11.09
G23	31.5	161.1	0.95	0.1623	0.0020	1.6074	0.0308	0.0719	0.0013	969.4	22.1	973.1	27.9	981.7	23.5	0.4	1.2	981.7	23.47
G24	99.5	1263.0	1.09	0.0633	0.0008	0.4782	0.0078	0.0548	0.0009	395.5	9.1	396.8	12.9	404.9	10.5	0.3	2.3	395.5	9.09
G25	99.9	567.0	0.60	0.1589	0.0019	1.5411	0.0243	0.0703	0.0011	950.8	21.0	946.9	23.5	938.3	18.3	-0.4	-1.3	938.3	18.28
G26	115.5	402.8	0.36	0.2722	0.0032	3.6380	0.0549	0.0970	0.0014	1551.8	32.6	1557.9	29.5	1566.4	22.7	0.4	0.9	1566.4	22.72
G27	370.8	646.6	0.96	0.4700	0.0056	11.3018	0.1653	0.1744	0.0024	2483.6	48.8	2548.4	33.8	2600.5	25.7	2.5	4.5	2600.5	25.68
G28	78.2	445.0	0.70	0.1547	0.0018	1.5230	0.0246	0.0714	0.0011	927.0	20.5	939.7	23.9	969.7	19.2	1.3	4.4	969.7	19.24
G29	24.0	116.6	1.03	0.1664	0.0022	1.7474	0.0450	0.0762	0.0020	992.4	24.5	1026.2	37.4	1099.3	34.6	3.3	9.7	1099.3	34.56
G30	26.7	177.1	0.83	0.1292	0.0016	1.1901	0.0240	0.0668	0.0013	783.4	18.2	796.0	25.7	831.5	22.4	1.6	5.8	783.4	18.15
G31	61.7	186.5	0.82	0.2796	0.0034	3.7603	0.0612	0.0976	0.0015	1589.2	33.9	1584.3	31.4	1578.0	24.8	-0.3	-0.7	1578.0	24.79
G32	24.8	138.9	0.49	0.1664	0.0021	1.6168	0.0323	0.0705	0.0014	992.4	22.8	976.8	29.1	942.1	24.0	-1.6	-5.3	942.1	24.04
G33	22.8	284.8	0.77	0.0696	0.0009	0.5354	0.0117	0.0558	0.0012	433.6	10.4	435.4	17.6	445.2	15.5	0.4	2.6	433.6	10.37
G34	92.4	1521.6	1.06	0.0498	0.0006	0.3726	0.0078	0.0543	0.0011	313.0	7.5	321.6	13.2	384.3	13.2	2.7	18.5	313.0	7.49
G35	20.6	156.7	0.47	0.1235	0.0015	1.0936	0.0232	0.0642	0.0013	750.7	17.7	750.3	25.8	749.5	22.1	-0.1	-0.2	750.7	17.67
G36	40.0	128.6	0.41	0.2935	0.0037	4.4876	0.0850	0.1109	0.0021	1659.0	36.8	1728.7	37.1	1814.4	31.2	4.0	8.6	1814.4	31.25
G37	15.0	178.9	0.81	0.0723	0.0009	0.5584	0.0141	0.0560	0.0014	450.2	11.1	450.5	20.4	452.0	18.2	0.1	0.4	450.2	11.06
G38	18.0	246.1	0.54	0.0675	0.0009	0.5072	0.0120	0.0545	0.0013	421.3	10.3	416.6	18.1	390.9	15.1	-1.1	-7.8	421.3	10.27
G39	48.7	524.7	1.66	0.0661	0.0008	0.5052	0.0097	0.0555	0.0010	412.5	9.7	415.2	15.2	430.8	13.2	0.7	4.3	412.5	9.67
G40	88.6	247.4	1.03	0.2881	0.0034	4.0741	0.0644	0.1026	0.0015	1632.2	34.4	1649.1	31.3	1671.0	24.6	1.0	2.3	1671.0	24.61
G41	31.2	317.8	0.16	0.1013	0.0012	0.8479	0.0161	0.0607	0.0011	622.0	14.4	623.5	20.6	629.3	17.3	0.2	1.2	622.0	14.40
G42	388.3	906.1	0.10	0.4249	0.0050	9.4211	0.1383	0.1608	0.0022	2282.6	45.2	2379.9	33.2	2464.5	25.4	4.1	7.4	2464.5	25.44
G43	38.8	213.6	0.88	0.1526	0.0019	1.5101	0.0308	0.0718	0.0014	915.5	21.3	934.5	28.8	980.0	25.2	2.0	6.6	980.0	25.22
G44	23.8	61.4	1.13	0.3054	0.0038	4.5681	0.0873	0.1085	0.0020	1718.1	37.9	1743.5	37.6	1774.4	31.4	1.5	3.2	1774.4	31.38
G45	54.4	93.9	1.00	0.4554	0.0055	10.0920	0.1624	0.1607	0.0025	2419.3	49.0	2443.2	36.2	2463.5	28.4	1.0	1.8	2463.5	28.45
G46	50.8	453.5	0.12	0.1165	0.0014	1.0293	0.0179	0.0641	0.0011	710.4	16.2	718.6	21.2	744.6	17.6	1.1	4.6	710.4	16.17
G47	67.5	397.4	0.34	0.1656	0.0020	1.6625	0.0300	0.0728	0.0013	987.9	22.2	994.3	26.9	1008.9	22.3	0.6	2.1	1008.9	22.31
G48	12.2	77.0	1.06	0.1269	0.0017	1.1591	0.0295	0.0662	0.0017	770.4	18.9	781.5	31.1	814.0	28.4	1.4	5.4	770.4	18.88
G49	6.5	60.5	0.26	0.1054	0.0014	0.8694	0.0274	0.0599	0.0019	645.9	16.8	635.2	32.6	598.2	28.7	-1.7	-8.0	645.9	16.80

Table 4

Gr. No.	Pb (ppm)	U (ppm)	Atomic Th/U	Ratios						Ages (Ma)						% concord. (206/238 / 207/235)	% concord. (206/238 / 207/206)	Best Age (Ma)	±2s
				206/238	± s.e.	207/235	± s.e.	207/206	± s.e.	206/238	± 2s	207/235	± 2s	207/206	± 2s				
G50	60.4	318.6	0.66	0.1695	0.0020	1.6512	0.0284	0.0707	0.0012	1009.6	22.5	990.0	25.9	947.3	20.4	-2.0	-6.6	947.3	20.40
G51	48.7	183.8	1.55	0.1912	0.0023	2.0492	0.0372	0.0778	0.0014	1127.8	25.2	1132.0	29.2	1140.5	24.1	0.4	1.1	1140.5	24.15
G52	121.7	549.6	0.45	0.2074	0.0025	2.3430	0.0372	0.0820	0.0012	1215.0	26.3	1225.4	27.2	1244.3	21.5	0.9	2.4	1244.3	21.53
G53	37.3	335.6	1.36	0.0833	0.0010	0.6524	0.0131	0.0568	0.0011	515.8	12.1	510.0	18.6	484.2	15.2	-1.2	-6.5	515.8	12.14
G54	79.6	362.7	0.71	0.1918	0.0023	2.0651	0.0344	0.0781	0.0012	1130.8	24.8	1137.3	27.2	1150.2	21.8	0.6	1.7	1150.2	21.85
G55	45.0	723.2	0.51	0.0582	0.0007	0.4579	0.0107	0.0571	0.0013	364.4	8.9	382.8	16.9	496.2	18.3	4.8	26.6	364.4	8.89
G56	21.8	113.5	1.75	0.1334	0.0018	1.2212	0.0331	0.0664	0.0018	807.5	20.1	810.3	33.7	818.7	30.5	0.4	1.4	807.5	20.13
G57	29.4	230.1	0.83	0.1111	0.0015	1.1674	0.0291	0.0762	0.0019	679.1	16.8	785.4	30.8	1100.9	33.5	13.5	38.3	679.1	16.83
G58	55.8	320.4	0.64	0.1556	0.0019	1.5040	0.0266	0.0701	0.0012	932.4	21.0	932.0	25.6	931.3	20.9	0.0	-0.1	931.3	20.87
G59	233.5	415.7	0.98	0.4457	0.0053	10.0405	0.1543	0.1634	0.0024	2376.1	47.2	2438.5	34.6	2491.4	26.9	2.6	4.6	2491.4	26.92
G60	114.7	757.9	0.60	0.1365	0.0016	1.2996	0.0212	0.0691	0.0011	825.0	18.4	845.5	22.5	900.2	18.7	2.4	8.4	825.0	18.38
G61	20.6	249.2	0.99	0.0675	0.0008	0.5153	0.0120	0.0554	0.0013	420.8	10.1	422.0	18.0	428.8	16.0	0.3	1.9	420.8	10.15
G62	5.4	36.5	0.79	0.1311	0.0021	1.3057	0.0548	0.0723	0.0031	793.9	24.1	848.2	52.5	993.8	54.2	6.4	20.1	793.9	24.05
G63	102.9	190.9	0.82	0.4444	0.0054	9.8621	0.1597	0.1610	0.0025	2370.5	47.8	2422.0	36.1	2465.9	28.5	2.1	3.9	2465.9	28.53
G64	29.9	349.4	1.16	0.0679	0.0009	0.5285	0.0135	0.0565	0.0014	423.6	10.5	430.8	20.0	470.5	19.2	1.7	10.0	423.6	10.50
G65	25.8	209.6	0.33	0.1199	0.0015	1.0828	0.0243	0.0655	0.0015	730.1	17.4	745.0	26.9	790.4	24.3	2.0	7.6	730.1	17.38
G66	30.7	123.7	1.23	0.1912	0.0024	2.0453	0.0401	0.0776	0.0015	1128.1	25.5	1130.7	31.1	1136.4	26.3	0.2	0.7	1136.4	26.26
G67	88.1	482.9	0.40	0.1762	0.0021	1.8368	0.0314	0.0756	0.0012	1046.0	23.1	1058.7	26.7	1085.6	21.9	1.2	3.6	1085.6	21.86
G68	33.3	376.1	1.36	0.0665	0.0008	0.5018	0.0106	0.0547	0.0011	415.1	9.9	412.9	16.4	401.2	13.8	-0.5	-3.5	415.1	9.91
G69	50.3	784.6	0.23	0.0651	0.0008	0.4969	0.0091	0.0554	0.0010	406.3	9.4	409.6	14.5	428.4	12.5	0.8	5.2	406.3	9.44
G70	58.0	369.8	0.29	0.1565	0.0019	1.5357	0.0305	0.0712	0.0014	937.0	21.5	944.8	28.3	963.4	24.1	0.8	2.7	963.4	24.12
G71	49.3	244.3	0.90	0.1683	0.0020	1.6343	0.0303	0.0705	0.0013	1002.5	22.5	983.5	27.4	942.1	22.1	-1.9	-6.4	942.1	22.13
G72	72.5	341.3	0.70	0.1863	0.0022	1.9283	0.0335	0.0751	0.0013	1101.1	24.3	1091.0	27.6	1071.4	22.2	-0.9	-2.8	1071.4	22.21
G73	109.3	177.6	0.67	0.5041	0.0061	11.6851	0.1895	0.1682	0.0026	2631.5	51.9	2579.5	36.6	2539.3	28.8	-2.0	-3.6	2539.3	28.83
G74	27.6	135.3	0.69	0.1791	0.0022	1.8193	0.0366	0.0737	0.0015	1062.2	24.3	1052.4	30.5	1032.7	25.5	-0.9	-2.9	1032.7	25.51
G75	48.9	128.6	1.40	0.2812	0.0034	3.8342	0.0695	0.0989	0.0017	1597.3	34.6	1600.0	34.5	1604.0	28.4	0.2	0.4	1604.0	28.36
G76	128.4	193.6	1.00	0.5345	0.0065	16.9115	0.2761	0.2296	0.0036	2760.2	54.2	2929.8	37.7	3049.0	30.0	5.8	9.5	3049.0	30.01
G77	36.7	404.1	1.17	0.0716	0.0009	0.5550	0.0116	0.0563	0.0012	445.5	10.6	448.3	17.3	463.0	15.2	0.6	3.8	445.5	10.59
G78	87.6	289.3	0.64	0.2678	0.0032	3.5651	0.0605	0.0966	0.0016	1529.8	32.7	1541.8	32.1	1558.7	25.9	0.8	1.9	1558.7	25.91
G79	32.9	418.3	0.63	0.0708	0.0009	0.5438	0.0113	0.0558	0.0011	440.7	10.5	440.9	17.1	442.8	14.7	0.1	0.5	440.7	10.48
G80	81.7	135.7	1.17	0.4592	0.0056	10.2717	0.1735	0.1623	0.0026	2435.9	49.1	2459.6	37.4	2479.7	30.0	1.0	1.8	2479.7	30.05
G81	30.2	368.5	0.67	0.0730	0.0009	0.5820	0.0124	0.0578	0.0012	454.1	10.8	465.7	18.1	523.7	17.1	2.5	13.3	454.1	10.81
G82	91.6	236.8	0.70	0.3332	0.0040	5.2275	0.0889	0.1138	0.0019	1853.9	38.8	1857.1	34.6	1861.3	27.9	0.2	0.4	1861.3	27.88
G83	18.5	225.2	0.68	0.0730	0.0009	0.5729	0.0137	0.0569	0.0014	454.1	11.1	459.9	19.9	489.2	18.4	1.2	7.2	454.1	11.05
G84	49.9	240.3	0.95	0.1712	0.0021	1.7240	0.0367	0.0730	0.0015	1018.9	23.6	1017.5	31.4	1015.1	26.9	-0.1	-0.4	1015.1	26.89
G85	16.1	89.0	3.34	0.0936	0.0013	0.7919	0.0230	0.0614	0.0018	576.7	14.7	592.2	28.8	652.6	28.1	2.6	11.6	576.7	14.74
G86	24.0	104.1	0.67	0.1991	0.0026	2.0920	0.0540	0.0762	0.0020	1170.3	28.4	1146.2	39.9	1101.4	34.7	-2.1	-6.3	1101.4	34.74
G87	72.3	959.9	0.74	0.0657	0.0008	0.5085	0.0095	0.0562	0.0010	410.1	9.6	417.4	14.8	458.7	13.3	1.7	10.6	410.1	9.56
G88	72.0	110.4	0.77	0.5241	0.0064	13.1822	0.2278	0.1825	0.0030	2716.7	54.1	2692.8	38.9	2675.4	31.3	-0.9	-1.5	2675.4	31.30

Table 4

Gr. No.	Pb (ppm)	U (ppm)	Atomic Th/U	Ratios						Ages (Ma)						% concord. (206/238 / 207/235)	% concord. (206/238 / 207/206)	Best Age (Ma)	±2s
				206/238	± s.e.	207/235	± s.e.	207/206	± s.e.	206/238	± 2s	207/235	± 2s	207/206	± 2s				
G89	22.8	260.8	1.09	0.0702	0.0009	0.5425	0.0157	0.0561	0.0016	437.2	11.2	440.1	22.7	455.9	21.2	0.7	4.1	437.2	11.20
G90	45.0	559.4	0.74	0.0704	0.0009	0.5414	0.0109	0.0558	0.0011	438.5	10.4	439.4	16.4	444.8	14.1	0.2	1.4	438.5	10.36
G91	52.3	221.2	0.83	0.2003	0.0024	2.1884	0.0413	0.0793	0.0015	1176.7	26.2	1177.4	30.6	1179.1	25.5	0.1	0.2	1179.1	25.51
G92	10.0	73.9	0.78	0.1145	0.0016	0.9974	0.0311	0.0632	0.0020	699.0	18.2	702.5	34.7	714.3	32.1	0.5	2.1	699.0	18.16
G93	53.5	163.8	0.58	0.2924	0.0036	4.1279	0.0793	0.1024	0.0019	1653.7	36.1	1659.8	36.7	1668.3	30.7	0.4	0.9	1668.3	30.71
G94	78.3	473.1	0.10	0.1727	0.0021	1.7458	0.0328	0.0734	0.0013	1026.9	23.1	1025.6	28.3	1023.6	23.6	-0.1	-0.3	1023.6	23.56
G95	45.9	373.4	0.77	0.1066	0.0013	0.8984	0.0196	0.0612	0.0013	652.8	15.4	650.9	23.8	645.2	20.5	-0.3	-1.2	652.8	15.38
G96	103.9	352.5	1.70	0.2054	0.0025	2.2852	0.0413	0.0807	0.0014	1204.0	26.5	1207.7	30.0	1215.1	24.7	0.3	0.9	1215.1	24.75
G97	174.4	851.8	0.74	0.1767	0.0021	1.8580	0.0331	0.0763	0.0013	1049.1	23.2	1066.3	27.7	1102.2	23.1	1.6	4.8	1102.2	23.10
G98	46.9	203.4	1.02	0.1862	0.0023	1.9175	0.0385	0.0747	0.0015	1100.8	24.9	1087.2	31.0	1060.7	25.9	-1.2	-3.8	1060.7	25.90
G99	11.0	142.9	0.51	0.0713	0.0009	0.5382	0.0154	0.0547	0.0016	444.2	11.3	437.2	22.4	401.2	19.0	-1.6	-10.7	444.2	11.31
12061801 - Song Trac																			
G1	23	256	1.02	0.0722	0.0009	0.5508	0.0118	0.0549	0.0009	449.6	10.8	445.5	15.0	408.2	12.7	-0.9	-10.1	449.6	10.8
G2	30	435	0.09	0.0730	0.0009	0.6333	0.0124	0.0630	0.0009	454.4	10.7	498.1	15.1	706.5	16.4	8.8	35.7	454.4	10.7
G3	28	48	1.52	0.4125	0.0052	7.9377	0.2054	0.1464	0.0018	2226.3	47.0	2224.0	31.8	2304.4	23.8	-0.1	3.4	2304.4	23.8
G4	169	277	0.77	0.4983	0.0058	11.9822	0.1971	0.1794	0.0017	2606.3	49.9	2603.0	28.4	2647.1	19.5	-0.1	1.5	2647.1	19.5
G5	114	699	0.30	0.1594	0.0019	1.5390	0.0241	0.0708	0.0007	953.5	20.7	946.1	19.4	950.5	14.3	-0.8	-0.3	950.5	14.3
G6	16	414	0.21	0.0390	0.0005	0.2809	0.0063	0.0514	0.0010	246.4	6.1	251.3	10.0	260.6	10.2	1.9	5.4	246.4	6.1
G7	101	1202	1.65	0.1555	0.0018	1.6197	0.0252	0.0753	0.0008	931.9	20.2	977.9	19.7	1076.3	15.3	4.7	13.4	1076.3	15.3
G8	118	1388	0.01	0.0922	0.0011	0.7819	0.0129	0.0603	0.0007	568.7	12.7	586.6	14.6	615.8	12.3	3.1	7.7	568.7	12.7
G9	48	431	0.42	0.1048	0.0013	0.9407	0.0177	0.0652	0.0009	642.3	14.7	673.2	17.9	779.5	16.3	4.6	17.6	642.3	14.7
G10	18	247	0.23	0.0725	0.0009	0.5562	0.0124	0.0557	0.0010	450.9	10.8	449.0	15.7	440.8	14.1	-0.4	-2.3	450.9	10.8
G11	79	1239	0.15	0.0667	0.0008	0.5137	0.0088	0.0554	0.0007	416.2	9.5	421.0	12.0	427.6	10.4	1.1	2.7	416.2	9.5
G12	148	481	0.40	0.2885	0.0034	4.0153	0.0664	0.1021	0.0012	1633.9	33.8	1637.3	26.5	1662.3	19.8	0.2	1.7	1662.3	19.8
G13	151	1234	0.50	0.1165	0.0014	1.1216	0.0185	0.0689	0.0008	710.6	15.8	763.7	17.8	895.7	15.6	7.0	20.7	710.6	15.8
G14	36	493	0.42	0.0711	0.0009	0.5462	0.0101	0.0562	0.0008	442.5	10.2	442.5	13.3	461.1	11.8	0.0	4.0	442.5	10.2
G15	123	424	0.80	0.2465	0.0029	3.0544	0.0532	0.0904	0.0011	1420.3	30.0	1421.3	25.8	1433.1	19.9	0.1	0.9	1433.1	19.9
G16	46	159	0.81	0.2429	0.0030	3.2517	0.0704	0.0994	0.0014	1401.5	30.8	1469.6	29.3	1612.3	24.3	4.6	13.1	1612.3	24.3
G17	97	634	0.20	0.1555	0.0018	1.5001	0.0259	0.0709	0.0009	931.7	20.4	930.4	21.1	953.7	16.9	-0.1	2.3	953.7	16.9
G18	31	420	0.35	0.0728	0.0009	0.5574	0.0109	0.0558	0.0009	452.8	10.6	449.8	14.2	443.2	12.4	-0.7	-2.2	452.8	10.6
G19	66	761	0.27	0.0857	0.0010	0.6927	0.0130	0.0597	0.0009	529.8	12.2	534.4	15.8	593.1	14.3	0.9	10.7	529.8	12.2
G20	47	234	4.31	0.0884	0.0011	0.7392	0.0164	0.0607	0.0011	545.9	13.0	561.9	18.4	628.6	17.6	2.8	13.2	545.9	13.0
G21	444	3362	0.34	0.1276	0.0015	1.2680	0.0159	0.0720	0.0005	774.3	17.0	831.5	15.0	985.1	14.3	6.9	21.4	774.3	17.0
G22	76	224	1.18	0.2631	0.0032	3.4694	0.0631	0.0977	0.0009	1505.5	32.6	1520.3	24.3	1580.5	21.5	1.0	4.7	1580.5	21.5
G23	107	531	0.46	0.1878	0.0023	1.9837	0.0332	0.0760	0.0007	1109.4	24.5	1110.0	20.6	1094.0	19.1	0.0	-1.4	1094.0	19.1
G24	13	116	1.29	0.0817	0.0011	0.6558	0.0194	0.0598	0.0014	506.3	13.6	512.0	22.4	596.0	27.7	1.1	15.1	506.3	13.6
G25	146	697	1.31	0.1594	0.0019	1.5972	0.0227	0.0724	0.0006	953.5	21.0	969.1	17.7	996.1	16.2	1.6	4.3	996.1	16.2
G26	189	2173	0.74	0.0761	0.0009	0.7193	0.0095	0.0685	0.0005	473.0	10.8	550.2	11.8	884.3	15.0	14.0	46.5	473.0	10.8

Table 4

Gr. No.	Pb (ppm)	U (ppm)	Atomic Th/U	Ratios 206/238	± s.e.	207/235	± s.e.	207/206	± s.e.	Ages (Ma) 206/238	± 2s	207/235	± 2s	207/206	± 2s	% concord. (206/238 / 207/235)	% concord. (206/238 / 207/206)	Best Age (Ma)	±2s
G27	24	610	0.08	0.0410	0.0005	0.3186	0.0063	0.0552	0.0009	259.2	6.4	280.8	9.8	418.7	17.2	7.7	38.1	259.2	6.4
G28	24	398	0.23	0.0615	0.0008	0.5036	0.0090	0.0593	0.0008	384.8	9.2	414.1	12.2	576.7	17.8	7.1	33.3	384.8	9.2
G29	44	546	0.34	0.0778	0.0010	0.6573	0.0126	0.0608	0.0008	482.8	11.6	512.9	14.9	631.5	19.4	5.9	23.5	482.8	11.6
G30	216	1542	0.36	0.1352	0.0016	1.4090	0.0183	0.0750	0.0005	817.3	18.1	892.7	16.0	1067.4	15.2	8.4	23.4	817.3	18.1
G31	24	447	0.22	0.0529	0.0007	0.4340	0.0084	0.0595	0.0009	332.5	8.1	366.0	12.0	586.5	19.7	9.2	43.3	332.5	8.1
G32	109	1275	1.34	0.0646	0.0008	0.5011	0.0077	0.0563	0.0006	403.4	9.3	412.5	10.7	465.4	14.1	2.2	13.3	403.4	9.3
G33	242	1903	0.82	0.1104	0.0013	1.0295	0.0141	0.0674	0.0005	675.1	15.1	718.7	14.4	848.6	15.1	6.1	20.4	675.1	15.1
G34	43	537	0.97	0.0655	0.0008	0.5627	0.0100	0.0631	0.0008	409.1	9.8	453.3	13.1	712.3	19.5	9.8	42.6	409.1	9.8
G35	263	1358	0.57	0.1764	0.0021	1.8713	0.0257	0.0767	0.0006	1047.4	22.8	1071.0	18.2	1113.4	16.1	2.2	5.9	1113.4	16.1
G36	55	744	0.79	0.0632	0.0008	0.4882	0.0087	0.0559	0.0007	395.0	9.3	403.7	11.8	448.8	15.7	2.2	12.0	395.0	9.3
G37	76	529	1.16	0.1122	0.0014	1.0067	0.0173	0.0643	0.0007	685.5	15.8	707.2	16.6	749.9	18.1	3.1	8.6	685.5	15.8
G38	185	1156	0.55	0.1464	0.0017	1.4673	0.0207	0.0714	0.0006	881.0	19.5	917.0	16.9	970.0	16.0	3.9	9.2	881.0	19.5
G39	30	381	0.64	0.0715	0.0009	0.5488	0.0097	0.0555	0.0007	445.4	10.5	444.2	12.6	430.8	15.3	-0.3	-3.4	445.4	10.5
G40	93	502	0.36	0.1771	0.0021	1.8628	0.0321	0.0755	0.0008	1051.3	23.4	1068.0	20.7	1081.3	19.8	1.6	2.8	1081.3	19.8
G41	162	1043	0.43	0.1463	0.0017	1.5468	0.0221	0.0758	0.0006	880.2	19.5	949.2	17.5	1090.6	17.0	7.3	19.3	880.2	19.5
G42	26	189	1.40	0.1005	0.0013	0.8876	0.0181	0.0623	0.0009	617.2	14.8	645.1	17.9	685.1	20.6	4.3	9.9	617.2	14.8
G43	43	312	1.08	0.1098	0.0014	0.9928	0.0197	0.0671	0.0009	671.3	15.9	700.2	18.9	842.1	21.9	4.1	20.3	671.3	15.9
G44	107	822	0.24	0.1298	0.0015	1.2559	0.0181	0.0696	0.0006	786.8	17.6	826.0	16.2	915.4	16.3	4.8	14.0	786.8	17.6
G45	94	578	0.29	0.1601	0.0019	1.5739	0.0255	0.0712	0.0007	957.1	21.3	960.0	19.0	961.7	18.3	0.3	0.5	961.7	18.3
G46	27	379	0.47	0.0659	0.0008	0.5111	0.0102	0.0563	0.0009	411.5	9.9	419.2	13.4	465.8	17.7	1.8	11.6	411.5	9.9
G47	46	220	2.19	0.1326	0.0016	1.2192	0.0236	0.0672	0.0009	802.6	18.7	809.4	19.8	844.9	20.9	0.8	5.0	802.6	18.7
G48	91	435	1.16	0.1655	0.0020	1.6278	0.0243	0.0714	0.0006	987.0	21.8	981.0	18.3	968.3	16.9	-0.6	-1.9	968.3	16.9
G49	214	1323	0.89	0.1351	0.0016	1.3198	0.0187	0.0710	0.0006	816.9	18.2	854.4	16.5	956.8	16.2	4.4	14.6	816.9	18.2
G50	58	492	0.22	0.1188	0.0014	1.2012	0.0199	0.0728	0.0008	723.8	16.6	801.1	17.6	1008.4	19.6	9.6	28.2	723.8	16.6
G51	210	1751	0.27	0.1183	0.0014	1.2166	0.0157	0.0730	0.0005	720.7	16.0	808.2	14.9	1012.6	15.0	10.8	28.8	720.7	16.0
G52	355	1043	0.98	0.2762	0.0033	3.8261	0.0535	0.0983	0.0007	1572.0	32.8	1598.3	21.9	1592.1	17.5	1.6	1.3	1592.1	17.5
G53	183	1273	0.33	0.1394	0.0017	1.4940	0.0208	0.0768	0.0006	841.5	18.7	927.9	17.0	1115.2	16.6	9.3	24.5	841.5	18.7
G54	42	826	0.11	0.0535	0.0006	0.3958	0.0062	0.0534	0.0006	335.7	7.8	338.6	9.3	347.1	12.8	0.9	3.3	335.7	7.8
G55	143	718	0.44	0.1871	0.0022	1.9789	0.0291	0.0763	0.0006	1105.6	24.1	1108.3	19.3	1101.9	17.1	0.2	-0.3	1101.9	17.1
G56	22	355	0.29	0.0611	0.0008	0.4551	0.0086	0.0552	0.0008	382.3	9.2	380.9	12.1	418.7	16.1	-0.4	8.7	382.3	9.2
G57	157	1199	1.09	0.1038	0.0012	0.9200	0.0138	0.0648	0.0006	636.5	14.5	662.4	14.7	768.2	16.2	3.9	17.1	636.5	14.5
G58	21	477	0.77	0.0385	0.0005	0.2681	0.0052	0.0510	0.0008	243.2	6.0	241.2	8.5	239.0	12.9	-0.8	-1.8	243.2	6.0
G59	272	885	0.39	0.2887	0.0034	4.3521	0.0598	0.1076	0.0007	1635.1	34.0	1703.3	22.3	1759.5	17.6	4.0	7.1	1759.5	17.6
G60	104	448	0.39	0.2191	0.0026	2.6659	0.0444	0.0874	0.0008	1277.3	27.8	1319.1	22.0	1370.2	19.8	3.2	6.8	1370.2	19.8
G61	44	504	1.07	0.0696	0.0009	0.5431	0.0094	0.0557	0.0007	433.4	10.2	440.5	12.2	440.4	15.1	1.6	1.6	433.4	10.2
G62	37	582	0.18	0.0654	0.0008	0.5587	0.0091	0.0615	0.0007	408.3	9.6	450.7	11.9	658.2	17.1	9.4	38.0	408.3	9.6
G63	31	420	0.63	0.0659	0.0008	0.5180	0.0106	0.0556	0.0009	411.4	10.0	423.8	13.7	435.2	17.5	2.9	5.5	411.4	10.0
G64	16	229	0.38	0.0661	0.0008	0.4936	0.0109	0.0546	0.0009	412.8	10.2	407.3	14.4	395.9	17.7	-1.3	-4.3	412.8	10.2
G65	290	1444	0.46	0.1881	0.0022	2.0468	0.0268	0.0775	0.0005	1111.2	24.0	1131.2	18.3	1133.8	15.4	1.8	2.0	1133.8	15.4

Table 4

Gr. No.	Pb (ppm)	U (ppm)	Atomic Th/U	Ratios						Ages (Ma)						% concord. (206/238 / 207/235)	% concord. (206/238 / 207/206)	Best Age (Ma)	±2s
				206/238	± s.e.	207/235	± s.e.	207/206	± s.e.	206/238	± 2s	207/235	± 2s	207/206	± 2s				
G66	27	349	0.36	0.0739	0.0009	0.6090	0.0108	0.0599	0.0008	459.5	10.9	482.9	13.5	601.4	17.7	4.8	23.6	459.5	10.9
G67	173	1003	0.18	0.1752	0.0021	1.8895	0.0260	0.0779	0.0006	1040.7	22.7	1077.4	18.3	1143.0	16.3	3.4	9.0	1143.0	16.3
G68	42	232	0.47	0.1696	0.0021	1.6689	0.0289	0.0724	0.0007	1010.1	22.6	996.8	20.2	998.3	19.4	-1.3	-1.2	998.3	19.4
G69	28	217	2.05	0.0851	0.0011	0.6946	0.0154	0.0590	0.0010	526.3	13.0	535.6	17.4	568.6	20.8	1.7	7.4	526.3	13.0
G70	182	2280	0.66	0.0730	0.0009	0.6202	0.0087	0.0602	0.0005	454.3	10.3	490.0	11.0	610.1	14.0	7.3	25.5	454.3	10.3
G71	186	494	0.53	0.3374	0.0040	6.0664	0.0897	0.1306	0.0009	1874.0	38.5	1985.4	23.9	2105.9	18.8	5.6	11.0	2105.9	18.8
G72	41	237	0.50	0.1622	0.0020	1.6825	0.0340	0.0725	0.0009	968.8	22.3	1001.9	22.2	999.4	22.4	3.3	3.1	999.4	22.4
G73	163	885	0.06	0.1929	0.0023	2.1831	0.0304	0.0822	0.0006	1136.8	24.6	1175.7	19.4	1249.1	16.9	3.3	9.0	1249.1	16.9
G74	65	379	0.65	0.1530	0.0019	1.5487	0.0269	0.0721	0.0008	917.5	20.7	950.0	19.5	987.6	19.5	3.4	7.1	987.6	19.5
G75	6	111	1.31	0.0413	0.0006	0.3201	0.0116	0.0558	0.0018	260.9	7.9	282.0	17.6	445.6	29.8	7.5	41.5	260.9	7.9
G76	320	934	0.83	0.2879	0.0034	4.1761	0.0615	0.1055	0.0008	1631.1	34.1	1669.3	22.7	1723.2	18.3	2.3	5.3	1723.2	18.3
G77	62	401	0.75	0.1341	0.0016	1.2180	0.0199	0.0659	0.0007	811.2	18.3	808.9	17.4	802.9	17.5	-0.3	-1.0	811.2	18.3
G78	36	483	0.30	0.0736	0.0009	0.5617	0.0095	0.0556	0.0007	457.7	10.7	452.6	12.4	434.8	14.8	-1.1	-5.3	457.7	10.7
G79	89	455	0.35	0.1896	0.0023	2.0360	0.0302	0.0781	0.0006	1119.1	24.4	1127.6	19.6	1148.1	17.5	0.8	2.5	1148.1	17.5
G80	31	459	0.22	0.0678	0.0009	0.5419	0.0116	0.0586	0.0010	422.6	10.4	439.7	14.9	551.5	20.3	3.9	23.4	422.6	10.4
G81	14	312	0.38	0.0432	0.0006	0.3373	0.0070	0.0567	0.0009	272.3	6.8	295.1	10.7	479.1	19.1	7.7	43.2	272.3	6.8
G82	76	123	1.04	0.4736	0.0058	10.3344	0.2163	0.1623	0.0014	2499.3	50.7	2465.2	27.6	2480.1	22.2	-1.4	-0.8	2480.1	22.2
G83	703	1156	0.69	0.5043	0.0059	12.5393	0.1689	0.1793	0.0011	2632.3	50.7	2645.7	24.9	2646.7	17.9	0.5	0.5	2646.7	17.9
G84	108	714	0.23	0.1500	0.0018	1.4607	0.0222	0.0701	0.0006	901.2	20.1	914.3	17.7	929.8	17.0	1.4	3.1	929.8	17.0
G85	18	329	0.22	0.0554	0.0007	0.4100	0.0094	0.0551	0.0010	347.4	8.8	348.9	13.6	414.7	19.0	0.4	16.2	347.4	8.8
G86	27	169	1.11	0.1250	0.0016	1.1528	0.0272	0.0648	0.0011	759.3	18.5	778.6	22.3	768.8	24.0	2.5	1.2	759.3	18.5
G87	194	1264	0.21	0.1549	0.0018	1.4889	0.0210	0.0702	0.0005	928.4	20.4	925.9	17.2	934.2	15.8	-0.3	0.6	934.2	15.8
G88	127	413	0.32	0.2935	0.0035	4.4562	0.0726	0.1085	0.0009	1659.0	35.0	1722.9	23.7	1773.9	19.7	3.7	6.5	1773.9	19.7
G89	292	1741	0.78	0.1433	0.0017	1.4405	0.0188	0.0723	0.0005	863.4	18.9	905.9	16.2	993.6	15.0	4.7	13.1	863.4	18.9
G90	128	675	0.46	0.1765	0.0021	2.0078	0.0304	0.0807	0.0007	1047.7	23.0	1118.1	19.5	1214.9	18.1	6.3	13.8	1214.9	18.1
G91	68	1036	0.17	0.0688	0.0008	0.5895	0.0095	0.0611	0.0007	429.1	10.0	470.5	12.1	643.8	16.8	8.8	33.3	429.1	10.0
G92	81	1789	0.94	0.0377	0.0005	0.2774	0.0043	0.0524	0.0006	238.8	5.6	248.6	7.0	304.2	12.1	3.9	21.5	238.8	5.6
G93	146	1308	0.61	0.1011	0.0012	0.8625	0.0132	0.0613	0.0006	621.0	14.2	631.5	14.3	648.0	15.5	1.7	4.2	621.0	14.2
G94	60	377	0.51	0.1467	0.0018	1.4601	0.0284	0.0708	0.0009	882.2	20.4	914.0	20.8	952.2	21.6	3.5	7.4	882.2	20.4
G95	200	1286	0.40	0.1477	0.0018	1.4747	0.0209	0.0708	0.0006	888.3	19.7	920.0	17.0	951.6	16.0	3.5	6.7	888.3	19.7
G96	163	886	0.20	0.1855	0.0022	1.9596	0.0275	0.0765	0.0006	1096.9	23.8	1101.8	18.8	1106.9	16.4	0.4	0.9	1106.9	16.4
G97	21	256	0.55	0.0747	0.0009	0.5770	0.0122	0.0560	0.0009	464.4	11.3	462.6	15.2	450.8	18.1	-0.4	-3.0	464.4	11.3
G98	46	502	0.05	0.0975	0.0012	0.8069	0.0137	0.0599	0.0007	599.6	13.9	600.7	15.0	598.9	16.7	0.2	-0.1	599.6	13.9
G99	25	335	0.45	0.0724	0.0009	0.5714	0.0115	0.0567	0.0009	450.4	10.9	458.9	14.4	479.9	17.9	1.9	6.2	450.4	10.9
G100	37	146	1.91	0.1672	0.0021	1.6809	0.0376	0.0724	0.0010	996.6	23.3	1001.3	24.0	996.9	24.3	0.5	0.0	996.9	24.3
G101	26	170	0.94	0.1227	0.0017	1.1283	0.0312	0.0694	0.0014	745.9	19.1	766.9	26.2	909.5	30.1	2.7	18.0	745.9	19.1
G102	73	396	0.85	0.1561	0.0026	1.5083	0.0621	0.0710	0.0010	934.9	29.4	933.8	27.0	958.3	23.9	-0.1	2.4	958.3	23.9
G103	304	1958	0.49	0.1504	0.0017	1.5057	0.0312	0.0713	0.0014	903.0	18.6	932.7	26.8	966.6	30.3	3.2	6.6	966.6	30.3
G104	89	1323	0.22	0.0686	0.0018	0.5695	0.0201	0.0594	0.0005	427.6	21.4	457.7	19.8	581.4	13.8	6.6	26.5	427.6	21.4

Table 4

Gr. No.	Pb (ppm)	U (ppm)	Atomic Th/U	Ratios 206/238	± s.e.	207/235	± s.e.	207/206	± s.e.	Ages (Ma) 206/238	± 2s	207/235	± 2s	207/206	± 2s	% concord. (206/238 / 207/235)	% concord. (206/238 / 207/206)	Best Age (Ma)	±2s
G105	131	955	0.30	0.1352	0.0022	1.3121	0.0446	0.0712	0.0010	817.5	24.8	851.0	24.3	963.7	23.2	3.9	15.2	817.5	24.8
G106	113	480	0.71	0.2058	0.0016	2.2312	0.0187	0.0808	0.0006	1206.4	17.1	1190.9	14.8	1217.6	16.4	-1.3	0.9	1217.6	16.4
G107	19	232	0.40	0.0796	0.0009	0.6205	0.0122	0.0558	0.0008	493.4	10.5	490.2	14.3	444.0	17.1	-0.7	-11.1	493.4	10.5
G108	16	211	0.44	0.0724	0.0020	0.5673	0.0266	0.0561	0.0006	450.6	23.4	456.3	21.2	456.3	14.5	1.2	1.3	450.6	23.4
G109	33	362	0.88	0.0757	0.0015	0.5911	0.0174	0.0554	0.0007	470.5	17.5	471.6	16.8	427.2	14.6	0.2	-10.1	470.5	17.5
G110	104	982	0.04	0.1134	0.0010	1.0415	0.0161	0.0665	0.0013	692.3	11.5	724.6	22.0	821.8	28.3	4.5	15.8	692.3	11.5
G111	213	593	0.40	0.3361	0.0009	6.1323	0.0117	0.1336	0.0008	1867.6	9.1	1994.9	11.7	2146.1	17.2	6.4	13.0	2146.1	17.2
G112	64	103	0.65	0.5231	0.0014	13.8736	0.0164	0.1998	0.0007	2712.1	11.5	2741.1	7.9	2824.6	12.6	1.1	4.0	2824.6	12.6
G113	1054	1779	0.16	0.5974	0.0040	25.4057	0.0931	0.3012	0.0010	3019.2	32.2	3323.9	14.4	3476.3	12.6	9.2	13.1	3476.3	12.6
G114	60	701	0.31	0.0836	0.0067	0.6886	0.3706	0.0593	0.0020	517.8	79.1	532.0	70.9	577.0	35.4	2.7	10.3	517.8	79.1
G115	79	1129	0.46	0.0655	0.0010	0.5147	0.0122	0.0566	0.0007	408.7	12.3	421.6	13.9	474.0	16.2	3.0	13.8	408.7	12.3
G116	94	1543	0.57	0.0561	0.0039	0.4844	0.1039	0.0605	0.0011	352.0	47.6	401.1	46.4	622.9	22.5	12.2	43.5	352.0	47.6

Table 5

Details			**Summary**				
Sample No.	14052705		Central age	54.5	± 3.6 Ma		
Irrad. No.	GAR 60		Age dispersion	22.7	%		
Position	0						
Date	22/04/15		Pooled age	54.4	± 2.6 Ma		
			Mean age	57.5	± 2.1 Ma		
zeta (CN5)	338						
zeta error	5		Chi squared	53.67	with	61	df
No. of grains	31		P(chi-sq)	73.61	%		
Total Ni	2907	tr					
Total Nd	4640	tr					
rho-d (CN5)	1.674E+06	tr/cm^2					
mean rho-s	8.375E+05	tr/cm^2					
mean rho-i	4.091E+06	tr/cm^2					
mean U	30.6	ppm					

Crystal	**Ng**	**Ns**	**rho-s**	**Ni**	**rho-i**	**Ns/Ni**	**U (ppm)**	**Age (Ma)**	**Error**
1	16	20	9.019E+05	116	5.231E+06	0.1724	39.1	48.6	11.8
2	15	61	2.934E+06	261	1.255E+07	0.2337	93.7	65.8	9.4
3	10	15	1.082E+06	121	8.730E+06	0.1240	65.2	35.0	9.6
4	12	40	2.405E+06	107	6.433E+06	0.3738	48.0	104.9	19.5
5	18	9	3.608E+05	21	8.418E+05	0.4286	6.3	120.1	47.9
6	12	41	2.465E+06	158	9.500E+06	0.2595	70.9	73.0	12.8
7	18	29	1.162E+06	158	6.333E+06	0.1835	47.3	51.7	10.5
8	10	26	1.876E+06	97	6.999E+06	0.2680	52.3	75.4	16.7
9	21	5	1.718E+05	28	9.620E+05	0.1786	7.2	50.3	24.4
10	20	11	3.968E+05	83	2.994E+06	0.1325	22.4	37.4	12.0
11	9	12	9.620E+05	49	3.928E+06	0.2449	29.3	68.9	22.2
12	12	1	6.013E+04	11	6.614E+05	0.0909	4.9	25.7	26.8
13	30	44	1.058E+06	237	5.700E+06	0.1857	42.6	52.3	8.6
14	18	13	5.211E+05	86	3.447E+06	0.1512	25.7	42.6	12.7
15	20	16	5.772E+05	89	3.211E+06	0.1798	24.0	50.7	13.8
16	25	17	4.906E+05	110	3.175E+06	0.1545	23.7	43.6	11.4
17	14	30	1.546E+06	156	8.040E+06	0.1923	60.0	54.2	10.8
18	21	22	7.559E+05	92	3.161E+06	0.2391	23.6	67.3	16.0
19	36	4	8.017E+04	19	3.808E+05	0.2105	2.8	59.3	32.6
20	20	8	2.886E+05	28	1.010E+06	0.2857	7.5	80.3	32.2
21	8	21	1.894E+06	64	5.772E+06	0.3281	43.1	92.2	23.2
22	16	11	4.960E+05	82	3.698E+06	0.1341	27.6	37.8	12.2
23	18	10	4.008E+05	57	2.285E+06	0.1754	17.1	49.4	17.0
24	18	28	1.122E+06	226	9.059E+06	0.1239	67.6	35.0	7.0
25	30	13	3.127E+05	92	2.213E+06	0.1413	16.5	39.9	11.8
26	40	4	7.215E+04	11	1.984E+05	0.3636	1.5	102.1	59.6
27	40	10	1.804E+05	116	2.092E+06	0.0862	15.6	24.3	8.0
28	32	9	2.029E+05	58	1.308E+06	0.1552	9.8	43.8	15.7
29	25	15	4.329E+05	73	2.107E+06	0.2055	15.7	57.9	16.4
30	12	11	6.614E+05	71	4.269E+06	0.1549	31.9	43.7	14.2
31	40	5	9.019E+04	30	5.411E+05	0.1667	4.0	47.0	22.7

Table 6

Production rate including topographic shielding

Sample	AMS-measured $^{10}Be/^{9}Be$ ratio	Analytical (1σ) uncertainty (%)	^{10}Be Production Rate: nucleogenic (atoms/g*yr)	stopped muons (atoms/g*yr)	fast muons (atoms/g*yr)	^{10}Be (atoms/g_{qtz})	Error (atoms/g_{qtz})	Denudation Rate (mm/kyr)	Error 1 (mm/kyr)	Total Error 2 (mm/kyr)	Apparent age (kyr BP)
12061807	5.52×10^{-13}	3.92	3.176	0.114	0.081	9.55E+04	3.82E+03	35.7	1.5	2.8	28.5
12061807-Carbonate corrected			2.749	0.088	0.067			29.5	1.3	2.4	33.2

Note that for the carbonate correction, the production rate was set to zero for DEM pixels covered by Devonian carbonate lithology.

Table 7

Sample number	Number of aliquots[1]	Equivalent Dose, De (Gy)[3]	Overdispersion (%)[4]	Dose Rate (Gy/ka)	OSL Age (ka)[5]	Depth (m)	Grain size (μm)	*In-situ* H_2O (%)[6]	U (ppm)	Th (ppm)	K (%)	Rb (ppm)	Cosmic (Gy/ka)[7]
12061803	**21 (38)**	0.84 ± 0.21	58.9 ± 21.7	2.61 ± 0.15	**0.32 ± 0.09**	1	90-180	9.4	2.5±0.2	13.8±1.2	1.17±0.03	69.5±2.8	0.14±0.01
12061804	**19 (35)**	0.40 ± 0.35	108.0 ± 31.7	2.61 ± 0.16	**0.15 ± 0.14**	5	125-212	8.9	4.0±0.3	14.1±1.3	0.86±0.02	47.1±1.9	0.08±0.01
12061706	**23 (28)**	23.99 ± 1.79[2]	13.1 ± 3.5	2.81 ± 0.16	**8.55 ± 1.08**	4	90-180	10.6	2.3±0.2	12.5±1.1	1.60±0.04	101.5±4.1	0.10±0.01
12061707	**20 (28)**	21.75 ± 1.74[2]	10.7 ± 4.3	2.95 ± 0.17	**7.36 ± 0.96**	8	90-180	9.8	3.1±0.2	13.1±1.2	1.54±0.04	97.8±3.9	0.06±0.01
12061709	**20 (41)**	1.77 ± 0.58	53.6 ± 10.3	3.24 ± 0.19	**0.55 ± 0.19**	4	90-180	11.9	2.6±0.2	12.8±1.2	2.03±0.05	124.0±5.0	0.09±0.01

1 Number of aliquots used for age calculation, number of aliquots measured in parentheses. Rejection of aliquots follows standard rejection criteria
2 De calculated using the Central Age Model of Galbraith et al (1999); Excel macros written by Sébastien Huot (UQAM). Error on De is 2-sigma standard error.
3 De calculated using the Minimum Age Model of Galbraith et al (1999) unless otherwise noted; Excel macros written by Sébastien Huot (UQAM).
4 Overdispersion represents scatter in De beyond calculated uncertainties in data, OD >20% is considered significant.
5 Error on age is 2-sigma standard error.
6 Assume 3±3%wt H2O is representative of burial history.
7 Contribution of cosmic radiation to the dose rate was calculated by using sample depth, elevation, and longitude/latitude following Prescott and Hutton (1994).